Using Publicly Available Data and Battery Models for Energy Consumption Estimation in Electric Vehicles

Saad Alateef

School of Computing, Newcastle University

2022

Dedicated to the Soul of my Father

DECLARATION

I declare that this thesis has not been previously submitted for a qualification or degree at Newcastle University or any other institution. I state that this thesis is my own work unless otherwise stated.

Saad Alateef

ACKNOWLEDGEMENTS

First of all, I would like to thank my supervisors, Dr Nigel Thomas and Dr John Colquhoun, for their academic and spiritual support. I am grateful and indebted to them for their guidance, endless motivation and advice throughout my PhD journey. They assisted me in overcoming all difficulties and challenges from the beginning to the end of my research.

I would also like to express my thanks to my external examiner, Prof William Knottenbet (Imperial College London) and my external examiner Dr Matthew Forshaw for their rich and valuable discussion.

I would also like to thank my colleagues and friends at the school of computing for their help and encouragement.

I am extremely thankful to my mother for her patience, support and endless prayers to ease all hardships. I would also like to thank my supportive wife and my kids, for their support, love and inspiration.

ABSTRACT

Improving the driving range of a battery-powered electric vehicle (EV) has been a significant concern in the automotive industry. The driving range is the actual distance an EV travels on a single charge. It strongly relies on the battery capacity and several other factors, such as road topology, traffic density, and weather conditions. These factors also influence the velocity profile or driving cycle of an EV which countries or organisations use as the standard procedure to assess the performance of vehicles. In contrast, less work was conducted to improve estimating the potential velocity profile for the vehicle based on the real-time traffic situation before the journey started. Estimating the driving profile or driving cycle on a particular route will enhance the state-of-charge (SOC) estimation accuracy. Hence, it will improve studying the influential factors towards battery behaviours and discharge processes. This thesis used public data from different resources related to the range estimation to predict the battery's remaining charge in a single trip. We further conducted several experiments to understand the battery behaviour of different models and used industrial open-source data to analyse the battery performance.

The state-of-charge (SOC) is crucial in predicting battery life, defined as the charge level relative to the battery's capacity. In this thesis, the determining factors of SOC are examined using traffic data obtained from Google Maps, HERE Maps and TomTom routing data providers. Some data were collected using the API for these three map information providers based on two different routes on the map, including time, distance and road segments. The data were collected at different times to better understand the route traffic situation. The route segmentation was first performed manually by specifying the waypoints on the map to separate the road parts where the speed is likely to be reduced due to possible stops. Furthermore, the waypoints were specified by the API dynamically to provide more route segments and to avoid API restrictions.

This approach helps us construct realistic driving profiles to a certain extent despite lower accuracy due to insufficient data. This step neglected the traffic light's waypoints

due to insufficient data, which has been applied as a random process. We added some noise to the velocity profile to emulate the driving behaviour since the data returned from the API is for the average velocity for each segment. The final driving profiles were used to discharge the batteries, and the results were investigated. Moreover, another approach was conducted to construct reliable driving profiles based on the route information. In this approach, we collected real-time data from different APIs, including route information, weather data, traffic light coordinates, and electric vehicle model. We incorporated these datasets into the SOC estimation algorithm. MATLAB and Simulink code was implemented, using the different datasets from different sources to estimate the real-time remaining range calculation.

Throughout this thesis, we have investigated different battery models used in electric vehicle applications and analysed the battery behaviours under various conditions. In addition, we explored the public data in different scenarios, integrated different APIs to predict driving behaviours in different routes, and analysed and compared the results of the data sources. As a result, we generated different power demand profiles based on different data sources to estimate the energy consumption of electric vehicles. Some of the representative driving cycles were further analysed and validated using an actual battery in the lab. The validation results showed that our battery's estimation is within the range of the actual battery in terms of power demand and energy consumption. It also showed that the battery model dynamics are similar to the real one, which gives the model more validity to conduct further experiments and rely on its results.

PUBLICATIONS

During my PhD, I have published the following papers:

1. Saad Alateef and Nigel Thomas. Battery models investigation and evaluation using a power demand generated from driving cycles. *In Proceedings of the 12th EAI International Conference on Performance Evaluation Methodologies and Tools.* (2019), pages 189–190 .[1]

2. Saad Alateef and Nigel Thomas. Energy consumption estimation for electric vehicles using routing API data. *18th European Performance Engineering Workshop.* (2022). [2]

3. Saad Alateef and Nigel Thomas. Trip driving cycle development and energy consumption estimation based on route API information for battery powered vehicles. *36th Annual UK Performance Engineering Workshop, Newcastle University.* (2020). [3]

CONTENTS

LIST OF FIGURES

LIST OF TABLES

1

INTRODUCTION

Contents

Introduction

1.1 Motivation

Primarily due to the zero-emissions characteristics of battery-powered electric vehicles (EVs), changes are expected over the immediate term regarding EVs acquiring a significant role in transportation markets. However, lengthening the life span of the batteries and their charge duration is crucial to the most efficient use of the batteries, which requires improvement due to their limited storage capacity. Attempting to restrict energy use at specific points is not necessarily successful in attaining a longer battery life span. Rather, battery life span is crucially affected by the existing levels and extraction patterns utilised, which influence how power is used up. Ultimately, a battery model is required to understand the effects on a battery and its characteristics stemming from energy usage. Live simulation of formulation, alongside state-of-charge (SOC) and state-of-health (SOH) predictions, are typically aspects and features of batteries. Consequently, models are crucial to ensure risk-free charging and discharging, maximum battery performance, and effective estimation of battery performance in various situations.

1.2 Introduction

The Paris agreement of 2015 [6] resulted in targets for reducing CO_2 emissions worldwide. In addition, it has led to governments and businesses investing in low-carbon technology for electricity generation and transport. For many years electric vehicles (EVs) were a niche technology used only for indoor or short distances, e.g. golf carts and milk floats. However, the development of more efficient high-speed motors and improvements in storage and charging technology for lithium-ion batteries have led to much more widespread use of electric vehicles for business and personal use. Figure 1.1 shows the electric vehicle ownership in the last few years in the United Kingdom, from 2012 until 2020..

There are several advantages in utilising the technology of the electric vehicle, including:
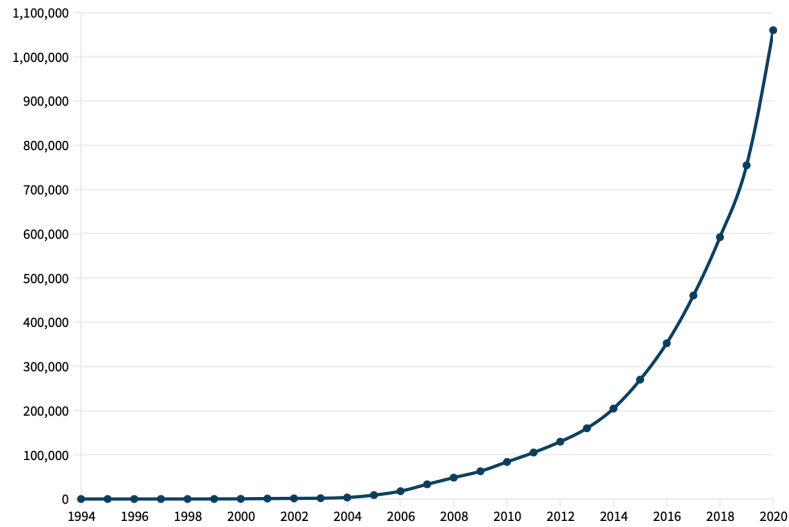
Figure 1.1: Electric vehicle ownership in the UK [4]

- Environmental friendly with zero-emission.

- Most of the countries have declared tax exempted.

- Smooth drive at cheap rates.

- The maintenance is minimal due to fewer moving parts.

Even though electric vehicles have significant advantages, many obstacles and challenges exist. These challenges have delayed the spread of utilising this technology for some years, such as:

- The limited range coverage varies depending on the vehicle's model and capacity.

- Extended charging time varies according to the battery and the charger capability.

- Batteries replacement after a few years, typically 5-10 years.

- Required a vast range of charging point networks in all parts of the country.

The internal combustion engine almost entirely led the transportation sector until the recent advances in electric vehicles in the last century. The improvements in this technology have been attracting both governments and the vehicle industry because

it is a green technology that decreases the dependence on fossil fuels and encourages the use of renewable energy [7]. The conversion to electric-powered vehicles started many years ago when hybrid vehicles were introduced, followed by plug-in-electric vehicles (PEV) until full EVs existed, which entirely depend on the battery [8]. Many countries improved the related infrastructure of electric vehicles as it will influence the attraction of both manufacturers and consumers [7]. This attention and consideration is mainly because of the impact of EVs use towards public health and safety as well as the environmental sustainability [7].

1.3 Aim of this thesis

This thesis aims to develop a method to estimate the energy consumption for electric vehicles using available public data. We investigate the existing battery models and energy consumption estimation methods and techniques. In addition, we will show how such methods and models can be used to generate realistic driving cycles for specific journeys over selected routes; hence, we can estimate the power demand for each trip. This process will involve integrating various factors into the models we implement, such as weather condition forecasting and road elevation degrees, to improve the power demand estimation. These parameters directly influence the driving profiles and the acceleration; therefore, they impact the energy consumption for EVs.

1.4 Problem Statement and Research Questions

Although electrical vehicle batteries work adequately, many studies in the literature [9–11], show that there are critical issues with battery life. However, battery life depends on different factors such as battery type, charge and discharge, charging current, battery temperature and battery usage patterns. There are outside factors that impact the driving modes, such as traffic, changes in road elevation and weather; thus, due to the influence of the driving patterns, there will be a different load on the battery. This study will investigate how significant this impact is by estimating the power demand of electric vehicles after taking these factors into account.

The research questions can be formed as follows:

- What factors most influence predictions of power demand and state-of-charge?

- How can these factors be determined from publicly available data?

- Hence, can we accurately predict power demand and reliably identify uncertainties in prediction?

To answer these research questions, we investigate publicly available data to find out how to generate a driving cycle without performing a single physical journey. Map service API data is very reliable nowadays. A Huge amount of data is collected from users every day to improve their services, including estimating the traffic and arrival times. We will use the API provided by maps service providers to generate speed profiles over the selected routes and then expand this process throughout the data to get the most realistic driving cycle. Other APIs will be investigated and used to integrate other factors that directly influence the driving patterns and energy calculations. For instance, weather data have significant impacts that directly affect energy consumption and driving patterns. These data include but are not limited to ambient temperature and wind speed/direction. In addition, we will obtain the road elevation information using the data provided from the map service providers to enhance the driving profiles and the energy consumption estimation.

1.5   Research Hypothesis

Our primary research hypothesis is that we can improve the remaining range estimation of electric vehicles by introducing API data.

1.6   Research Objectives

This thesis aims to investigate and study the traffic, map, and publicly available weather data and integrate them into an energy consumption estimation model for electric vehicles. It also aims to analyse their impact on the SOC and battery behaviour. This research seeks to address the abovementioned issues and answer the research questions. The thesis objectives are as follows:

- Investigation and understanding of the existing battery models using existing literature.

- Comparison of the most appropriate lithium-ion battery models for electric vehicles.

- Developing a generic energy consumption model that considers outside factors, including traffic data, route information and weather conditions and understand their influence on driving cycles.

- Using the constructed driving cycles as an input to generate the battery current for the electric vehicle.

- Investigating the battery dynamics and the SOC of the battery.

1.7 Research Methodology

While investigating and analysing existing related work in this thesis, the following methods were followed to achieve the research objectives:

- Understand how battery-powered vehicles perform under different conditions.

- Understand the battery models and how they function by looking at the established literature and meeting the battery modelling experts.

- Review the existing models implemented in the past.

- Experiment with some battery models to evaluate them and compare their outputs to determine which model is more stable and efficient.

- Explore traffic, map and weather data to identify what factors could influence the power demand for the battery.

- Integrate the data that could be influential by developing a model that processes these data from different sources to estimate the vehicle's power demand.

- Evaluate the battery model outputs to determine how much power would be consumed when these factors are taken into account.

1.8   Research Contributions

The contribution of this research can be broken down into the following points.

- Experiment with different battery models, use industrial open-source data to discharge the battery and analyse the results.

- Review of the related approaches that have been conducted to generate similar data using different sources.

- Investigate and evaluate publicly available map service APIs and generate velocity profiles for sample journeys based on their data.

- Generate scripts to collect data from map service providers such as Google Map, Here Map and Tom-Tom map. Capture and apply manual data segmentation so that the data collection methods meet our purposes.

- Develop an automated data capturing from different APIs, analyse the data's reliability, and then select the most accurate source API to generate our model's inputs.

- Generate power demand profiles based on these data and evaluate the effect of each type of data.

- Validate the generated profiles after using them to discharge batteries. The validation occurs in a lab using actual battery cells for electric vehicles.

1.9   Thesis structure

Chapter 1 Introduces the problem and emphasises the motivation behind the idea of this research. It also describes the research aims and objectives, the contributions, and how these objectives can be achieved.

Chapter 2 Highlights the importance of the transportation sector and gives an overview of batteries issues and previous studies related to batteries in EVs. It also provides an

overview of the map services API and what kind of data can be extracted and used for research purposes.

Chapter 3 Investigates the battery modelling techniques and evaluates the previous models for EVs. It also explains how the battery model can be implemented and tested. This chapter involves experiments of some battery models using some existing data.

Chapter 4 Focuses on the publicly available data, especially maps and related traffic information. It investigates previous studies on this domain, and it shows how we can obtain the data and how we can process them and use them with the battery inputs to estimate the state of charge.

Chapter 5 Integrates different data sources with the EV model and applies all mechanical and electrical parameters to generate the power demand profiles. It generates the velocity profiles but in more automated and efficient ways than the previous chapter's approach. In addition, it analyses the impact of considering the traffic lights on the route, which might impact the acceleration and deceleration rate.

Chapter 6 Discusses some of the generated profiles above and the battery estimation outputs. Moreover, it analyses the most reliable results and validates them using the existing battery to determine how reliable these data are. It also analyses the validated results using different approaches.

Chapter 7 Evaluates the entire thesis, including the data sources used to achieve the research goals. Additionally, it will present the limitation on developing such models and extracting the data. Moreover, it suggests possible future work in this field.

2

BACKGROUND AND RELATED WORK

Contents

Summary

2.1 Summary

This chapter introduces the technology of electric vehicles. It outlines the different technologies, including hybrid, plug-in hybrid, and fully electric cars. It also describes the EV fundamentals and outlines the challenges associated with this technology's adoption. This chapter will review the existing research on the remaining range estimation for EVs and classify different approaches. In addition, it reviews their strengths and drawbacks.

2.2 Introduction

This chapter will overview electric vehicle technology and its promising future. It explains the differences between battery-powered vehicles. It also involves reviewing the existing challenges in attracting consumers. Moreover, it illustrates the related issues that face EVs industry consumers and introduces possible solutions. This chapter highlights the gaps concerning the data extraction that can be useful for battery SOC and remaining range estimation and how this thesis tries to overcome these gaps.

2.3 Battery Powered Vehicles

The transportation industry consumes much energy and contributes to air pollution. Governments all around the globe are making attempts to decrease transportation-related energy and air pollution. A range of measures should be implemented to decrease transportation-related air pollution and its reliance on fossil fuels [12]. Electrifying transportation is one of the methods suggested by industrial, public agencies and research groups. Electric vehicles (EVs) are a viable alternative for achieving a low-emission and cleaner transportation system. Countries worldwide are setting ambitious goals to promote EV distribution among consumers, and some are even suggesting prohibiting the sales of conventional vehicles in the future [13]. China, for instance, plans to sell seven million electric vehicles per year by 2025, which is one-fifth

of all its local market demands. The United Kingdom and France declared that sales of conventional vehicles would cease by 2040. Norway wants electric vehicles to account for 100 per cent of new automobile sales by 2025. The automotive industry anticipates that EVs will be the primary transportation in the car market by 2030 [14].

Although the market has seen rapid growth in electric vehicles (EVs) due to the many environmental benefits they offer, there are still some concerns about range anxiety (the limited range to complete a trip or reach a charging station), that limits the broad adoption of EVs [15]. Estimating EV energy usage may help reduce range anxiety and assist EV users to plan their routes [16]. In addition, researchers and the industry have devoted considerable attention to electric vehicle-to-grid integration in recent years. This technology enables electric vehicles to interact with the power grid and offer services to help balance power loads [17]. In this instance, modelling the energy consumption for electric vehicles may help optimise charging and discharging operations while balancing energy usage and transportation requirements.

2.3.1 Electric vehicle history

The first electric vehicle, a tricycle powered by a battery, was developed in the 18th century. However, as the internal combustion engine (ICE) improved, ICE vehicles have taken a greater part of the market; pure electric vehicles (PEVs) have nearly vanished since the 1930s. With the rapid growth of the human population, if all vehicles are powered by internal combustion engines, gasoline and diesel oil will be overused and possibly depleted soon, as well as resulting in greenhouse gas emissions. As a result, energy saving and environmental protection are becoming increasingly important concerns all over the world [18]. An electric vehicle (EV) is a road vehicle that runs on electricity [18, 19]. Pure electric vehicles (PEVs), hybrid electric vehicles (HEVs), and plug-in hybrid fuel vehicles (PHEVs) are the three categories of electric cars. Due to current technology, they are currently in various stages of development; the major characteristics and features of three categories of EVs are shown in Table 2.1.

Types	PEV	HEV	PHEV
Source of energy	- Battery	- Battery/ultra-capacitor - Internal combustion engine	- Larger battery - Internal combustion engine
Propulsion system	- Electric motor	- Electric motor - Internal combustion engine	- Electric motor - Internal combustion engine
Features and characteristics	- Zero emission - Short driving range - High initial cost	- Low emission - Long driving range - Low initial cost	- Low emission - Longer range - Medium initial cost
Major techniques	- Electric motor control - Battery management system - Charging device	- Electric motor control - Battery management system - Motor regenerative braking charge	- Electric motor control - Battery management system - Motor regenerative braking charge - External charging device
Regenerative braking	- Yes	- Yes	- Yes

Table 2.1: Comparison of the main features of the three types of electric vehicles

2.3.2   Hybrid Electric-Vehicles

The hybrid electric vehicle is a technology where the vehicle combines both an engine and batteries to run the vehicle [20]. Hybrid vehicles feature two or more energy sources and/or two or more power sources on board. A battery, a flywheel, or other energy sources can be used. An engine, a fuel cell, a battery, an ultracapacitor, and other power sources are possible. Two or more of these power or energy sources may be employed depending on the vehicle design. Hybrid cars economize energy and reduce pollution by combining an electric motor with an (ICEs) in a way that takes use of each's best features. Series hybrids and parallel hybrids are the two types of hybrid cars. The engine of a series hybrid vehicle powers the generator, which then powers the electric motor. The engine and the electric motor are linked to operate the vehicle in a parallel hybrid car. In a city driving cycle, a series hybrid vehicle can save fuel consumption by ensuring that the ICE operates at its most efficient level during frequent stops and starts. In the highway driving cycle, when the ICE is at its most efficient and the car is travelling at constant speed, a parallel hybrid vehicle can consume less gasoline. Mild hybrids, power hybrids, and energy hybrids are the different categories of hybrid cars, based on the role of the engine and electric motor, as well as the mission that the system is meant to accomplish [21].

2.3.3   Plug-in Hybrid Electric-Vehicles

In both the industry and academia [22], as well as by different government organisations across the world, PHEVs have been regarded as a significant development in hybrid vehicle technology. PHEVs have a high-energy-density battery pack that can

be externally charged, allowing them to run on electric power for longer periods of time than standard HEVs, resulting in longer range and more efficiency [23]. The battery pack may be recharged in the garage or at a nearby AC outlet charger. Because the batteries are charged at night, PHEVs enhance the efficiency of utility power usage.

2.3.4 Full Electric-Vehicles

The first electric vehicle (EV) was developed in 1828, and the first manufactured electric vehicle was presented in 1884 [24]. Full EVs are a recent and mostly new technology that will help to decrease pollution and gas emissions. Fuel cells, traction motors, and electric motors are used to power these vehicles. This kind of vehicle should not be equipped with gasoline ICE or diesel engines. Rechargeable battery packs, as well as flywheels or ultra capacitors (UCs), are used to supply electricity. External charging stations or power points located in parks, as well as ordinary electrical outlets at home, can be used to recharge the battery pack. When compared to HEVs and PHEVs, the FEV does not produce any gas emissions when it operates. In comparison to PHEVs, FEVs have a considerably greater potential for emission reduction [25]. Because the battery packs can drive the EV motor with greater torque, the car accelerates considerably more quickly. In comparison to traditional diesel and gasoline cars, the performance of FEV is superior [26]. In today's market, there are a variety of manufacturers offering various types of EVs, as shown in Table 2.2. In comparison to previous batteries like NiMH, earlier versions of Li-ion, and so on, recent FEVs use state-of-the-art Li-ion batteries for greater performance.

Vehicle type	Battery type	Battery capacity
Renault Twizzy	Li-Ion	6.1 kWh
VW E-Golf	Li-Ion	24.2 kWh
Hyundai Ioniq	Li-Ion	28 kWh
Nissan Leaf	Li-Ion	30 kWh
Tesla Model S	Li-Ion	100 kWh

Table 2.2: Comparison of some of electric vehicle's battery available in the market

2.4 EVs Challenges

A variety of problems and obstacles obstruct the adoption of the use of electric vehicles. Some of these factors are listed and discussed below.

2.4.1 Driving range

There are some disadvantages to EVs, like less driving range and lengthier charging time. Therefore, this issue might affect the advancement of the market penetration of EVs and may be a vital obstacle. Despite an increase in the number of electric vehicle sales, they are still not widely accepted by a more significant segment of the population of targeted buyers. Except for Sweden, China, and Norway, most nations have an average EV share of less than 1 per cent [27]. This statistic demonstrates that, despite the rise in popularity of electric vehicles, growing environmental concerns, and technological progress, electric vehicles are still not as prevalent on the road as they should be. Several pieces of research are being conducted in order to solve this particular EV adoption issue. For example, a phenomena known as range anxiety is the most critical factor in determining whether or not to purchase an electric vehicle [28]. In the context of electric vehicles, range anxiety is described as the worry of running out of energy before reaching a nearby charging station or final destination [29].

2.4.2 Cost

The economics of electric vehicles is one of the essential factors in determining their societal acceptability. It is critical for the widespread adoption of electric cars (EVs) to be economically competitive with conventional internal combustion engines vehicles (ICEs). One of the most severe issues with this is a problem with the battery. Some automobile manufacturers sell this battery together with the vehicle, whereas others (such as Renault) just rent the battery. The market policy adopted here differs from the previous one and is dictated by the local area and market needs. Battery cost now accounts for 23-58 per cent of the overall cost of a electric vehicles [30]. The advancement of electric mobility is closely connected to technological advancement in

general. The characteristics of batteries are presently one of the critical challenges to the widespread adoption of electric vehicles. Battery prices vary according to the characteristics of their storage systems and operating models. As a result, the costs of batteries for passenger vehicles and those for buses vary considerably. It is expected that within this decade, battery technology will improve enough to address one of the major disadvantages of current electric vehicles, namely their short operational range. Furthermore, batteries are expected to be considerably cheaper than they are now. A reduction in battery costs is one of the reasons anticipated to minimise the price gap between an electric car and an internal combustion vehicle [31].

2.4.3 Charging points

Even though EVs have very low greenhouse gas emissions and excellent energy efficiency, there are still issues with charging infrastructure [32]. A sufficient number of charging stations in convenient places is required for widespread adoption of this technology. The charging site infrastructure issue is divided into two stages: first, the cost of the charging infrastructure is reduced, and then the network flow is optimised. Decent research and modelling work has been done in this area, but each model is overly narrow in how it addresses certain issues, and there is an urgent need for a more comprehensive solution that addresses all of the challenges that are preventing the large-scale adoption of electric vehicles [33].

2.5 Background

The need for reducing global emissions and making the use of energy more efficient have become essential for the entire globe [25]. Therefore, electric vehicles (EVs) are gaining global attention and more popularity mainly because they have smaller impact to the environment than the internal combustion vehicles (ICVs). Additionally, EVs have zero emission when they operate [34]. Many countries have set EV achievement goals for the next few years. However, some challenges and barriers for consumers reduce their trust in purchasing EVs. As mentioned above one of these challenges is known as range anxiety where the user is not assured to have enough energy in

the battery to drive in a certain route [35]. This makes it difficult to travel through unknown routes, therefore, every trip should be well planned taking into consideration the remaining charging and the availability of the charging stations. Nevertheless, EV travel ranges vary dramatically due to road gradients and traffic situations. As a consequence, average users struggle to come up with an accurate plan for unfamiliar roads [36].

One of the features of EVs is regenerative braking. This mechanism allows the vehicle to retrieve the energy while braking [37]. In particular, the wheels generate the energy during the excessive braking and pass it back to the motor which returns it to the battery. Past investigations found that EVs were substantially more effective when driving on urban roads than driving in motorways as the regenerative braking helps in energy recovery. The opposite occurs in ICE vehicles where they exert extra energy in urban driving due to braking and thermal energy losses [38].

The energy consumption estimation of vehicles has been an intense research topic globally as the dominance of EVs will substantially reduce transportation fuel dependency and emission levels [39]. In this chapter, we will identify and review the existing studies conducted in energy consumption estimation for electric vehicles. We have identified a strategy to review the relevant studies to achieve this goal. We first searched for relevant research papers published in recent years in scientific databases. Then we used a set of keywords, including EVs energy consumption estimation, state-of-charge estimation for EVs and electric vehicle power demand estimation, to find the relevant papers. Then we scanned the titles and excluded the irrelevant studies; this step is followed by scanning the abstract of the collected paper and then excluding any irrelevant study. In addition, irrelevant papers include but are not limited to charging infrastructure, grid integration and hybrid electric vehicles related papers. The process for this strategy is depicted in Figure 2.1.

2.5.1 Battery Management System (BMS)

BMS is developed to handle and manage battery pack control and activities, as well as the energy, flows from the pack to the motor [40]. The main features of BMS are as follows:
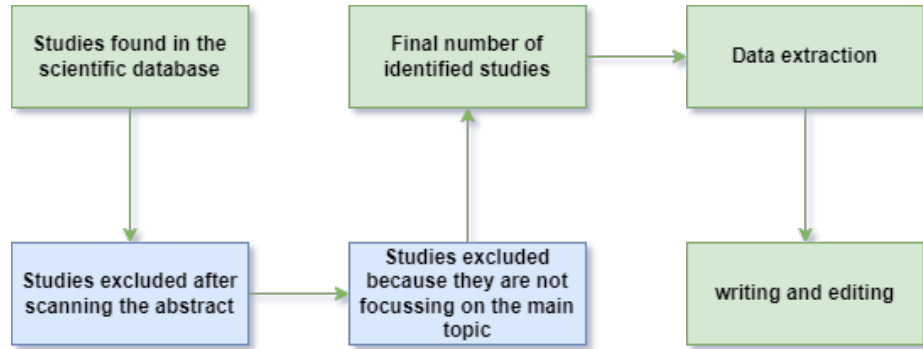
Figure 2.1: The review process workflow

- Voltage and current measurements at the input and output.

- Charge equalisation for the battery cells.

- Controlling voltage in electrochemical cells for monitoring and balancing.

- Preventing the risk of overcharging and/or over-discharging in electrochemical cells.

- Control of battery charging and discharge depending on the powertrain's energy requirement and available energy.

- Diagnose, analyse, and show defects and flaws.

- Electrical and electronic systems control and command.

- Temperature monitoring and control.

A BMS is composed of hardware modules such as sensors and actuators, thermal management components, protection circuits, and a communication network. In addition, a software module including models for predicting, estimating, and computing state-of-charge (SOC), state-of-health (SOH), cell balance, and fault detection [41]. Some BMS technological solutions regulate the functioning of hardware elements/subsystems and assess the condition of battery cells. The BMS software controls the cell load/discharge, actuators, and safety circuits. In addition, the BMS software analyses data for continuous process management and updating of battery operations, estimating the in-service (currently operational) state (a crucial determinant for successful battery operation)

and identifies potential problems. The evaluation of two fundamental parameters primarily assesses the battery's functional condition: the state-of-charge SOC level and the internal degradation level state-of-health SOH. The SOC parameter is computed using voltage, current and operating temperature data, while the SOH parameter is determined based on the deterioration of the electrochemical process performance in battery cells, which decreases charging/discharging capacity and available energy. Because the battery discharge and charge operations include complicated chemical and physical processes, estimating the SOC parameter's value correctly is a critical task. SOC and SOH are calculated using various mathematical models and methods, including conventional, non-linear, hybrid, neural networks, fuzzy logic etc [41].

2.5.2   General concepts

The estimation of the potential EV range is usually based on three main factors: vehicle design, driving behaviours and the surrounding environment as shown in Figure 2.2. According to studies on this area, each of these groups is dependent on the change of direct or indirect factors [42–44]. Some parameters are fixed, such as vehicle type, transmission type, number of seats, vehicle's mass, weight, battery type, road infrastructure and available battery charging infrastructure. In addition, others are variable such as battery state-of-charge SOC, battery state-of-health SOH, driver behaviours [45], traffic flow [46], EV dynamic performance and battery management system. However, the majority of the work in this area that analyses and addresses these problems is directly linked to the linear estimation of the maximum that an electric vehicle may accomplish based on real-time SOC battery estimation [47].
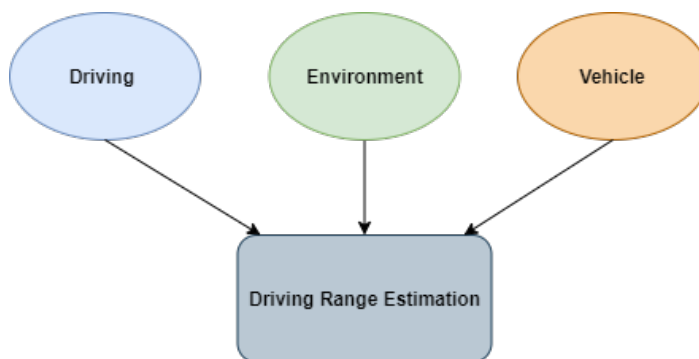
Figure 2.2: Main variables that influence the remaining range estimation

2.5.3   EV design

An electric vehicle's total energy efficiency is linked to the design of the car, which is influenced by many variables including consumer's preferences in the automative industry. These variable includes the capacity of passengers, the vehicle's body type, volume capacity for baggage, wheels, frontal area, type of tyre and type of cooling and heating system. An electric vehicle's design and construction begins with consideration of physical forces following Newton's second law of motion.
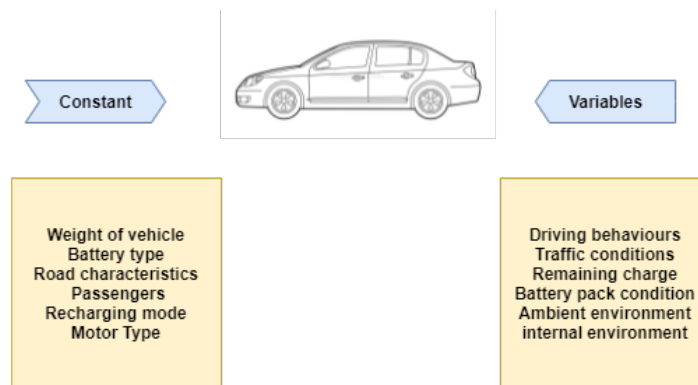
Figure 2.3: Main influential factors on EV energy consumption

2.5.4   Driving behaviour

The impact of drivers on EV energy efficiency when driving the vehicle in real-world traffic may be divided into two categories. First, an EV's energy efficiency is affected by its usage or how aggressive the driving behaviours are. Second, it is mainly related to how the accelerator pedal is used. A study by Mruzek et al. [48] discovered that an EV's range is affected not just by designing factors but also by driving patterns. Real-world driving cycles were used in simulations to evaluate how these variables affect the range of EVs. Four acceleration instances were compared, with the starting condition being the vehicle's continuous departure until it reached 50 km/h after 10, 15, 26, and 36 seconds. There was a difference in the estimated energy consumed by 4% between the quickest and slowest acceleration at the EV's estimated weight of 1000 kg and about 2.7% when the estimated weight of the vehicle is 1500.

The driver's psychology may be considered an influential factor through the impression of the travel distance that the electric vehicle may have reached (range anxiety) [49].

Consumers deliberately avoid critical range circumstances by conserving an extensive range of safety buffers since it has been demonstrated that range and range of anxiety are strongly linked notions (on average, only about 80 per cent of their actual range available). According to Eisel et al. findings [50], experienced EV drivers had substantially lower negative range ratings and range stress than novice EV drivers. As a result, the EV driver's experience directly impacts range anxiety on behavioural, cognitive, emotional levels.

Other influential factors on the energy efficiency of an EV include those linked to how the driver uses the vehicle in various traffic situations (with negligible effect on the energy consumption and efficiency of the battery). These factors include the proper usage of the brake, being harsh to accelerate and decelerate in traffic congestion, usage of auxiliary equipment such as air conditioning and lights. It is very challenging to develop precise algorithms that correctly predict the impact of these variables on an EV's range estimation since the driver's behaviours and the psychological response for each driver is different.

2.5.5   Environment

The EV range is closely related to the external environment, such as ambient temperature, wind speed/direction, and the interior environment, such as temperature in the passenger chamber and auxiliary systems. Additionally, the presence of minimum thermal comfort throughout an EV's operation is a critical requirement for consumers' fast and widespread adoption of this technology. For this reason, EVs must be fitted with proper heating, ventilation and air conditioning systems. The total thermal load of an EV is the sum of the thermal loads generated by the environment, both internal and external. The total thermal load of an EV can be expressed by the following equation:

$$L_{total} = L_{AC} + L_{amb} + L_{rad} + L_{vent} + L_{inh} \tag{2.1}$$

Where L_{total} represents the entire heat gained in the cabin, L_{AC} is the thermal load produced by the AC or heating system, L_{amb} is the ambient temperature load, L_{rad}

is a load of solar radiation, L_{vent} is a load of ventilation, L_{inh} is the interior thermal load for passengers.

Air conditioning and heating systems have been demonstrated in some studies to produce substantial range reductions in hot and cold conditions. For example, under various simulation circumstances, the load of AC showed a reduction of 17-37% in summer, while a load of the heating system reduced the range by 17-54% in cold conditions [51]. Furthermore, considering Nissan Leaf, the impact of the variety of ambient conditions was investigated in [52]. Finally, the author experimented with various industrial driving cycles (NEDC, FUDS and SFUDS) to consider different driving behaviours, such as rural and motorway driving patterns. The findings revealed that the EV's range was extended to 150km when the ambient temperature was at 20°C. Furthermore, the range drops to 85km at 0°C and drops again to 60km at -15°C.

When developing predictive tools, high values of range loss due to this factor must be considered, along with the necessity of further research in this area. In addition, the usage of heating pumps and the correlation between battery thermal management, air conditioning and heating systems in vehicles should also be considered. Additionally, it is feasible to explore utilising energy-independent auxiliary equipment from the EV energy source to generate heating and cooling systems. Furthermore, an independently fuelled air heating system may be utilised to accomplish this idea. However, there is a tradeoff between energy efficiency and weight, simplicity of use, and safety which are regarded as obstacles to consumers' acceptance of EVs.

The battery thermal management directly affects the external environment, either via its operation or by other heat sources. The amount of heat produced by the running battery is proportional to the amount of energy needed by the powertrain. The greater the energy demand, the greater the power transmitted and, as a result, the occurrence of higher temperature in the battery pack. The general conclusion is that limiting a battery pack's operating temperature is essential and leads to an enhanced lifespan [47].

2.5.6 EVs Configuration

EVs are defined broadly to include battery electric cars (BEVs), hybrid electric vehicles (HEVs); plug-in hybrid electric vehicles (PHEVs); and fuel cell electric vehicles (FCEVs). The typical energy flow within EV is shown in Figure 2.4, which is made up of three main subsystems: electric propulsion, energy source, and auxiliary. As shown in Figure 2.5, the electric propulsion subsystem comprises a motor(s), transmission, power converter, and electronic control units. The energy source subsystem is composed of three components: an energy storage unit, an energy management unit, and an energy replenishment unit. In reality, the most often used energy storage technology for EVs is a battery, owing to its high energy density, small size, and dependability [53]. Additionally, an ultracapacitor, flywheel, and hydrogen tank may be used as an auxiliary or hybrid energy source [54, 55]. Finally, the auxiliary subsystem is made up of three components: an auxiliary power supply unit, a power steering unit, and an air conditioning control unit.
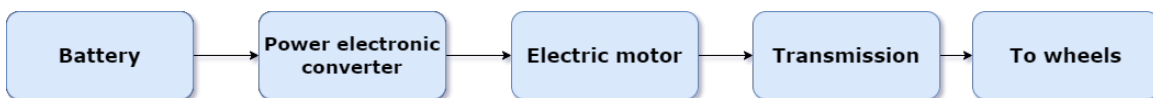
Figure 2.4: The flow of energy within the EV
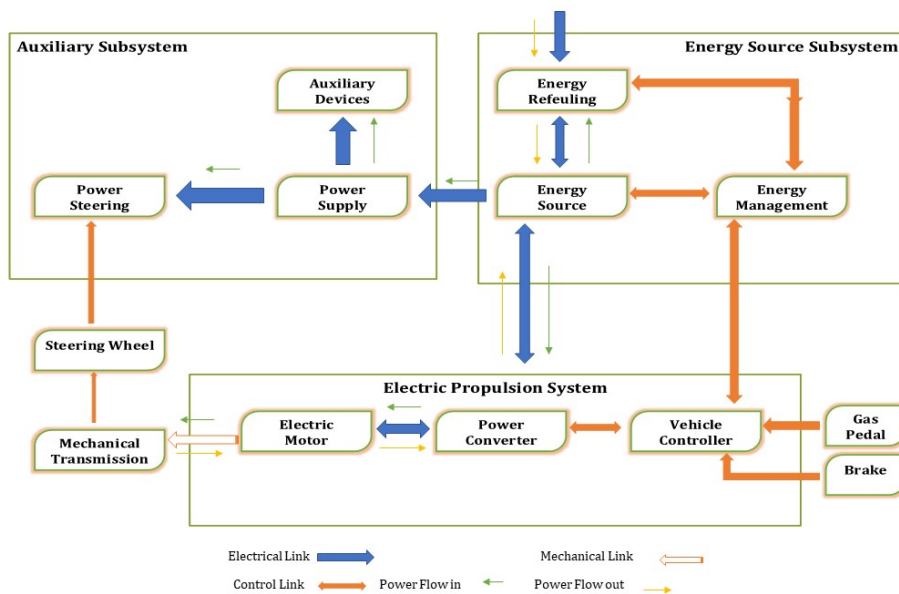
Figure 2.5: The configuration of electric vehicle

2.5.6.1 Regenerative braking and energy consumption

Estimating BEV energy consumption is crucial for environmental sustainability and marketplace acceptance due to restricted charging infrastructure and battery capacity and long charging periods. Energy consumption for BEVs is an integration of the power output measured at the battery's terminals (unit in kWh), with the battery charging and discharging modes handled independently [56].

It is possible to estimate the power output P_{out} (W) when in the propulsion mode. The power output is determined by dividing the tractive power at the wheels P_{wheel} (W) by the powertrain's efficiency, which may take into account the loss of power in the motor drive and gearbox. Traction power at the wheels is calculated as the result of vehicle speed v (m/s) and tractive force at the wheels F_{wheel} (N), which may be estimated as the sum of rolling resistance F_{rr} (N), aerodynamic force F_{ad} (N), road slope force F_{rg} (N), and acceleration force F_{accel} (N).

The battery output power is given as:

$$P_{out} = \frac{P_{wheel}}{\eta_m \eta_t} \tag{2.2}$$

Where η_m and η_t represent the motor and transmission efficiency, The tractive power at the wheel in terms of speed and tractive force is given as: $P_{wheel} = v.F_{wheel}$. The tractive force at the wheel is used to compensate the rolling resistance F_{rr}, aerodynamic force F_{ad}, road gradient F_{rg} and acceleration force F_{accel}, so:

$$F_{wheel} = F_{ad} + F_{rg} + F_{rr} + F_{accel} \tag{2.3}$$

All these forces can be individually defined as:

$$
\begin{aligned}
F_{ad} &= \frac{\rho_\alpha}{2} C_d A_f v^2 \\
F_{rg} &= mg\sin(\alpha) \\
F_{rr} &= C_r mg\cos(\alpha) \\
F_{accel} &= m\delta\frac{dv}{dt}
\end{aligned}
\tag{2.4}
$$

Rolling resistance and aerodynamic drag coefficients are represented by C_r and C_d, m is the mass of the vehicle in (kg), g is the gravitational acceleration, α is the road slope, ρ_a is the air density, A_f is the frontal area of the vehicle and δ is the rotational inertial factor of the vehicle.

Equations 2.3 and 2.4 can be expressed by:

$$
\begin{aligned}
F_{wheel} &= F_{ad} + F_{rg} + F_{rr} + F_{accel} \\
F_{wheel} &= \frac{\rho_a}{2} C_d A_f v^2 = mg\sin() + C_r mg\cos(\alpha) + m\delta\frac{dv}{dt}
\end{aligned}
\tag{2.5}
$$

All the above equations can be rearranged as:

$$
\begin{aligned}
P_{wheel} &= v.F_{wheel} \\
P_{wheel} &= v.\left[\frac{\rho_a}{2} C_d A_f v^2 + mg\sin(\alpha) + C_r mg\cos(\alpha) + m\delta\frac{dv}{dt}\right]
\end{aligned}
\tag{2.6}
$$

Therefore:

$$
P_{out} = \frac{v.\left[\frac{\rho_a}{2} C_d A_f v^2 + mg\sin(\alpha) + C_r mg\cos(a) + m\delta\frac{dv}{dt}\right]}{\eta_m \eta_t}
\tag{2.7}
$$

Battery charging in electric vehicles takes place during coasting and braking. During these modes the kinetic energy of EV is restored and regenerated as electrical power. During regenerative braking, the motor of electric vehicle which drives the vehicle is acting as a generator so it returns the energy back to the battery. The input power at the battery terminal can be defined in terms of output power as:

$$
P_{in} = kP_{out}
$$

So,

$$
P_{in} = k\frac{v}{\eta_m \eta_t}\left[\frac{\rho_a}{2} C_d A_f v^2 + mg\sin(a) + C_r mg\cos(a) + m\delta\frac{dv}{dt}\right]
\tag{2.8}
$$

Where k is the braking factor varies from 0 and 1 and determines how much percentage of overall braking energy is recovered by electric motor. Regenerative braking cannot

alone stop the electric vehicle safely so the friction brake is also connected to the wheels.

The battery energy can be determined from power as:

$$E_{batt} = \int_t^T P_{batt} dt \tag{2.9}$$

But in traction mode

$$P_{batt} = P_{out} \tag{2.10}$$

While in braking mode

$$P_{batt} = P_{in} \tag{2.11}$$

2.5.7 EV energy consumption influential variables

2.5.7.1 Variable classification

Variables linked to vehicle energy consumption may be categorised into four groups: (a) components of the vehicle, (b) vehicle dynamics, (c) traffic, and (d) the environment.

2.5.7.2 EV components variables

Several factors associated with vehicle components control significant propulsion operations components such as the motor, transmission, and energy flow in the auxiliary system and energy storage. For instance, the efficiency of the motor and transmissions determines the proportion of produced energy from the source that may be utilised for propulsion [44, 57–61]. They vary depending on the particular designs of EVs and the motor, and the technology of transmission. In addition, the state-of-charge (SOC) is observed to influence the energy consumption rate in electric vehicles [44, 62–65]. Several studies have shown that the battery SOC may affect the instantaneous efficiency and mechanism of the charging and discharging for the battery; as a result, it is regarded as a key explanatory variable [44, 65]. Other studies have shown that the initial battery SOC may exacerbate or alleviate range anxiety in EV drivers, leading them to alter their driving habits, influencing energy consumption on their vehicles [62, 64]. According to [66], variations in battery quality, for instance, degradation rate, is used

to predict changes in the trip-level energy consumption rate for electric vehicles as they age. Under certain climatic circumstances, the auxiliary power required to support the feed conditioning, radio, monitor panel, and lights is not simple to generate. Therefore, the auxiliary load has been considered constant or approximated based on real-time observed auxiliary load data in many studies [57, 63, 66–69]. The new technologies in modern vehicles such as safety sensors, cameras, and wireless devices may impact energy consumption. In the future, academics and engineers may pay more attention to this subject due to its importance. Studies have also been conducted to directly establish statistical connections between vehicle characteristics (such as the size of the vehicle's engine and its engine technology and the kind and efficiency of its transmission) and energy usage [70]. The coefficients of rolling resistance and aerodynamics are incorporated in models that predict EV energy consumption at each moment of operation according to the principles of physics [71–74].

2.5.7.3 EV dynamics variables

Variables in vehicle dynamics encompass motion-related factors, including speed, acceleration, and tractive or braking torque. These variables directly connect to kinetic energy used by vehicles, and the laws of physics control them. For this reason, the variables are utilised often in electric vehicle energy estimate models. The current literature offers data on vehicle dynamics in many ways, including on an immediate or aggregated basis, for instance, every second, every segment or every trip. Speed is a critical metric for estimating road loads since it is physically linked to aerodynamic drag, rolling resistance and road slope [44, 57, 58, 75]. Furthermore, instantaneous speed correlates significantly with instantaneous electric vehicle energy usage [61, 65, 73, 76–78].

Energy consumption is calculated at the trip level by considering the average speed [62, 79–81] and its higher-rate of speed [82–86]. In addition to speed and acceleration data, researchers have also utilised other indicators to estimate the energy consumption of electric vehicles. Drivers' maximum instantaneous speed and acceleration, for example, were utilised in research [87, 88] to estimate the trip-level energy consumption of electric vehicles. Based on the speed distribution throughout a journey, one

may estimate EV energy consumption by looking at drivers' driving behaviour [39]. Estimating the regenerative braking capability of EVs is based on the speed trajectory profile [89]. As with kinetic energy, the energy used by EVs when in motion is closely linked to the change in kinetic energy.

2.5.7.4 Traffic variables

Traffic signals operation, traffic density levels and types of vehicles on the road may all impact the consumption of EVs as described by Fetene et al.. These factors are considered to predict and validate the dynamics of the vehicles within the route segment or the whole route, therefore improve the energy estimation. The traffic condition variables can be categorised as interval and categorical variables. Trip time such as rush-hours, the day of the month or the week the trip was performed are categorical. Fetene et al. developed a multiple linear regression model using "rush hour" as a dummy variable to determine if a journey occurred during peak times (in the morning or afternoon).

Masikos et al. [63] developed a model based on a general regression neural network [90] using categorical variables to show the journey time during the day, during the week, month, and hour. Their mode findings revealed that those factors were statistically significant in predicting EV energy consumption. They depict traffic conditions as a consequence of a vehicle's dynamics or overall traffic circumstances. For example, idle time and stops ratio over time may indicate the traffic state, denser if the ratio is greater during the travel time. Several studies have shown that this variable is very significant statistically in their EV energy modelling [79, 87, 91, 92]. The creation of indices of congestion, which might be used to measure the energy consumption of EVs, has been attempted. Other studies [79, 93, 94] defined and found importance in the model of a congestion index, dividing the standard deviation by the vehicle's average speed, and they noticed its significance in their model.

2.5.7.5 Environmental variables

Weather conditions and road characteristics are considered to be environmental factors. These factors influence energy consumption on EVs by adding extra loads into the

battery, for instance, AC or heating power. The road gradient [60, 61], road type [62, 65, 95], wind speed and direction [62, 68, 95], humidity and ambient temperature [63, 64], have an impact on the energy consumption to some extent and were considered and examined in these studies. One example of this is how the slope of the road may influence tractive forces required to overcome the resistance of the road gradient. Some of global positioning systems technologies GPS provides real-time road gradient data, and several researches have used it in implementing energy estimation models for EVs at either instantaneous level [58, 59, 67] or a trip level [63, 68, 77, 79, 84, 96, 97] Another variable related to the road characteristics in current research is the road class, for instance, city and motorway roads [62, 65, 95, 98]. Furthermore, to estimate the energy consumption of EVs while driving, road infrastructure characteristics such as traffic signals and speed limit control are considered independent variables that influence the estimation [99].

Ambient temperature and weather humidity are climatic factors that influence the power demand of heating and cooling and the operational efficiency of the EV battery pack. The exact consequences of climatic conditions on power demand are generally difficult to estimate, but as a rule, trip-level models are designed to incorporate certain factors, including the usage of auxiliary power [52, 62, 63, 68, 100]. Sun et al. attempt to analyse the connection between battery performance and climatic factors by monitoring the battery cell thermal effects; however, these variables were not involved in their proposed model. Liu et al. adopted a dummy variable on their model to represent the needs of the light depending on the time of the day, and they found that lighting situation correlates strongly with energy estimation on EVs. In order to assess prospective energy consumption for cooling and heating, humidity and ambient temperature are estimated or calculated depending on the geolocation of the route [43, 52, 77].

2.5.8   *Energy consumption estimation approaches*

The energy efficiency of an EV also tends to vary less from component to component. In addition, Newton's Law was followed to estimate the energy consumption by calculating the tractive power at the EV's wheels, which was assumed to be constant

Table 2.3: Summary of most related papers and the considered factors in the literature for EV energy consumption estimation

Year/Ref	Factors				Data Source
	components	dynamics	traffic	environmental	
2017 [62]	✓	✓	✓	✓	Real world
2017 [77]	✓	✓	✗	✗	Real-world
2017 [82]	✓	✓	✗	✗	Real-world
2017 [86]	✓	✓	✗	✓	Real-world
2017 [97]	✗	✓	✗	✓	Real-world
2017 [102]	✓	✓	✗	✗	Real-world
2017 [77]	✗	✓	✗	✓	Real-world
2018 [67]	✗	✓	✗	✓	Real-world
2018 [103]	✗	✓	✗	✗	Simulation
2018 [104]	✗	✓	✗	✓	Simulation
2018 [80]	✓	✓	✗	✗	Real-world
2018 [83]	✓	✓	✗	✓	Real-world
2018 [87]	✗	✓	✓	✗	Real-world
2018 [105]	✗	✓	✗	✓	Real-world
2018 [95]	✓	✓	✗	✗	Real-world
2018 [106]	✗	✓	✗	✓	Real-world
2019 [64]	✓	✓	✗	✗	Real-world
2019 [107]	✓	✓	✗	✗	Simulation
2019 [108]	✓	✓	✗	✓	Simulation
2019 [109]	✓	✓	✗	✗	Real-wold
2019 [52]	✗	✗	✗	✓	Real-wold
2019 [70]	✓	✗	✗	✗	Real-wold
2019 [66]	✓	✗	✗	✗	Real-wold
2019 [110]	✗	✓	✓	✓	Simulation
2019 [111]	✓	✓	✗	✗	Simulation
2020 [112]	✓	✓	✗	✗	Real-world
2020 [78]	✓	✓	✗	✓	Real-world
2020 [113]	✓	✓	✗	✓	Simulation

for the powertrain efficiency [58, 59, 67]. Another group of researchers implemented EV energy estimation algorithms based on car-following approach and downstream traffic data [57]. In some studies, fuzzy logic [103] was applied to simulate the effect of regenerative braking, while others assumed a direct relationship with the speed of the vehicle [114].

2.5.8.1 Predicting the driving behaviour

A discrete classification system, in which drivers are categorised into various efficiency levels, is one approach to deal with driving behaviours. For example, in studies [115, 116], driving behaviour was classified into ten levels from optimal driver corresponding to 0% to 60% of influence to battery efficiency. If the driver is in the tenth class, then the range prediction is reduced by 60%. The categorisation is based on the driving style such as velocity, acceleration and preferences of using AC and heating systems. However, this technique may not be effective for modelling driver's behaviour in real-world scenarios. Furthermore, the driver category is assumed to be constant and is not a time-dependent variable as other factors such as traffic status may change the driver's response.

A second method is using a data-driven approach to simulate the behaviour of the driver. Bär et al. gathered individualised route preferences by studying the driving behaviours of the observed users, applying an inverse reinforcement learning technique [118]. The model can forecast drivers' preferred routes. However, it does not predict the usage and the effect of the AC and heating systems. This technique does allow for a probability-based route to be planned. This approach, however, incorporates a probabilistic map of the destinations; therefore the chance of reaching any given destination is given. Data-driven approaches have shown high predictive accuracy and ease of use. Therefore, a data-driven energy consumption estimation technique for EVs was developed [119]. Furthermore, this method was produced to address the problem of energy-efficient routing. The proposed model can differentiate between variables that influence energy consumption (such as road features, weather, and altitude variations), making it well-suited to predict energy consumption for any particular route. Cascade of neural networks (NN) and multiple linear regression (MLR) models are used to

create this model. They used MLR model to estimate the energy consumption given multiple predictor factors, whereas NN model is used to forecast MLR model input variables that are unknown.

In contrast with the above method, there are other techniques for simulating the impact of the driver's response on the efficiency of EV usage based on a limited quantity of experimental data. The findings related to driver behaviour's effect on decreasing fuel consumption for an ICE vehicle by creating and implementing a control-based driving style model [120] provide an approach to this.

2.5.8.2 Several factors combination methods

Many factors may be handled concurrently by assigning them to road segments, i.e. splitting the route into multiple chunks. In Google Maps, for instance, this kind of discretisation technique is often employed. In addition, the road network may then be seen as a graph. To help with the range prediction issue, characteristics such as traffic density, temperature, road slope are given to each road segment. An algorithm to process road networks was created to deal with large-scale road networks effectively [121]. Additionally, other authors modified the method to account for negative cycle costs generated by energy recovery, which is unique to EV exploitation circumstances [122]. Another model was developed for remaining range prediction using Markov chains and particle filter [123]. A probability distribution function approximates the range prediction, described as a collection of weighted particles. This model only contains a comprehensive battery model, vehicle dynamics model and electric motor. It considers various sources of uncertainty, such as the unpredictability of the driving profile, noise measurement and inaccuracies in the battery status estimation. A simulation was used to verify the model's accuracy, and the authors claim that the method forecasts the EV's remaining range with an acceptable level of precision and computation. Another approach uses fuzzy c-means clustering method to estimate the battery state-of-function (SOF) [124]. The parameters of SOF specifies the power output capacity of the battery and its ability of transfers to the electric motor. The SOF parameter is highly correlated with the battery's state of charge and may be an indirect parameter for the remaining charge prediction problem. The fuzzy c-means

(FCM) algorithm was used to optimise the fuzzy prediction algorithms considering (SOC, SOH and charge-discharge rate) as the inputs. The average estimate error was about 8.69 per cent, and the authors reported that the prediction method has the benefits of being simple to build, quick to respond, and capable of future accuracy improvement.

Fetene et al. considered real-world driving data, another research analysed EVs' energy consumption rate and driving range and offered insight into the elements that influence energy consumption. Some data for 741 drivers were collected and analysed, including driving characteristics, type of road, driving patterns and weather conditions.

In addition, according to their results, EV energy consumption rates are at 0.183 kW h/km, with a 34% increase in winter driving distance and a 25% drop in summertime distance. Driving speed and acceleration have a nonlinear influence on energy consumption, while season and precipitation levels have a significant linear influence [62].

2.5.8.3 Machine learning approach

The state of charge (SOC) estimation is one of the essential factors that helps to solve an important problems of safety and monitoring for a battery of an electric vehicle. Several studies have been conducted to improve the SOC estimation and energy consumption on EVs considering different approaches. Zahid et al. [125], developed an advanced machine learning algorithm under diversified driving cycles was implemented to estimate the power consumption of an electric vehicle. They have implemented subtractive clustering based on the neuro-fuzzy system that is evaluated and presented through simulation experiments with the aid of vehicle simulator. Some of the inputs in this study include temperature, current, battery thermal effect, cooling air temperature and power demand. The data were collected from 10 different standard driving cycles that have been created for testing purposes. The results from the experiments revealed that their proposed model shows more accurate state of charge estimation than both Elman and neural network techniques when compared to them. In addition, their proposed model shows significant advancement in state of charge estimation under varies driving cycles with high potential to address the drawbacks in existing

methods [125].

Besides, eco-driving reduces the braking energy loss of conventional vehicles and enables the vehicles to reduce the loss of engine mechanical energy. Another research in implementing machine learning with the main focus on real-time range estimation method with no destination knowledge for BEVs conducted by Yavasoglu et al. [126]. They proposed an advanced estimation model based on test data, including dynamic vehicle parameters and environmental factors with road type and driver predictions. Their focus was to predict the remaining range without knowing the future driving profiles and giving ideas on the distance that a car can travel with the amount of energy left. They utilised periodogram and decision tree techniques to estimate driver profile and road type, respectively. The utilised decision tree made an accurate classification of a road type. In addition, they used a machine-learning algorithm to estimate vehicle range based on train data sets through chassis dynamometer tests. For real-world verification, the car is driven 50.4 kilometres on a road with predominantly urban driving characteristics. They established that the outcomes of the real-life evaluation indicate that the proposed technique predicts a range with a lower error than the rated one. Accurate estimation of EVs consumption of power in the future will assist in reducing the range anxiety of users that results from an electric range of EVs, and inadequate charging facilities. Real-world tests indicate that the suggested approach forecasts range with a narrow margin of error and estimates the ultimate remaining capacity 11.3 per cent better than the rated method. [126].

Qi et al. used a machine learning model to estimate the trip energy consumption. They analysed the EV's usage data to estimate the consumption and claimed that this method could be used in a larger EVs fleet in the future. They concluded that the distance of trips, vehicle's velocity, temperature, and the initial SOC influence energy consumption at different levels. Although the effect on energy consumed when the trip distance is changed is stable, they also claimed that the initial SOC does not significantly influence energy consumption [80].

De Cauwer et al. used real-world data to predict energy consumption on EVs. However, their main objective was to detect and quantify the relationship between energy consumption and the vehicle's kinematic parameters and to use the energy consump-

tion data to create consumption models. They used multiple linear regression based on the dynamics equation of the vehicle as a physical base model to establish three models. All three models use a unique level of aggregation that allows predictions to use different input parameters. One of the three models allows prediction with basic available parameters such as temperature, travel time, and distance by using the trip's kinematic parameters. The second model is a little bit advanced as it encompasses detailed acceleration data, while the third model predicts energy consumption using the raw data of the kinematic parameters as input parameters [72].

2.5.8.4 Modelling and measurements approach

A modelling approach was employed by Fiori et al. as they developed a model that can show how electric vehicles consume energy. The authors claimed that the limited driving range is one of the manufacturer's issues they have been trying to overcome in the EVs industry. Thus there is a need to develop a simple and accurate energy consumption model, and it is essential to develop real-time driving and eco-routing to improve the energy efficiency in EVs, hence extend the driving range. Even though they have limited themselves to the existing industrial driving cycles, they developed an energy model that computes instantaneous energy consumption using acceleration, vehicle velocity and road gradient information. In addition, the braking energy regeneration function is implemented in their model [58]. They found that their model can be well used in smartphones, eco-routing, transportation simulation, and eco-driving. Their proposed energy consumption model uses instantaneous variables of a vehicle to compute the regenerative braking efficiency of EVs.

As people agree that the EVs will reduce the dependency on oil and reduce the carbon emissions to the environment, Wu et al. studied the measurement and evaluated the energy consumption rate of electric vehicles. Both the local and federal governments have looked at some of the potential benefits of electric vehicles and allocated funds, and taken regulatory and legislative steps to enhance the deployment and adoption of EVs. This momentum shows a high possibility for EVs to gain excellent market penetration in the future, particularly in highly populated urban centres that experience air quality issues. Soon, people will experience issues concerning the right way to improve

the efficiency of the transport system [59]. They have taken a step to reduce the issue by focusing on the right way to measure and estimate the energy consumption of EVs. Their research first presented a system to collect vehicle driving data and in-use EVs by installing it on the vehicle for research and experiments purposes. The authors collected about five months of electric vehicle data to analyse driver behaviours and EV performance. Furthermore, they argued that the car is more efficient when the driving is more in-city roads than driving on motorways. They have investigated further and found that the driver route selection balances the trade-off between energy consumption and travel time. They claimed that more data is needed to make their findings more generic. However, they emphasised the importance of their study and that their observation could change traffic and transportation in the future concerning EVs. In addition, they have analysed the relationship between EV's acceleration, power demand, vehicle's velocity and road slope [59].

Hu et al.demonstrate that distinct patterns in power consumption exist throughout a route, which is partially related to variations in infrastructure design, traffic situation and individual driving habits. In the future, the suggested technique for evaluating time series data on energy usage along routes may be utilised to research with bigger fleets of EVs [100].

The accurate prediction of electric vehicles' energy consumption is essential in removing the anxiety that drivers experience. Moreover, it is an essential foundation for managing charging infrastructures and spatial planning [77]. Therefore, Wang et al. focused on improving estimation accuracy for electric vehicle's energy consumption by developing a model that considers the impact of ambient temperature.

Their observation of sparse GPS in 68 electric vehicles in Japan, then proposed and verified an energy consumption model through multilevel linear regression and traditional linear regression. Based on the outcomes of their study, their proposed energy consumption model indicates an effective performance of estimation. For a steeper road gradient, the parameters show a higher difference between downhill energy regeneration and uphill energy consumption. They claimed that the relationship between ambient temperature and energy efficiency produced an asymmetrical 'U' shape, and the best energy efficiency occurred at about 17.5 degrees Celsius [77].

In addition, Qi et al. developed a model to estimate and analyse how electric vehicle consumes energy under the real-world traffic situations. The research investigated EV power consumption in Shanghai, China. Their study made use of a database that was collected from 50 EVs. They started by examining the travel patterns of the driver's usage data and analysed the influence of initial SOC, speed, ambient temperature and trip distance on energy consumption. Since traffic conditions, infrastructure design and driving behaviour affect energy consumption; they chose three routes with enough vehicle in-use information as the test objects for the study [80].

Hu et al. investigated the differences in energy use in electric vehicles. They explored how individual driving styles, driving behaviour, infrastructure design, and traffic conditions affect the energy efficiency of electric vehicles. Their tests were done in Beijing road network under a typical driving cycle using Nissan LEAF to understand variations among drivers in different urban traffic situations. The operation parameters and energy consumption were monitored and recorded in both off-peak and peak hours for 13 drivers [100].

The development of a driving cycle was introduced by Brady and O'Mahony to evaluate the economy of electric vehicles in urban areas. They discussed that knowing real-world driving needs in driving cycles is essential in developing efficient energy storage systems and powertrains for electric vehicles. Moreover, driving cycles facilitate the evaluation of the life-cycle and economic costs of vehicle technologies. However, there are deviations in real-world driving conditions and measured driving cycles due to some factors such as inadequate data, inadequate methodologies, and techniques for assessing developed driving cycles [127]. They used real-world data from EVs gathered for more than six months to develop a driving cycle appropriately for the EVs assessment. They used a statistical and stochastic methodology to develop and assess the optimum driving cycle compared to real-world driving cycles data. The used datasets consist of six months velocity versus time record collected in Dublin, Ireland. They used this data to develop a driving cycle considering the same parameters, such as the driving style, road and traffic conditions. They claimed that real-world driving style varies significantly from the industrial driving cycles developed to design EVs in Japan, Europe and the United States. They noticed that the standard driving cycles have

lower velocity rates and higher acceleration in general, making them not the optimal choice to design purposes of EVs. In addition, they emphasised that the driving cycles developed in their study would help in allowing electricity grid economic, analysis and life-cycle studies to be performed with more confidence [127].

Qiu et al. used the past energy consumption rate and variations of electric vehicles to predict energy consumption. They discussed that an electric vehicle should have a data storage module that can keep high energy consumption rates and a controller to calculate the energy consumed depending on the energy across the range. Therefore, the operation of an EV should be configured to respond to the predicted energy consumed [128] .

The adoption of connected and automated vehicle technologies (CAV) can enhance the development of innovative systems and applications that promote the efficiency of vehicles and improve transportation systems. Moreover, Gao et al. [129] present an evaluation of the performance of an electric vehicle performance based on the eco-driving cycles was performed. They presented simulation research on various EVs and compared performance when EV is driven on a real road cycle to when driven on a highly optimised e-driving cycle using CAV technologies. The EVs under their investigation included seven standard delivery trucks, a transit bus, and a compact vehicle.

An estimation model was developed by Xu and Wang of mileage power-based consumption for EVs. Their proposed method was based on prediction and driving cycle identification. First, the driving cycles and their respective energy consumption were categorised through screening, component analysis, fuzzy C clustering, and sectioning. Then, they predicted future car speed curves based on past information, real-time congestion data, and the estimation mileage model and elevation information. Finally, they carried out real-time vehicle tests on the experimental vehicle. As a result, based on ten groups of vehicle testing, the average error between the predicted value of the mileage power consumption and the test value is about 4.15%, and they claimed that it meets the standards for everyday usage of electric cars [87].

Zhu and Gonder used map service API to detect the driving cycles. The authors established that GPS and smartphones have improved studies and surveys in the trans-

portation sector. However, detecting driving cycles from wearable GPS devices has not been well researched. They focused on distinguishing driving cycles from trips of motorists like taking a bus [130]. They claimed that API route data may be obtained using a driving detection approach that uses APIs and a trajectory segmentation algorithm to determine the best potential API route. In addition, a logistic regression machine learning model can be trained with probability methods for car and non-car modes using actual route data and API information [130].

2.6   Conclusion

EV range anxiety may be decreased in the following ways for EV consumers:

- The EV user must understand the EV's technical specifications to assess its energy efficiency.

- Installation of an interactive map on-board that shows the areas that can be covered by the vehicle while travelling.

- Apart from interactive maps, an ideal solution could advise an energy-efficient path and indicate accessible places near the destination if the destination is known. Additionally, if the range of the vehicle is less than the distance to the nearest charging station after reaching the destination, the system should warn the driver and create a new route that includes a stop at a charging station.

Numerous studies are being conducted presently on the prediction of the remaining range for EVs efficiency usage. However, it is worth noting that most of this research examined a limited number of factors that impact the EV range. SOC estimation is given special attention for range prediction, and relatively fewer studies have been conducted to integrate a complex combination of all possible influential variables of the EV's range estimation into a single mathematical model. The current research integrates multiple Maps API to generate representative driving cycles at trip and segment levels in a specific route. Furthermore, it analyses the possible APIs to obtain detailed route information in real-time and adapt it to any road covered by the

map service. In addition, since the instantaneous vehicle's speed is very significant on energy consumption, this thesis aims to obtain the traffic information and route information from several APIs to predict the car's speed along the route. Moreover, it will retrieve the weather data on the selected journey and applies its variables to the energy consumption calculation. Finally, these variables will be integrated with a generic electric vehicle model that includes a lithium-ion battery to generate the power demand for multiple journeys.

3

BATTERY MODELLING FOR ELECTRIC VEHICLES

Contents

Summary

This chapter investigates the dynamics and performance of lithium-ion battery used in Electric Vehicles (EVs). We evaluate the impact of different driving patterns on the energy consumed. The investigation discussed in this chapter was based on a power demand obtained using four different standard driving cycles, representing driving patterns corresponding to different geographical areas and road topology. In our investigation we used an equivalent circuit battery model and a mathematical battery model, which were configured using MATLAB and Simulink. The findings show that the equivalent circuit model emulates the dynamics of the real battery more accurately than the mathematical model, However, both models show almost similar estimation of the battery state-of-charge.

3.1   Introduction

This chapter will explore the battery modelling techniques. In addition it will demonstrate some of the generic battery models. The battery components will be presented along with the battery behaviours. The inputs and the outputs of the batteries will be identified. This chapter will discuss early stage experiments performed to understand the battery behaviours and the influential factors that play a significant role on the SOC estimation and the energy consumption.

In full battery-powered vehicles, the key component is the battery, and it is the only source of power that stores the vehicle's energy. As a result, it requires a significant portion of the vehicle's volume and weight, as well as influencing the vehicle's price [8]. Every electric vehicle now has a rechargeable battery consisting of many cells connected to each other that convert the chemical energy on the battery into electrical energy. Each cell contains positive electrodes and negative electrodes connected by an electrolyte. The chemical reaction between the electrolyte and the electrodes produces the battery current that generates the direct current electricity (DC) on the battery for discharging. The same chemical reaction can happen in reverse while charging the battery to store the energy on it [8]. Numerous forms of battery technology have

been adopted in EVs since their development. However, the majority of major battery types that are widely adopted in EVs are Lithium-ion and nickel metal hydride (NiMH). Presently, the majority of Hybrid Electric Vehicles (HEVs) use nickel metal hydride batteries [131]. Certain HEVs that were produced until 2010, for example the General Motor EV-1, Toyota Prius, Ford Escape and Nissan Altima, utilised Nickel Metal Hydride Batteries due to their mature technology.

Nevertheless, lithium-ion battery has been expanding rapidly since 2010, growing in popularity as a battery technology compared with previous period, particularly for use in EVs. This is largely because of the advantage posed in obtaining higher energy density. The main modern EVs utilising this battery technology are: the Tesla-Roadster; the Daimler Benz Smart EV; the Nissan Leaf EV, as well as the Think EV [132].

3.2 Battery modelling

From complex stochastic models to in-depth electrochemical models, the body of the existing academic research covers numerous forms of battery models. Electrochemical, electrical circuit and mathematical models are three major classifications of battery models that may be distinguished [133].

3.2.1 Electrochemical modelling

The first approach of battery modelling is an electrochemical models, in this approach the batteries may be modelled on the basis of electrochemical process, as proposed in [133] and [9]. The battery's inner electrochemical characteristics can be comprehensively outlined through such models. Two joined partial differential equations (PDES) comprise a standard electrochemcial battery model. The means through which the cell's electrochemical reactions are contributing to and influencing the potential of the cell are illuminated by these equations.

3.2.2 Equivalent circuits modelling

Secondly, a battery's electrical characteristics were initially explored by Hageman [134] through an electrical circuit model commonly adopted in electrical engineering.

Therefore, precise explanations of the battery can be provided through such models. However, the impracticality of the combined model is a problem due to the in-depth explanations provided, meaning that establishing performance models requires an alternative approach [135].

Equivalent-circuit models provide a comprehensible interpretation of battery electrical characteristics. The open-circuit voltage (OCV) is represented by the voltage source U_{oc} and the cell internal resistance is represented by the resistor R_o both common to all models presented in Table 3.1 [5]. However, while the Rint model in 3.1 performs well with continuous-current loads, the addition of the cell internal resistance in parallel (Thevenin and GNL model) increases voltage-prediction accuracy. In addition, as they represent time constants during transients, conferring on the model the expected nonlinear behaviour [136]. Essentially, the networks composed by R_i and C_i are equivalent to the diffusion process [5].

By including the capacitance C_{cap} to the Thevenin model in Table 3.1, which accumulates the discharge current, the Partnership for a New Generation of Vehicle (PNGV) model in Table 3.1 is able to better represent the OCV variation. Furthermore, the General Nonlinear (GNL) model adds on RC branch to the PNGV model, describing the concentration polarisation effect [5]. Overall, the battery dynamics can be satisfyingly represented with one or two RC blocks. With larger numbers of blocks, the increment in accuracy becomes insignificant compared to the increase computational effort [137].

One of the great advantages of equivalent-circuit models is flexibility, as they can be implemented with multiple components in different ways [5]. Furthermore, it is possible to describe how their parameters are influenced by multiple factors such as ambient temperature and inner heat generated in the cell [137].
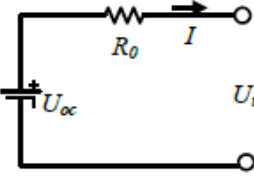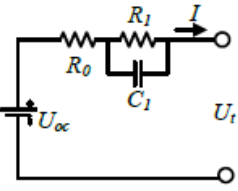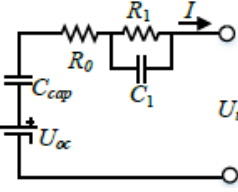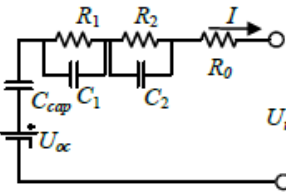
Model	Expression
Rint model [138]	$U_t = U_{0c} - I \cdot R_0$ U_t is the terminal voltage, U_{oc} indicates the OCV. I is the discharging current R_0 is the Ohm resistance.
Thevenin model [139] [140]	$u_t = U_{0c} - U_1 - I \cdot R_0$ R_1 is the polarization resistance and C_1 is the polarization capacitance, U_1 is the voltage of the RC network.
PNGV model [141]	$U_t = U_{0c} - U_{cap} - U_1 - I \cdot R_0$ C_{cap} is the bulk capacitance.
GNL model [142]	$U_t = U_{oc} - U_{cap} - U_1 - U_2 - I \cdot R_0$ R_2, C_2 are the concentration polarization resistance and capacitance.

Table 3.1: The expressions of the four common ECMs [5]

3.2.3 Mathematical modelling

Thirdly, mathematical modelling of batteries may be undertaken. Rakhmatov and Vrudhula [143] have introduce diffusion based model, as well as Manwell and McGowan [144] kinetic battery model (KiBaM), are examples of this approach, where the crucial battery characteristics and impacts are assessed through an abstract model. Little practical understanding of the battery is required, while application and incorporation of other models is possible, when utilising the KiBaM [10] and other sophisticated analytical models. Another example of incorporated model introduced by Oliva et al.

[123], which simulates battery load, and combined it with this type of model.

Consequently the defined load patterns can be used to determine the probability of the depletion of the battery through the combined model. The KiBaM battery model has been adopted in order to explore the manner in which the model captures the battery degradation, as well as to comprehend how the battery's efficiency evolves during the battery's life cycle [145].

This investigation was extended in [11] to assess and quantify the risk of premature battery depletion. Despite sound results being achieved while using the KiBaM or its variations for modelling lithium-ion batteries, this model is affected by significant limitations that remain unresolved. Firstly, the Kinetic battery model does not consider how the battery degrades, so it is uncertain how the parameters are affected. Battery wear-out, which is a trend of decreasing capacity over time, should be factored into the KiBaM model [133].

The basic mathematical models aim to describe the terminal voltage of the battery in terms of the state of charge (SOC) and the current [136]. They are simplified representations of electrochemical models; therefore, although estimation accuracy is compromised in a certain level, they require lower computing power [5].

Table 3.2 presents three well-known empirical models and their equations, in which k is the time index, y_k is the terminal voltage, E_o is the open-circuit voltage (OCV) for a fully-charged cell, R is the cell internal resistance, i_k is the output current, z_k is the state of charge (SOC), and K_i is a constant for curve fitting [136], [5].

Model Type	Model Equations
Shepherd [146]	$y_k = E_0 - R \cdot i_k - \frac{K_1}{z_k}$
Unnewehr universal model [147] [5]	$y_k = E_0 - R \cdot i_k - K_1 \cdot z_k$
Nernst model [148]	$y_k = E_0 - R \cdot i_k - K_2 \cdot \ln(z_k) + K_3 \cdot \ln(1 - z_k)$

Table 3.2: Generic mathematical models

3.2.4 Comparative analysis

The electrochemical models describe in detail the battery internal dynamics, presenting an appropriate approach for cell design [149]. Due to the complexity of their equa-

tions, they offer high estimation accuracy but are computationally expensive, time-consuming and, therefore, unsuitable for real-time applications [137]. Mathematical and equivalent-circuit models consist of simpler, more comprehensible representations of the electrochemical modes. As mentioned in the previous sections, the simplicity of their equations provide an increase in computational efficiency but also incurs lower estimation accuracy [5]. The pros and cons of the different modelling approaches are illustrated in Figure 3.1. Also Figure 3.2 shows the connection of different modelling approaches.

Modeling Methods	Empirical Model	Equivalent Circuit Model	Electrochemical Model
Modeling expression	$U_t = f(U_{oc}, SOC, I)$	$U_t = f(U_{oc}(SOC), I, R, C)$	$U_t = n \cdot f_{PDEs}$
Pros	Simple expression, computational efficiency	Easily understood, widely used in SOC estimation	High accuracy of voltage calculation
Cons	Limited capability of describing the terminal voltage	Complex parameter identification process	Require prior knowledge of the battery, time consuming

Figure 3.1: Pros and cons of battery modelling approaches
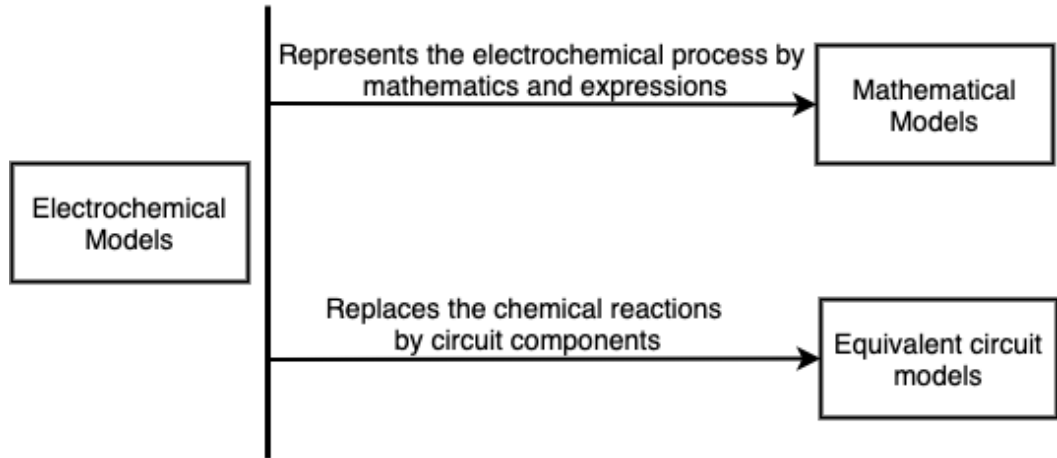
Figure 3.2: The connection of different modelling techniques

3.3 Battery state estimation

Primarily, there are two main types of estimation for battery state: state-of-charge and state-of-health. In addition, the most commonly used methods to estimate the

battery state are column counting, voltage, and the Kalman filter method. All of these approaches apply to all battery systems.

3.3.1 State-of-charge estimation

The state-of-charge estimation know as SOC is a technique of capturing the remaining level of the battery during the battery discharging process.

- **Coulomb Counting method**: Also known as ampere hour counting and current integration, is the most common technique for calculating the SOC. The integration of the current over time is known as the Coulombic counting method [150].

- **Voltage Method**: The SOC of a battery is its remaining capacity. It can be calculated using a discharging test under unknown measuring conditions. The voltage method uses the battery's voltage vs state-of-charge (SOC) curve to convert the voltage reading to a state-of-charge value. Nevertheless, the battery current influences the voltage more significantly. Mainly because of the electrochemical kinetics and temperature of the battery. This method can be more accurate by considering lookup tables of the battery open-circuit voltage vs temperature. However, this method is challenging because the battery voltage range is unstable. Moreover, the discharging tests include continuous recharging, which makes the task very time-consuming [150].

- **Kalman Filter Method**:

  To estimate the SOC Kalman filter is another algorithm that estimates any dynamic system's inner state; this method can also be used to estimate the SOC of the battery. Compared to other estimation approaches, the Kalman filter automatically provides dynamic error bounds on its state estimates. By modelling the battery system to include the wanted unknown quantities (such as SOC) in its state description, the Kalman filter estimates their values and gives error bounds on the estimates. It then becomes a model-based state estimation technique that employs an error correction mechanism to provide real-time predictions of the

SOC. It can be extended to increase the capability of real-time SOH estimation using the extended Kalman filter. Notably, the extended Kalman filter is applied when the battery system is nonlinear, and a linearisation step is needed. Although Kalman filtering is an online and dynamic method, it needs a suitable model for the battery and precise identification of its parameters. It also needs a large computing capacity and an accurate initialisation.[150].

3.3.2 State-of-health estimation

Compared to a new battery, the State of Health is a measurement that indicates how well a battery is performing in general and its capacity to provide the desired performance. In addition to charge acceptance, internal resistance, voltage, and self-discharge, it takes into consideration other variables as well. When it comes to the long-term capabilities of the battery, it provides an indication rather than an exact assessment, of how much of the battery's potential lifetime energy throughput has been used and how much is remaining.

3.4 Experiments set-up for existing models

Several experiments have been performed with some existing models using standard driving cycles to estimate the SOC. These experiments have been published in 2019.

In order to undertake these experiments, we have selected two different battery models to investigate their performance based on the demand we generated.

3.4.1 Battery models

The experiment of this chapter used MATLAB for the driving cycle power demand calculations, and SIMULINK for the two existing models that simulated the lithium-ion battery. In order to investigate the impact of the driving cycles on EV's battery, several assumptions have been made:

- The temperature dependency is not considered in the first model and ignored in the second model.

- The battery self-discharge phenomenon is not implemented.

- Gain blocks in SIMULINK are used to modify the number of cells in parallel/series to simulate the battery pack characteristics in EVs.

- Regenerative breaking, which provides energy restoration to the battery, is not considered.

3.4.1.1 Shepherd's Model

Shepherd's model is a mathematical representation of the battery's components such as internal resistance, open circuit voltage, terminal voltage and the state of charge [136]. The general Shepherd's Equation is given as

$$u_k = E_0 - RI_k - \frac{\mu}{SOC_k} \tag{3.1}$$

where k is a time index, u_k is the model voltage, E_0 is a DC gain, R is the cell internal resistance, I_k is the cell current and μ is a constant used for fitting the curve.

3.4.1.2 The Equivalent Circuit Model

The Equivalent Circuit model is a very common solution for battery modelling. It works by simulating the battery's electrical components such as resistor, capacitors and voltage sources [151, 152].

This modelling technique can be easily parameterised in such a way that when the battery block is stimulated, it responds as a real battery. This process relies on creating a model correlation with the experimental data [153]. In this paper, a battery model was obtained from [154] which is an EC model. It can be represented by modelling the terminal voltage of the battery as an open circuit. The battery terminal voltage of the model is given by:

$$U = OCV - U_S - U_0 \tag{3.2}$$

where OCV is the open circuit voltage, U_S is the transient response voltage and U_0 is the voltage drop over the internal resistance.

U_S can be obtained from the following equation.

$$\frac{dU_S}{dt} = \frac{-1}{R_S C_S} U_S + \frac{1}{C_S} I \tag{3.3}$$

and

$$U_0 = R_0 I \tag{3.4}$$

The State Of Charge (SOC) of the battery refers to the amount of energy in the battery compared to its nominal capacity. There are several methods to estimate the SOC. The method used to estimate the SOC in both models mentioned above is known as Coulomb counting. The Coulomb counting algorithm works by measuring the current while the battery is discharging, then it integrates it over time:

$$SOC(t) = SOC(0) - \frac{1}{Q} \int_0^t I(t) dt \tag{3.5}$$

where Q is some constant to relate the current with charges. The amount $SOC(t)$ is an estimate of energy consumed based on the open circuit voltage of the battery.

3.4.2 Extracting the power profiles

This section presents the method applied to generate the power demand from the available driving cycles. Velocity and acceleration data from the existing driving cycles were used to generate the power demand for each cycle. The power consumed by the EV is based on the mechanical energy generated during the journey, which is directly influenced by the driving patterns of the vehicle. In EVs, this energy will then transfer through the electric drive as the load on the battery. To calculate the power of the driving cycle, we have to convert the speed into metres per second instead of kilometres per hour. Then find the acceleration at each point to define the initial parameters derived from each driving cycle using the following formula:

$$a = \Delta_v / \Delta_t = (v_f - v_i)/(t_f - t_i) \tag{3.6}$$

Where a is the acceleration of the vehicle at every second of the cycle in mps, v_f is the final velocity of the journey, v_i is the initial velocity, t_f is the ending time of the journey and t_i is the starting time.
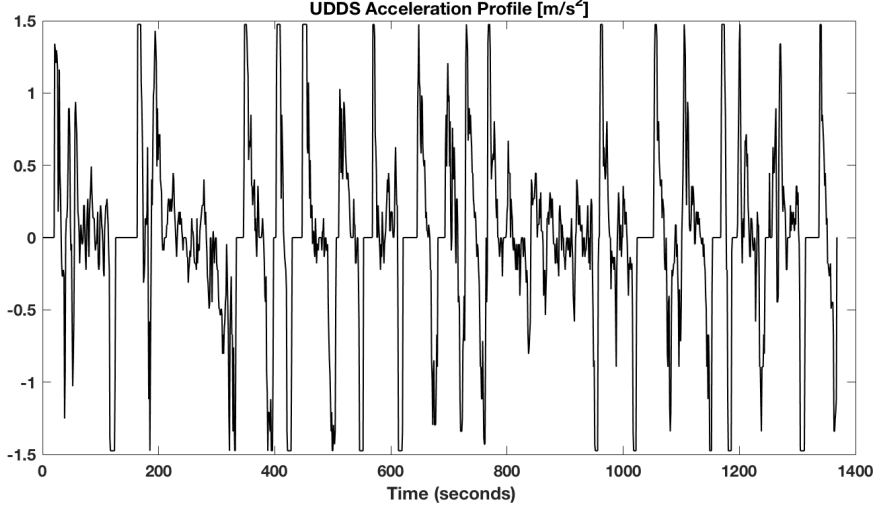
Figure 3.3: Acceleration of the EV for UDDS driving cycle

Note that acceleration and speed of the vehicle are known at every single point of the driving cycle. We can now express the input parameters in MATLAB and use them to calculate the propulsion force required for the vehicle to move, which we do as follows:

$$F_t = f_m M \alpha + M g C_{rr} \cos \theta + \frac{1}{2} \rho A C_d (V - V_w)^2 + M g \sin \theta \qquad (3.7)$$

where f_m is the mass factor, M is the vehicle mass in kg, C_{rr} is the coefficient of rolling friction between the road surface and the vehicle's tires, ρ is the air density, A is the frontal area of the vehicle expressed m^2, C_d is the air drag coefficient, v_w is the speed of the wind in the moving direction of the vehicle, g is the acceleration due to gravity and θ is the road elevation or angle, which is positive for going uphill, negative for going downhill and 0 on a flat road, as it is assumed to be in this experiment.

The total power P needed to drive the vehicle at speed V is as follows:

$$P = F_t V =$$

$$P = f_m M \alpha V + M g C_{rr} V \cos \theta + \frac{1}{2} \rho A C_d V (V - V_w)^2 + M g V \sin \theta \qquad (3.8)$$

In order to use the above equations, some input parameters of the EV that affect the propulsion power in Table 3.3 should be defined. In addition, this will enable us to estimate the battery dynamics of EVs using any battery model. Some input parameters are needed from the below table to generate the power needed for each cycle. These particular values were selected from previous experiments in the literature, as mentioned in [52] and [131].

Table 3.3: The static parameters from typical vehicle used to generate the power profile

Mass	1,360 kg
Mass Factor	1.05
Coefficient of rolling resistance	0.02
Air density	1.225 kg/m^3
Frontal area of the vehicle	$2m^2$
Air drag coefficient	0.5

3.4.3 Standard driving cycles

Driving cycles have been developed in recent decades as a standard tool for estimating fuel consumption and air pollution from vehicles by measuring the emissions for a certain journey profile [155]. There are many standard international driving cycles such as NYCC, UDDS, HWFET and FTP-75, which have been used to generate the power demand profile of an EV in this chapter. A driving cycle is a series of points of velocity versus time plots reflecting the driving pattern of the vehicle and the driver under given conditions. Figure 3.4 illustrates the Urban Dynamometer Driving Schedule (UDDS) driving cycle. Moreover, New York City cycle (NYCC), Federal Test Procedure (FTP-75) and Highway Fuel Economy Test (HWFET) were also used in this chapter. Creating driving cycles requires several set-ups and arrangements, so it can be a relatively costly task [156]. The driving cycles analysed in this article were selected to cover most of the typical driving modes and distances that can be obtained by drivers. That includes short distances which can occur in small cities, frequent stops that are common in urban areas, urban driving with high acceleration phase and motorway cycle.

The driving cycles used in this chapter are as follows:
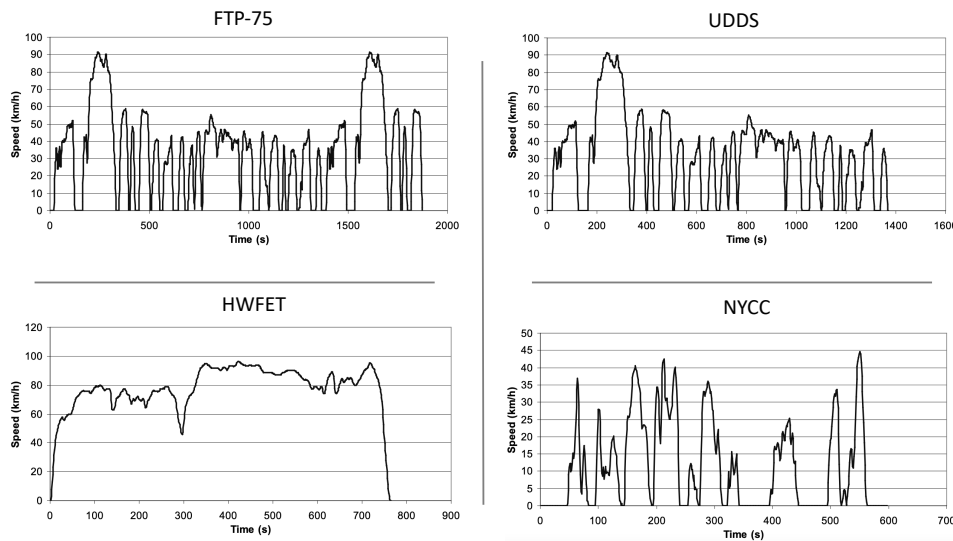
Figure 3.4: Velocity profile for all selected driving cycles

- Urban Dynamometer Driving Schedule (UDDS), simulates an urban route with a distance of 12.07 km with several stops. A sample of the driving cycle is depicted in Figure 3.4 for UDDS. It has a maximum velocity of 91.25 km/hour and 31.5 km/hour average velocity [157].

- New York City Cycle (NYCC) is a driving test performed for light-duty vehicles which simulates the vehicle dynamics at low speed in urban driving with multiple stops. This driving cycle has a short distance of 1.89 km with an average speed of 11.4 km/hour and the maximum speed of 44.6 km/hour [158].

- Federal Test Procedure (FTP-75) is derived from the UDDS by adding a third phase of 505 seconds. The distance travelled by this cycle is 17.77 km with an average speed of 34.12 km/hour and the maximum speed of 91.25 km/hour [159].

- Highway Fuel Economy Test (HWFET) is a driving cycle performed by the US EPA to measure the fuel consumption of light-duty vehicles. This cycle has total distance of 16.45 km, with the average speed of 77.7 km/hour in a total time of 765 seconds [160].

3.5 Battery discharge

3.5.1 Driving cycle load based

This section investigates the impact of each driving cycle used on the battery's discharging current, voltage measured and the SOC prediction. The driving cycles have been developed over various time limits, which means every driving cycle has a different distance travelled. They have therefore been implemented repeatedly for one

hour as a single journey, regardless of how many times they are repeated. The power profiles extracted from the driving cycles will be used as a power demand for the EV to investigate the battery discharging behaviour.
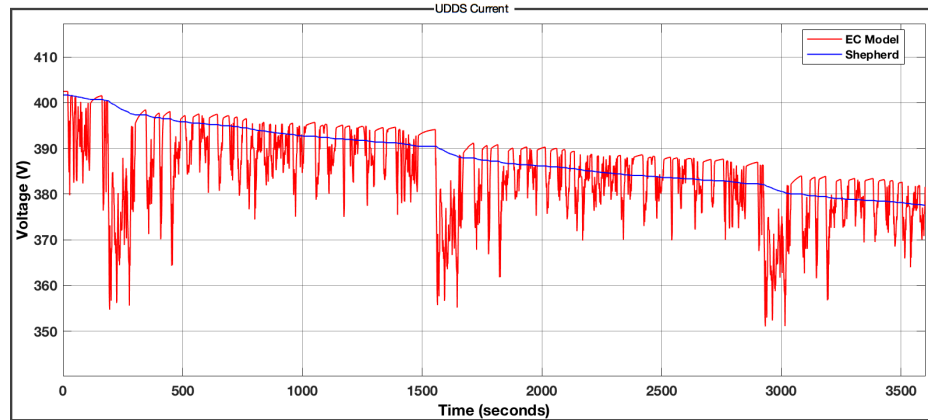
Figure 3.5: UDDS driving cycle voltage profiles
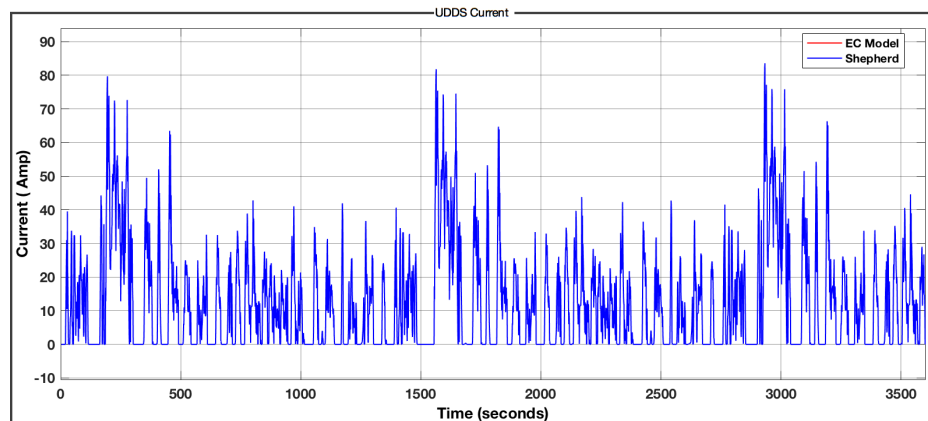
Figure 3.6: UDDS driving cycle current profile
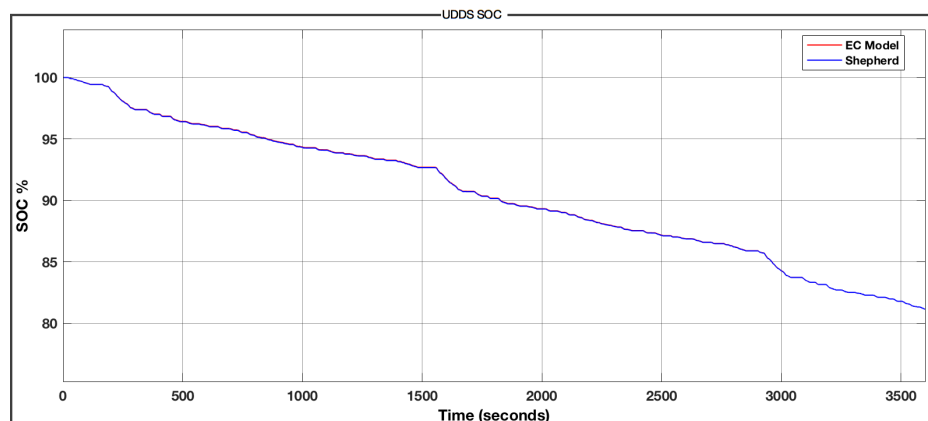
Figure 3.7: UDDS driving cycle state-of-charge

The first phase of the experiment was obtained using UDDS driving cycle parameters, followed by power demand calculations to measure the energy consumption for both models according to this driving cycle. The parameters were set for a typical journey as mentioned in Table 3.3, which shows the fixed parameters for the power calculations. We confirmed that the parameters of the driving cycles had been obtained correctly after validating the acceleration and velocity profiles. These profiles show that the speed is converted from the original speed of the UDDS. The discharge current of the UDDS shows 80 Amp as the highest discharge rate due to the acceleration attained at the beginning of this cycle. The voltage drop for the EEC model during the acceleration time is also noted with realistic voltage dynamics as in Figure 3.5 whereas, the Shepherd's model did not capture the voltage dynamics accurately. The SOC of the UDDS profile shows almost 18.4% of energy consumed, which was similar in both models due to the same method being used to estimate the state of charge as shown in Figure 3.7.
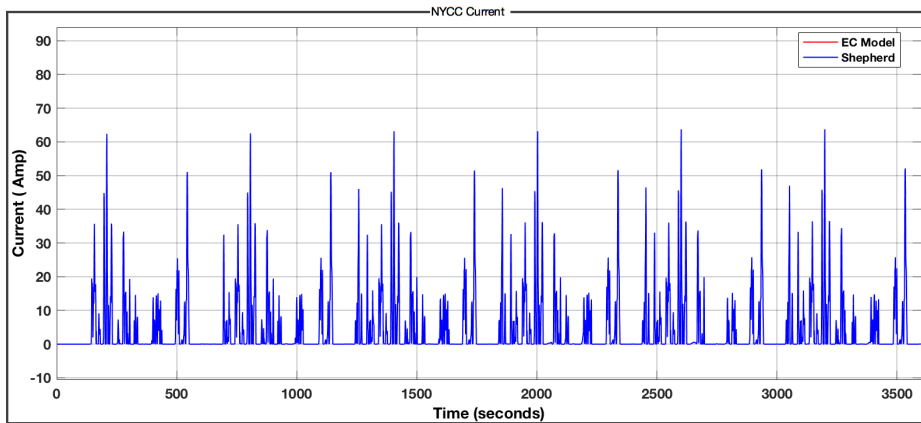
Figure 3.8: NYCC driving cycle current profile
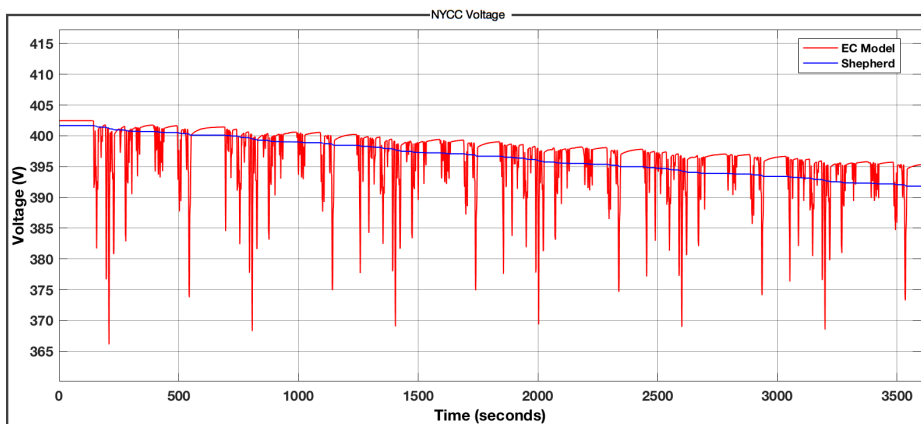
Figure 3.9: NYCC driving cycle voltage profile
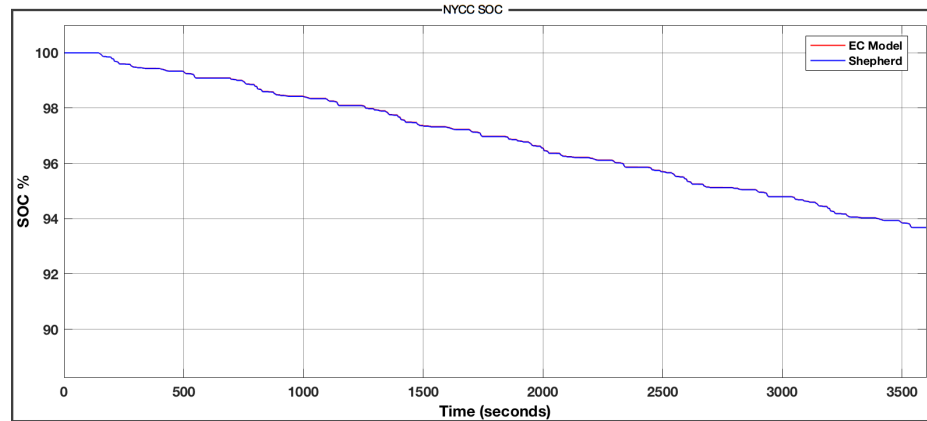
Figure 3.10: NYCC driving cycle state-of-charge

The second phase of this experiment is for the NYCC driving cycle. The same procedures were implemented in this cycle as for UDDS, in order to produce the power demand profile and to test the impact on the EV's battery.

This cycle shows a discharging current rate of almost 62 Amp and less significant voltage drop as shown in Figures 3.8 and 3.9, compared to the UDDS cycle. This is due to the city driving patterns with the frequent stops and the lower speed limits.

The SOC prediction for this profile is around 6.3% from the initial capacity for both models as in Figure 3.10. However, the frequent stops can be noticed as it works as a rest time for the battery where the battery can recover.

City driving, with lower speed limits and frequent stops could potentially increase the battery's life span for a single charge if the road topology is flat and the weather conditions are normal. Shepherd's model did not capture the voltage dynamics again due to the rapid changes in the load of this driving cycle. Compared to this cycle during the portion of time in which there are no pauses, Shepherd's model demonstrates better performance in terms of its ability to capture the battery dynamics throughout the UDDS driving cycle load.
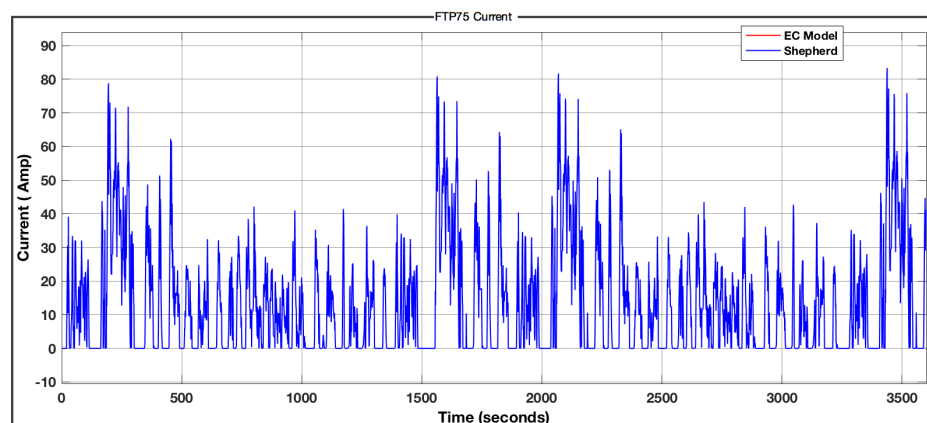
Figure 3.11: FTP-75 driving cycle current profile

- 57 -
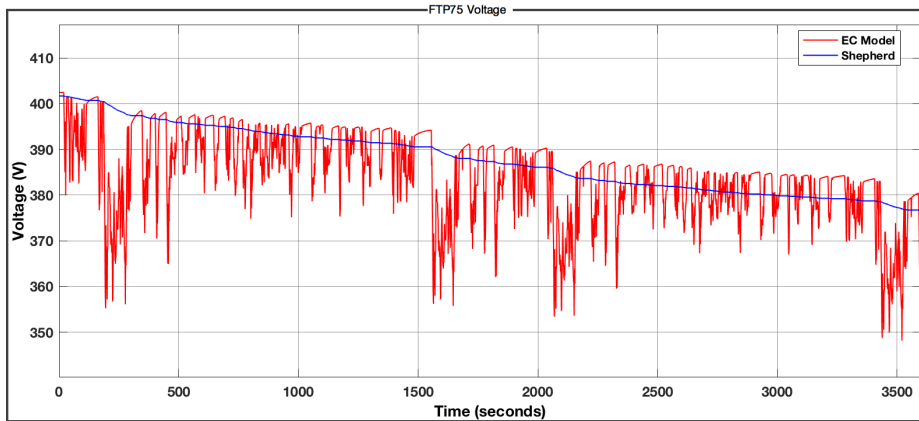
Figure 3.12: FTP-75 driving cycle voltage profile
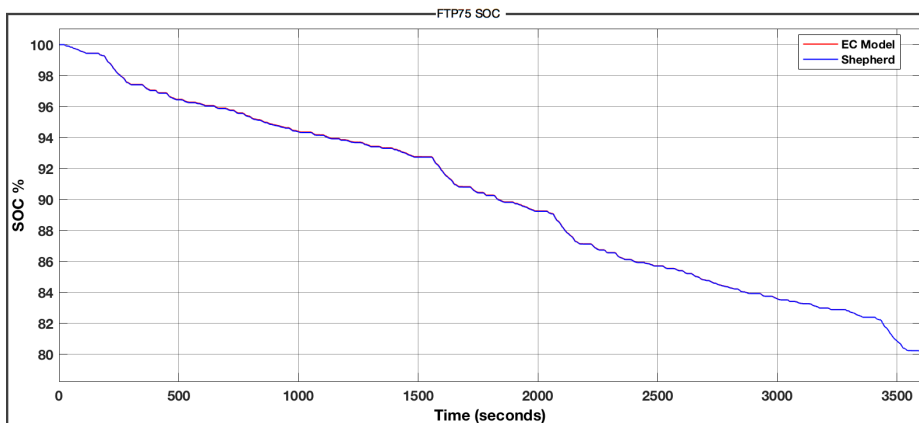
Figure 3.13: FTP-75 driving cycle state-of-charge

In this phase, the FTP-75 driving cycle was considered; this shares some of the characteristics with the UDDS.

This experiment shows almost the same discharging current rate as in the UDDS for both models because of the added phase of this cycle matches the first 505 seconds in the UDDS cycle. The energy consumed is almost 19.7% of the initial capacity. This makes a difference in the SOC prediction of only 1.3% compared to the UDDS and this is because the time scale of 1 hour while the UDDS and FTP-75 profiles are long compared to the other cycle profiles used in this paper.

The dynamics of the FTP-75's current and voltage profiles are very similar to those of the UDDS. However, the effect of the additional period added to the FTP-75 cycle can be seen in how the voltage behaves in the EC model, as shown in Figure 3.12.
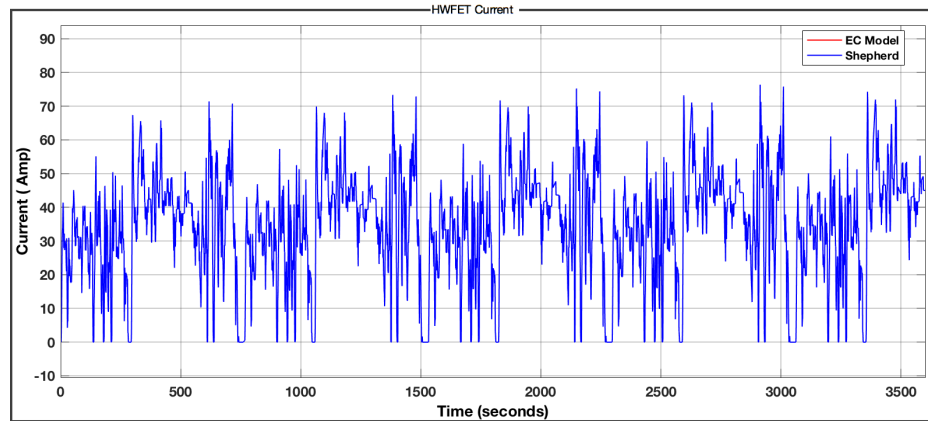
Figure 3.14: HWFET driving cycle current profile
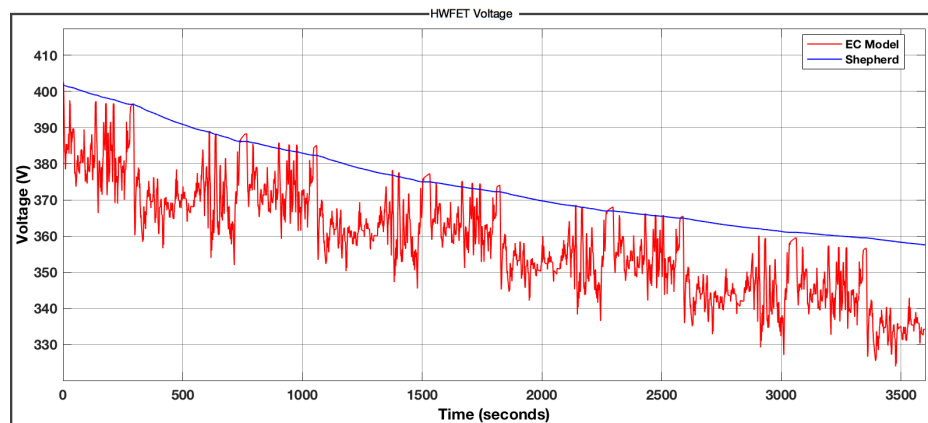
Figure 3.15: HWFET driving cycle voltage profile
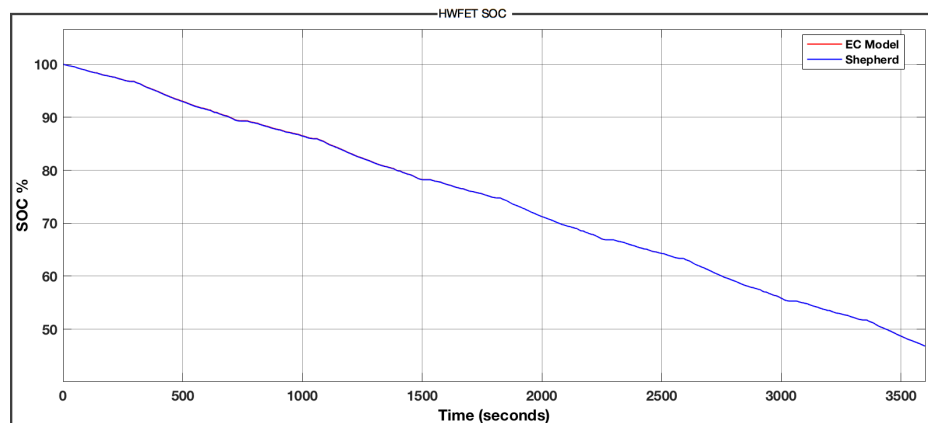
Figure 3.16: HWFET driving cycle state-of-charge

The last phase considers the power profile of the HWFET cycle, which is obtained for motorway driving. In this cycle no stops were performed during the entire journey, except at the end of each cycle before we repeated it. The maximum speed of this journey was almost 90 km/hour, however the maximum current rate was almost 75Amp

and this is because there was no excessively high acceleration during this cycle. The voltage dropped at a lower rate compared to the other cycles due to the energy consumed from the battery which was in this journey profile almost 54% for both models as shown in Figure 3.16.
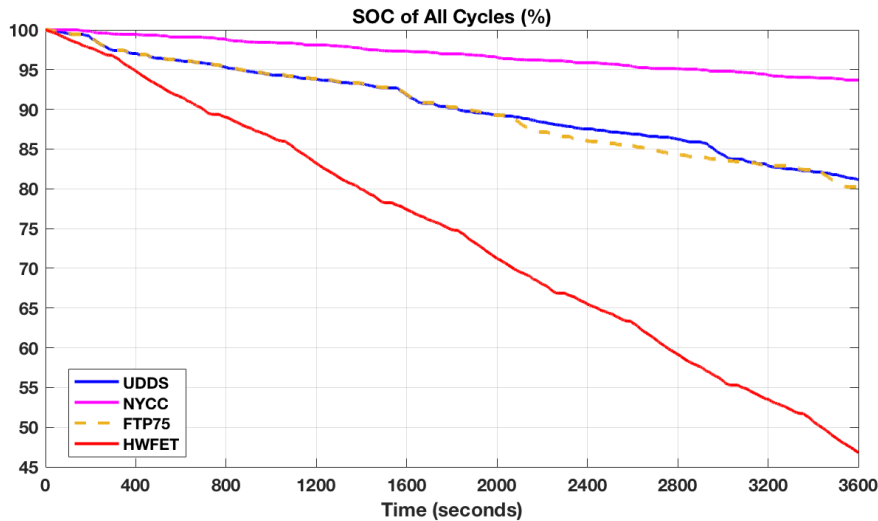
Figure 3.17: state-of-charge for all cycles

Figure 3.17 shows the energy consumption for the cycles used in this experiment. The impact of the NYCC city driving can be seen in the SOC for this cycle, which is very small compared to the other three cycles. The UDDS cycle is considered to be an urban test; however, it has a higher speed than the NYCC. Therefore, it involves quite high and sudden acceleration, which can consume high energy. Since both the UDDS and FTP-75 share the same characteristics, similarity in the battery state of charge can be seen, but when the difference accrues we can see that the SOC of FTP-75 drops more than that of the UDDS. In the HWFET SOC, it is noticed that motorway driving consumes a huge amount of energy compared to city and urban driving, where the stops provide a rest time for the battery to recover.

3.6 Conclusion

This chapter presents power profiles for four standard driving cycles. It processes the driving cycle data, which consists of velocity versus time, in order to find the parameters to calculate the power profile for each cycle. The power profiles were generated to show the differences in the SOC when the traffic conditions influence the driving patterns. Each profile were used as power inputs for two generic battery models, namely the Equivalent Circuit model and the Shepherd's mathematical model. These models were configured using MATLAB scripts and SIMULINK blocks to estimate the SOC and capture the voltage and current dynamics of the battery. Some adjustments have been made to the models to represent the battery pack for EVs by replicating the number of cells in series and in parallel. The models were explained in detail along

with their limitations. The results of the simulation, SOC estimation and the voltage measurement were discussed and analysed.

The SOC prediction of the experiments were varied depending on the cycle profile. For instance, the city driving NYCC cycle shows less energy consumption due to the continuous stops, low speed and less excessive acceleration, which can be classified as efficient driving patterns, whereas the UDDS and FTP-75 cycles show a drop in the SOC at the beginning of the journey due to the high acceleration.

Since the data provided from the driving cycles is only velocity and time, the generated power profile would not be exactly the same as in real life. This limitation could lead to inaccuracy, especially if we consider other factors that could potentially affect the power profile such as the traffic density on the road, the road elevation or weather conditions.

These experiments could be validated using the same power profile as an input to lithium-ion battery in the lab to estimate the SOC and the battery dynamics. It also can be extended by using more recent driving cycles provided by the battery manufacturers or by combining two or more driving cycles to represent a more detailed journey.

Generating a power demand profile using some existing traffic data and map services such as Google maps, Here maps or open street map could be considered. This will simulate the driving cycle based on the traffic conditions and road topology for a given origin and destination, which will help to produce a journey profile for a specific route. This would capture the sequences of a real-time journey, which could be converted to power, thus providing a more realistic driving cycle to estimate the performance of the EV battery.

- 62 -

4

DRIVING CYCLE CONSTRUCTION BASED ON MAP DATA API

Contents

Summary

This chapter introduces a velocity model based on route information for the range estimation of electric vehicles. It uses publicly available data sets obtained from several map services APIs and incorporates this data in the range estimation algorithm. Three map services APIs were used to collect the data for an extended period, and then we analysed this data to extract the most representative data to generate the velocity profiles. It uses MATLAB code and python libraries to process the representative data and apply the velocity model. Moreover, we have integrated it into an electric vehicle model, including the battery, to estimate the power demand for each trip and the remaining driving range. We observed that producing realistic driving cycles using public data is possible; furthermore, it simulates the driving patterns and satisfies the constraints of the vehicle.

4.1   Introduction

In addition to the enormous advantage of reducing the levels of pollution EVs have, this invention has some other benefits over conventional vehicles. These benefits include energy recovery when the battery restores some of the energy due to braking and the noise-freeness [161]. Regenerative braking is a crucial characteristic of EVs when the generator returns the energy to the battery system due to braking. According to previous studies, this feature is practical, especially in city driving and the daily commute. However, it is less effective on motorways, and long journeys [162]. In addition, conventional vehicles consume more energy in city driving because of the heat loss due to braking in contrast with EVs [59].

This chapter aims to develop a velocity model using publicly available routing data on specific routes. It attempts to construct the speed profile for a specific journey between origin and destination using the map API. After generating the potential realistic driving profile, we used a generic EV model to generate the potential power demand for the trip. Hence we apply the state of charge estimation method to analyse the impact of the route and traffic on the battery efficiency. This chapter concentrates on developing a data collection process using multiple maps service API. Many drivers rely on the GPS data provided by map services to navigate to their destinations [130]. This chapter uses the data collected from the drivers using the map API. The first step of this chapter involves exploring the routing information and using it to estimate energy consumption and improve the battery-powered vehicles' efficiency. It explores the data of three different map information providers through their API. Google Maps API [163], HERE Maps API [164], and TomTom Maps API [165] are the primary data sources in this chapter.

The amount of data collected from vehicles and drivers can significantly improve the range of electric vehicles [166]. The battery management system (BMS) installed in electric vehicles senses the battery's state of charge. It predicts the remaining range based on the battery status and other data installed on the system, such as the vehicles'

specifications. However, these data sets do not consider the route information ahead. Therefore, it uses the range values for its estimation. The proper use of the available data can improve driving range prediction and energy consumption estimation. In this chapter we construct near to real-time velocity profiles to allow us to generate power profiles and estimate the power consumption before performing the journey.

4.2   Route information

Many factors influence the energy consumption of EVs including road characteristics, topography information, traffic lights, roundabout, change in speed and road gradient. The information of the route needs to be obtained from different sources, hence, the energy consumption of the EV can be estimated. In this chapter, we will obtain similar data from different API sources, Google Map, HERE Map and Tom-Tom map. The data can be accessed manually by breaking the route into smaller chunks to get the most accurate data possible.

These three APIs allow developers to obtain the journey profile between two points, selecting different travel modes. In this case, we set the travel mode to (CAR) and send a query to get the average time taken between the origin and destination in regular traffic. In addition, it provides the distance in metres between these points and the time of the journey considering the real-time traffic situation. This approach was implemented to understand the route information and to study its feasibility for estimating the energy consumption of electric vehicles. Figures 4.1 and 4.2 show the selected routes, and the route selection will be justified in the forthcoming section.
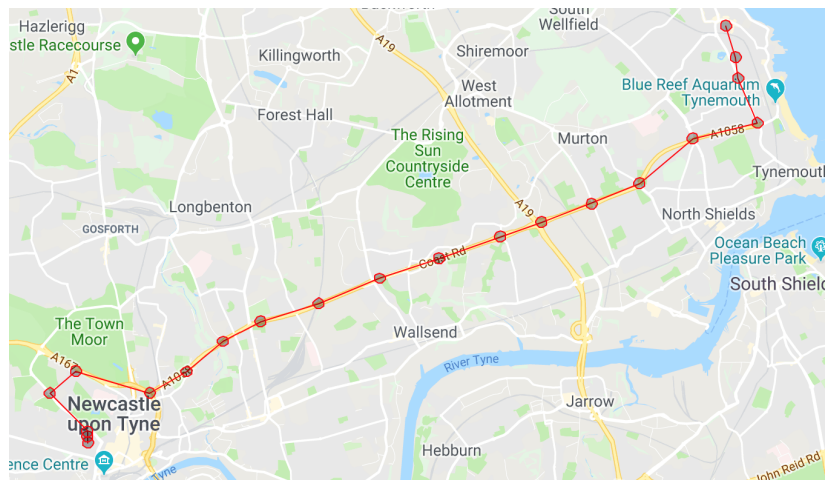
Figure 4.1: The first Route on the map with the way-points selected
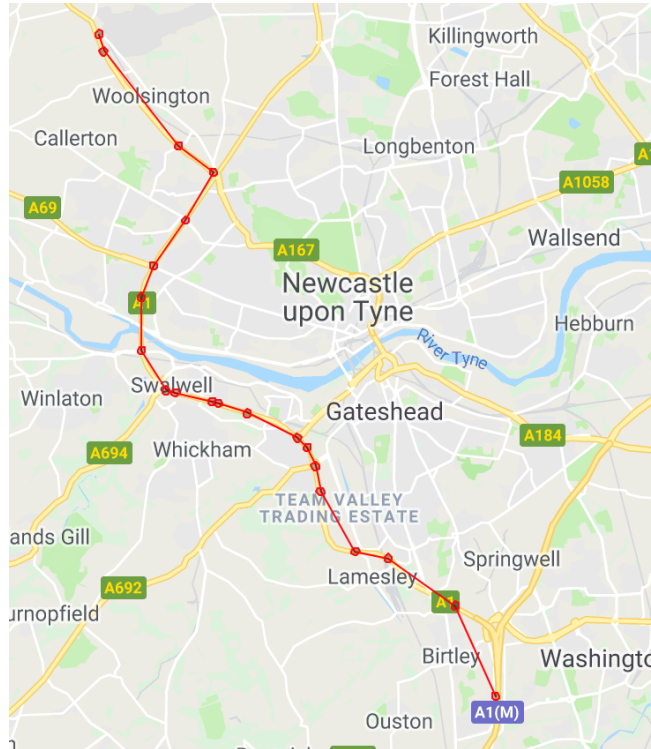
Figure 4.2: The second Route on the map with the way-points selected

4.3 Data collection process and analysis

4.3.1 Traffic data exploration

This section illustrates the process and the purpose of exploring the traffic data. In addition, the data collection process and the challenges faced are also presented.

1. Route Selection:

   The main objective of collecting the data from the map service providers is to create a generic script that gathers time-specific traffic data between two different Geographical locations following a specific route. We have specified the origin and destination on the map for two different routes with different road structures. These routes were sliced into multiple chunks to collect more accurate data for each chunk. Collecting the data for smaller segments is to separate the parts of the route with possibilities of speed reduction from more continuous high-speed such as motorways. Both routes use the main road but have different speed limit variations.

2. Data Analysis:

   APIs provide duration, distance, and segment information. Every segment profile contains time and distance information. Moreover, because distance and duration are known, we can determine the average speed for each segment and,

therefore, for the whole journey. The plots for these raw gathered data depict the average speed for each part of the trip, providing us with an understanding of the speed profile.

3. Data Manipulation:

Since the data obtained from the APIs are only average speed based on the duration in traffic and distance of the segment, it provides a constant speed for each chunk of the road. Therefore, the speed transition between the segments should be identified to mimic the actual velocity.

4.3.2   Data collection

1. Data collection methodology.

   - Extracting the data from the API provider.
   - Collecting data from the API response.
   - Scheduling the collection process for specific times.
   - Loading the data into a CSV format.

2. Source of traffic data.

   - Google Maps API
     The API products provided from Google Maps were used as follows:
     - Distance Matrix API: This API allows us to get the travel distance and time for the entire route and each identified segment. In addition, it allows us to obtain the estimated duration within the current traffic.
     - Directions API: Allows introducing the way-points which helps force the API to follow the route we specify; it is also responsible for the mode of transportation, which is "Car" in our case.
   - TomTom Maps API
     The API products provided from TomTom were used as follows:
     - Traffic Flow API : This allows developers to request the travel time from the origin and destination with respect to the real-time traffic.
     - Maps API: This product gives an access to the API data every time we make a request.
     - Routing API : This API gives highly detailed information about the route, with respect to directions and travel mode.
   - HERE Maps API
     The API products provided from HERE Maps were used as follows:
     - Routing API: This product informs the estimated arrival time between the origin and destination.

– Traffic API: This API is responsible for reporting the traffic flow, its consequences and the incidents information.

– Way-points sequence API: This allows us to specify the way-points on the route to divide it to the segments we require.

3. Extracting the time and speed data

- The data of the time taken during current traffic and the average speed calculated are added into separate files for each journey. These files are formatted in two columns that show the time in seconds for the whole journey versus the average speed at each second. These files are then processed to generate possible velocity profiles.

In Table 4.1, the main features of the used map services API are illustrated.

Table 4.1: The main features of the used map services API are illustrated

	Google map	HERE map	TomTom map
Free transactions	40000 requests per month	250000 requests per month	2500 requests per day
Pricing	$5 for up to 100,000 requests	$1 for 1000 ruquests	$0.5 for 1000 requests
Technology	Direction and distance matrix APIs are called. Response in JSON format	Routing API is called. Response in JSON format	Routing API is called. Response in JSON format
Way-points limit	23 way-point in each request	50 way-points in each request	No way-point limits

The data was collected at multiple time-slots for each API. These slots were at 8:15, 12:00, 16:45 and 12:00. This time selection was done to evaluate and analyse the differences between the peak traffic hours and when it is quiet.

During each time slot, the data is requested for an hour; then, the data is loaded into a CSV file in several rows. The row length depends on how many intermediate points are distributed throughout the route. Many columns start from the time of data collection until the journey's average speed is loaded. Figure 4.3 illustrates a step by-step-process of collecting the data through the APIs.

4.3.3 Data collection issues

Even though the data collection scripts were implemented to check the local time every minute and run on the specific times, the APIs dropped the connection due to unknown issues. Therefore, we had to check that our data collection was in progress regularly and the connection is not dropped. Another issue was selecting the way-points in terms of accuracy, as some of them seemed to be accurate with Google Maps, but not with others. To overcome this issue, the way-points were manually obtained from each map provider and used them for its API requests. Figure 4.4 shows the preliminary velocity profile profile obtained from the map API.
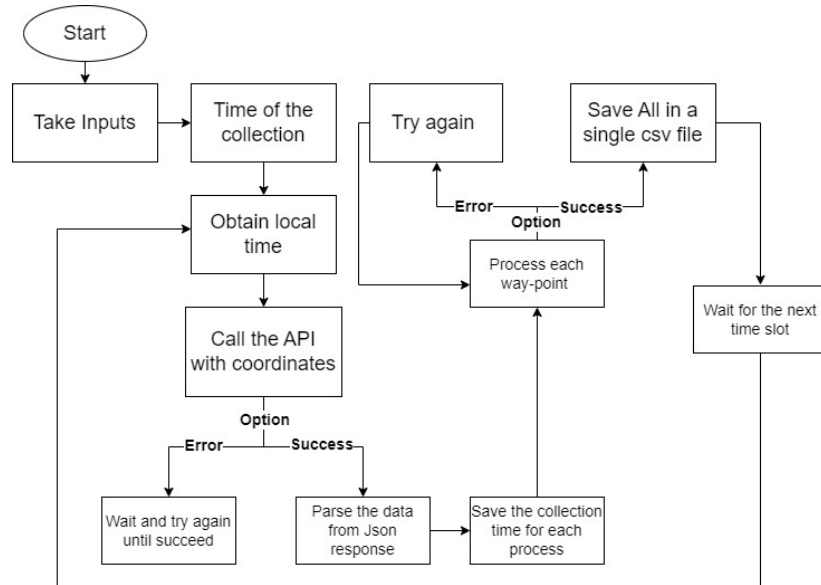
Figure 4.3: Data collection process
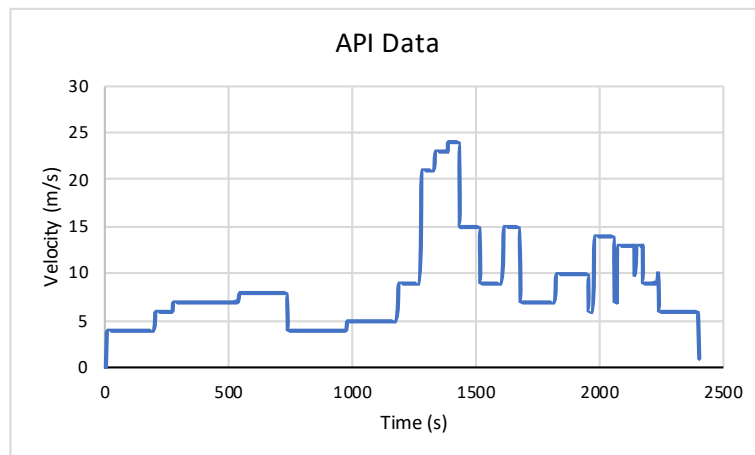
Figure 4.4: Mean velocity obtained from HERE Maps API

4.4   Data analysis

This section analyses the data collected using various methods and selects the representative profiles to generate the velocity profiles and use them to compute the energy consumption.

The script used to call the APIs and process their returns generates CSV files containing data from one or more calls. Table 4.2 presents the coordinates of origin and destination and the number of non-empty CSV files for each route.

To identify the route and the call, each API call – or sample – contains the date, coordinates of origin, coordinates of destination, departure time and arrival time. The route calculation data, which follows the arrival time, includes the distance, duration

Route	Origin	Destination	Number of files			Number of samples
			Google Maps	HERE	TomTom	
1	54.97º, -1.63º	55.04º, -1.44º	159	344	337	3818
2	55.04º, -1.71º	54.89º, -1.56º	248	339	337	3605

Table 4.2: Coordinates and number of files of studied routes

without considering the current traffic, duration within the traffic and average speed for the entire route and for each way point. The data was collected between September 6, 2019 and February 26, 2020, allowing the recording of seasonal variations in traffic.

The purpose of this study is to select samples that are representatives of the data set. The selected samples are later converted to time series and used to generate driving cycles and power profiles.

The CSV files are loaded and analyzed separately by route. Samples in which the date, origin or destination are empty or corrupted, as well as empty files are excluded from the dataset. Data types are converted according to the information they represent.

4.4.1 Data outliers

Outliers are the abnormal data points that appear unusual from most of our dataset. In this context, the outliers are detected on the entire route and are affected by multiple reasons. For example, one of the significant reasons severe accident forces for alternative routes result in longer distances. Furthermore, we consider the overall distance in our dataset to be within acceptable differences to make our samples more consistent. Therefore we established a range around the average distance where the inliers are located, and we excluded the data samples affected by the outliers from our analysis. In Route 1 Figure 4.5 (left), the majority of samples are located around 18 km and 20 km. In Figure 4.5 (right), for Route 2, we observe that most distances are around 26 km, while a small number of samples, the outliers, are above 28 km.

4.4.1.1 Data visualisation

Table 4.3 presents the mean and standard deviation of the main full-route variables, considering data from the three APIs.We observe that distance and duration present low standard deviation, which we aim to achieve with outlier filtering for route consistency. Duration in traffic and average speed, which is function of this last variable, present higher variation, reflecting traffic conditions in the respective routes.
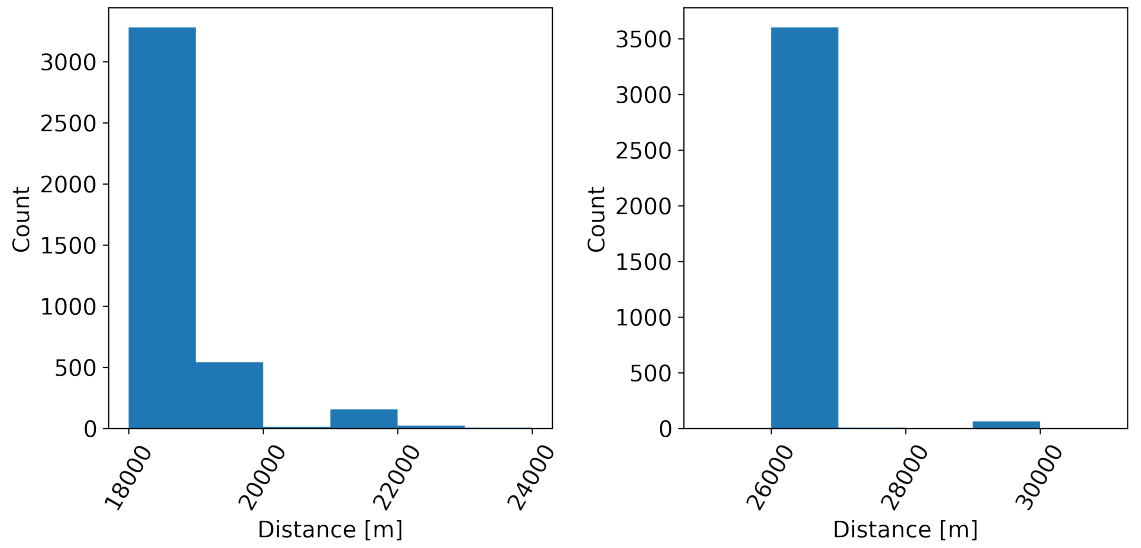
Figure 4.5: Histogram of full-route distance for each route.

Route	Distance [m]	Duration [s]	Duration in Traffic [s]	Average Speed [m/s]
1	18897.29 ± 263.52	1579.81 ± 180.09	1869.31 ± 370.28	10.46 ± 1.87
2	26300.22 ± 54.36	$12938.80 \pm 80.166^{\text{o}}$	1517.43 ± 409.26	18.23 ± 3.54

Table 4.3: Summary of main variables for each route (all APIs)

Figures 4.6 and 4.7 show the histograms of duration in traffic of each API for Route 1 and Route 2, respectively. Compared to HERE and TomTom, the Google Maps dataset presents less samples, as shown in Table 1, and its distributions have a lower range. We observe that, for both routes, peaks are located between 1000 s and 2000 s. Furthermore, the majority of samples are concentrated around low values of duration in traffic, which is a result of API call time parameters. The relation between traffic and departure time is explored in the next section.

(a)   (b)   (c)
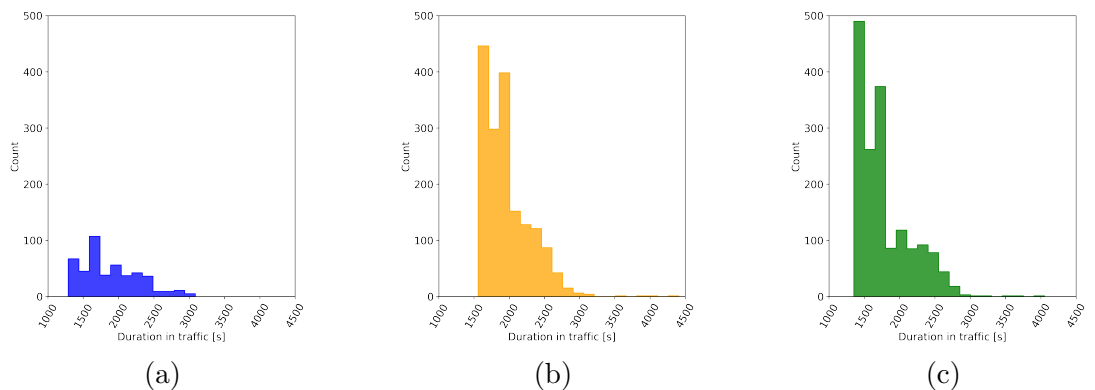
Figure 4.6: Histogram of duration in traffic for Route 1 on (a) Google (b) HERE (c) TomTom data
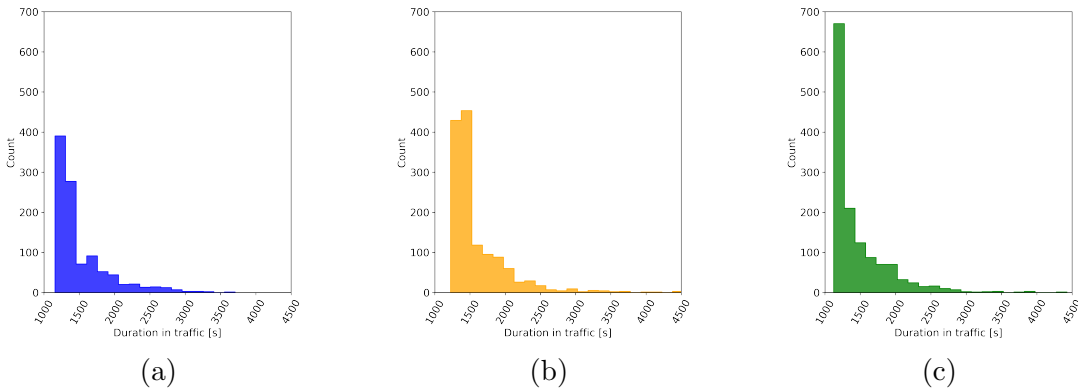
Figure 4.7: Histogram of duration in traffic for Route 2 on (a) Google (b) HERE (c) TomTom data

4.4.1.2 Traffic time vs departure time

Departure time values are between 12:00am and 5:37pm, and samples are not uniformly distributed in this interval. To represent the traffic in terms of time variation, we introduce the variable traffic time, which is calculated using Equation 4.1. Table 4.4 presents the mean and standard deviation of the traffic time for routes 1 and 2 of the three APIs.

$$traffic\ time = duration\ in\ traffic\ \text{-}\ duration \tag{4.1}$$

Route	Traffic Time [s]
1	289.49 ± 351.37
2	278.63 ± 405.77

Table 4.4: Summary of traffic travelling time for each route (all APIs)

In Figure 4.8, the scatter plots of traffic time in function of the departure time for Route 2 of Google Maps are shown. The time gap between samples is not represented; instead, they are organised in ascending order of departure and plotted sequentially.

It has been observed that the traffic is more intense from 8 am to 9 am and then from 4:30 pm to 5:30 pm. Overall, the high-traffic time intervals coincide with the beginning and ending of workdays, while in between these intervals, traffic is less intense.
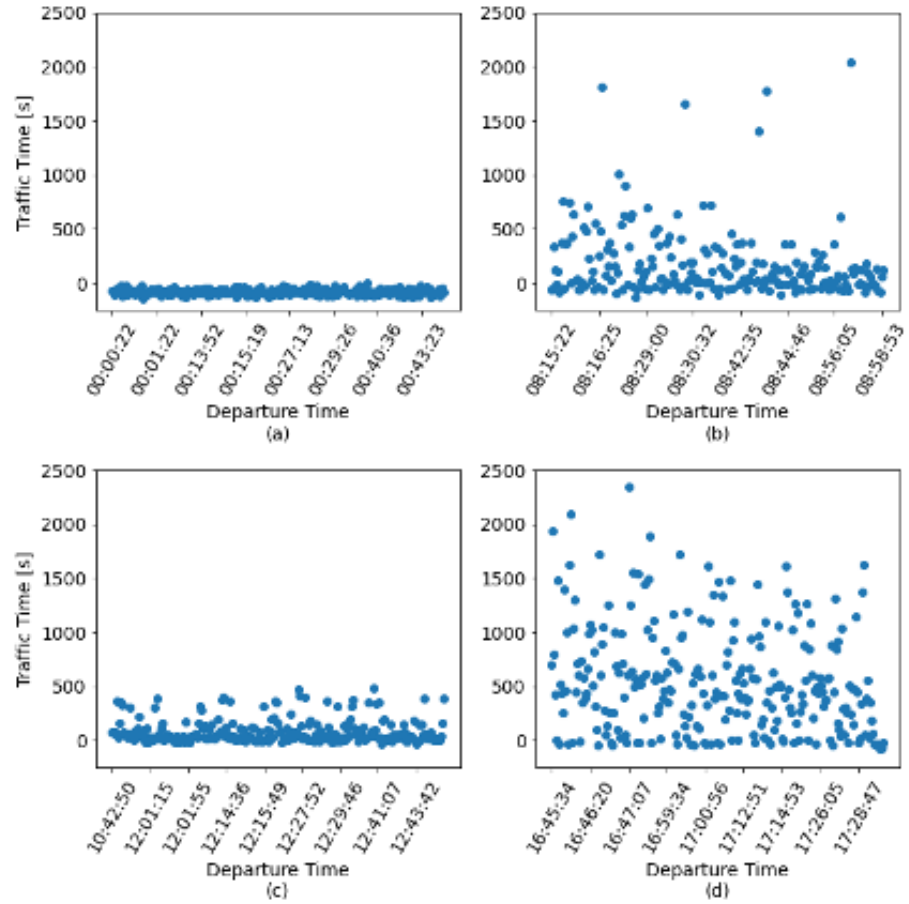
Figure 4.8: Traffic time in function of departure time for Route 2 from HERE Maps, in collection period (a) from 00:00 to 1:00 (b) from 8:15 to 9:00 (c) 12:00 to 13:00 (d) 16:45 to 17:30.

4.4.2 Selecting representative cycles

Before generating the driving cycles that will be further analysed, we select samples that are representatives of the APIs data-sets. We are not only interested in the average samples, but also in the ones that represent the variations in traffic observed throughout the day. Therefore, three samples were chosen for each API corresponding to low, average, and high traffic. The following steps are performed for each route and API.

4.4.2.1 Data classification

As showed in Figure 4.9, we clearly observe that the traffic time varies along the day. To help highlighting the patterns in these two variables, we assign four classes to the samples according to the departure time vs traffic time graphic. The classes correspond to the data collection intervals, starting at 00:00, 8:15, 12:00 and 16:45, as shown.
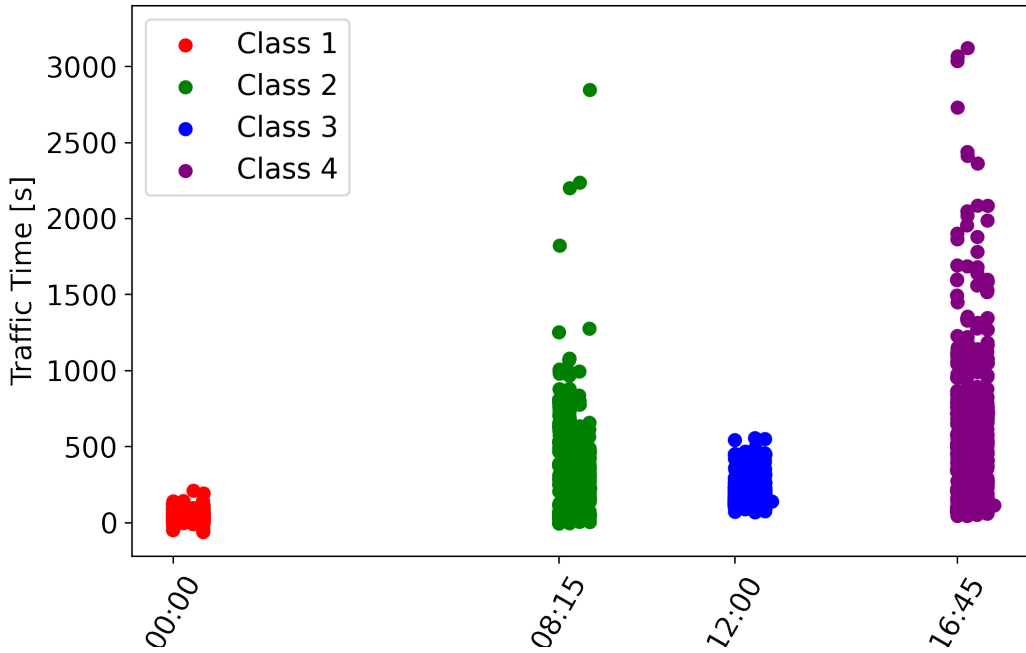
Figure 4.9: Traffic time in function of departure time for Route 2 of HERE, colored by class.

4.4.2.2 Statistical analysis of classes

With the datasets divided in classes, we can extract the representatives considering the identified patterns of traffic and time. As the aim was to capture the traffic variation within a typical-value range, the selection is based on the traffic time quartiles. From the table of quartiles and classes assembled for each API in Table 4.5, the upper-bound, average, and lower-bound samples (highlighted in blue) were selected. We establish that the samples must belong to different classes, which helps diversifying the representatives. The values of average speed corresponding to the selected samples are verified not to be outliers.

- The upper-bound sample: the highest value of the third quartile row (75%);

- The lower-bound sample: the lowest value of the first quartile row (25%);

- The average sample: the value in the second quartile row (50%) which is the closest to the average of upper and lower bounds.

By applying this method, we are able to select samples with diversified traffic conditions. Tables 4.6 and 4.7 present a summary of the representative samples' data per API for routes 1 and 2, respectively.

Clusters	Class1	Class2	Class3	Class4
3rd quartile (75%)	65	478	191	818
2nd quartile (50%)	47	230	153	564
1st quartile (25%)	31	53	128	264

Table 4.5: Quartiles for traffic time for classes on HERE data for Route 2

API	Sample	Distance [m]	Departure time	Duration in traffic	Average speed [m/s]
Google Maps	Upper bound	18699	17:09	2443	7.65
	Average	18699	09:04	1714	10.91
	Lower bound	18699	00:37	1294	14.45
HERE Maps	Upper bound	18796	16:57	2403	7.82
	Average	18796	08:39	1995	9.42
	Lower bound	18796	00:12	1625	11.57
TomTom Maps	Upper bound	18785	17:09	2455	7.65
	Average	18785	09:03	1747	10.75
	Lower bound	19738	00:00	1607	12.28

Table 4.6: Summary of representative samples per API from Route 1

API	Sample	Distance [m]	Departure time	Duration in traffic	Average speed [m/s]
Google Maps	Upper bound	26368	16:46	2116	12.46
	Average	26366	08:42	1370	19.25
	Lower bound	26368	00:29	11960	22.05
HERE Maps	Upper bound	26261	16:58	2146	12.24
	Average	26261	08:28	1530	17.16
	Lower bound	26261	00:13	1331	19.73
TomTom Maps	Upper bound	26290	16:45	2145	12.26
	Average	26290	08:55	1342	19.59
	Lower bound	26290	00:00	1131	23.24

Table 4.7: Summary of representative samples per API for Route 2

4.5 Route-based driving cycle construction

This section shows how the acceleration and deceleration approach calculates the speed transitions between route segments. Furthermore, it illustrates how the noise values are added to the constant speed of each segment, as well as how the sharp edges are addressed using the smoothing function.

4.5.1 Applying acceleration and deceleration between route segments

We applied the acceleration and deceleration rates to the beginning and ending intervals to smooth the velocity transition between segments. We determine the maximum acceleration on the car based on the Nissan leaf's 2019 [52] acceleration rate for 0/100 km/h. Furthermore, we consider that the acceleration and deceleration rates are the same. Therefore, even though that car can decelerate under braking faster than ac-

celeration, the maximum speed transition only occurs if the speed difference between the two segments is very significant and rarely happens in the case of acceleration.
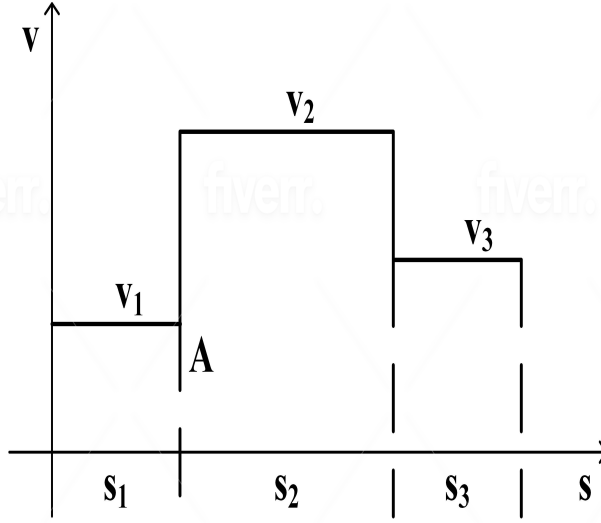
Figure 4.10: The initial driving cycle before the speed transition between segments

Using the data retrieved from the API, we obtain the initial driving cycle as shown in Figure 4.10. It is characterised by sharp edges, corresponding with unrealistic significant speed changes. In addition it does not take into account the technical constraints imposed by the vehicle and the road characteristics. Therefore, the final driving cycle needs to be developed realistically before performing the energy consumption estimation.

The process of developing the driving cycle is implemented in iterative manner. In Figure 4.11, the driving cycle shows three different segments which constant speeds. The velocity on the first segment is assumed to be at speed V_1, and since the recorded velocity on the second segment is higher than the vehicle's velocity on the second segment, the vehicle needs to accelerate gradually after exceeding point A. the determination of the acceleration is based on the speed difference between V_1 and V_2 using the following equation:

$$a = \begin{cases} 3.5, & v_2 - v_1 \geq 10\frac{km}{h} \\ \frac{1}{2}(v_2 - v_1), & v_2 - v_1 < 10\frac{km}{h} \end{cases} \tag{4.2}$$

After determining the acceleration, The time Δt needed for the vehicle to accelerate from the velocity in the first segment V_1 to the following velocity V_2 can be calculated as:

$$\Delta t = \frac{v_2 - v_1}{a} \tag{4.3}$$
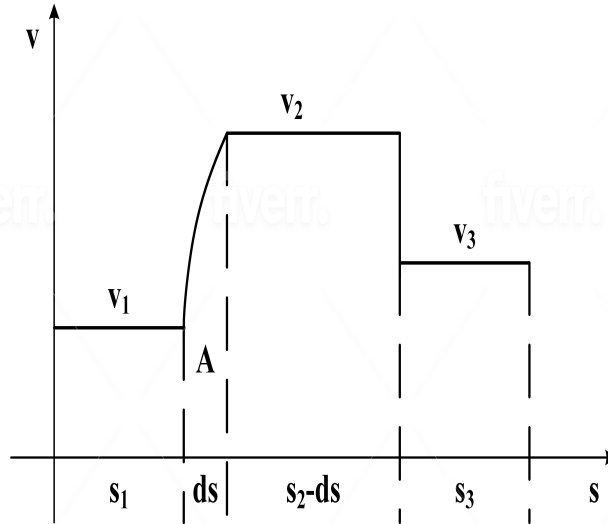
Figure 4.11: The gradual acceleration added to the driving cycle

Calculating the distance Δs the vehicle needs during the accelerating process leads to the division of the following segment into separated segments as shown in Figure 4.12

$$\Delta s = v_1 \Delta t + \frac{a \Delta t^2}{2} \tag{4.4}$$
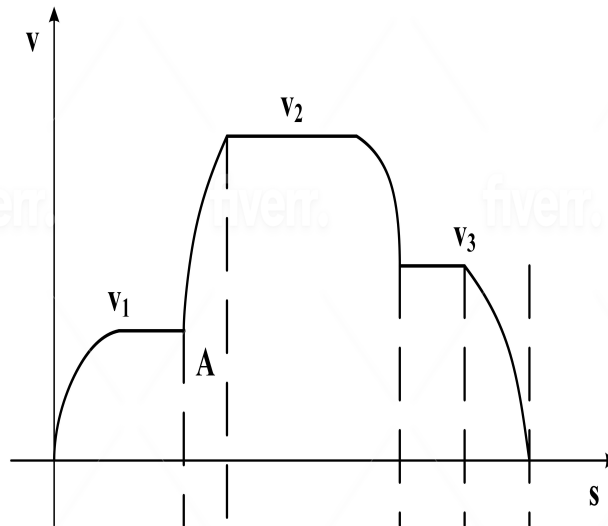
Figure 4.12: Final driving cycle after applying the acceleration method

The first segment has the length ds where the vehicle acceleration is applied until it reaches the speed V_2. The second segment has the length S_2 - ds when the vehicle's velocity is constant and equals V_2. The API data speed data are often imperfect and inconsistent; it deviates from real-life conditions and constraints. Herefore, the acceleration between velocities is only sometimes feasible; in other words, for the

above-analysed case of the acceleration from V_1 to V_2, sometimes the distance that the vehicle needs to accelerate is longer than the length of the following segment itself. To overcome this issue, the acceleration V_2 will not take place; moreover, we reduce the speed on the following segment by a small step Δ, and repeat the process where the speed on the next segment is V_2 - Δ. This process is repeated until it satisfies the feasibility of yielding the final driving cycle, as shown in Figure 4.12.

4.5.2   Introducing noise to the speed profile

To mimic a real driving cycle, we add noise to the intervals in which the speed is constant. The noise is generated as Gaussian distributed random numbers in the interval $[a, b]$. Considering that small variations in speed are accepted, a and b are defined as functions of the maximum and minimum speeds of an interval i.

$$a = -5 \times \frac{1}{minimum(v_i)} \quad \text{and} \quad b = 5 \times \frac{1}{maximum(v_i)} \tag{4.5}$$

The introduced noise slightly changes the constant speed; it is a speed variation to the average speed we obtained from the API. Therefore, it will impact the distance travelled. To keep the distance unchanged or with an acceptable difference, after the noise n is generated for N samples, it is corrected as follows.

$$n_{i\ corrected} = n_i - \overline{n}, \quad i = 1, 2, \cdots, N \tag{4.6}$$

4.5.3   Smoothing the sharp edges

As abrupt variations in speed remain after the acceleration method and noise adding, the last step consists of smoothing the speed curve. We apply the LOESS (locally estimated scatter plot smoothing) method, using 4% of the samples for calculating smoothed values.

LOESS is a method of non-parametric regression that produces a smooth curve by locally fitting polynomial functions. Thus, the fitted values are determined with neighbouring subsets of data. LOESS, among other methods, and the percentage of samples are chosen based on a qualitative evaluation of the final driving cycle – the main criteria are the decrease of sharp edges, preservation of noise-induced variations and preservation of the cycle when compared to its pre-processing shape. We determine that the cycle starts and ends at 0 m/s. The speed curve is linearly interpolated from *zero* to a speed point near the first and last segment's speed. Figure 4.13 illustrates the general framework of the entire process in this chapter, starting from the data collection to the state of charge estimation in electric vehicles.
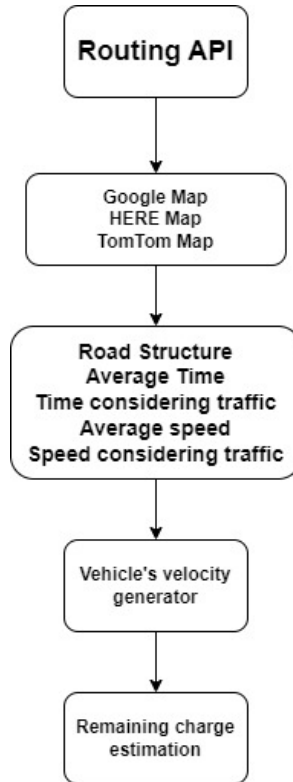
Figure 4.13: Data collection and energy consumption estimation framework

After applying the previous methods, the represented driving cycles are generated as shown in the Figures 4.14 to 4.16. These figures present the velocity profiles for all APIs after the representative driving cycles are selected for both routes. It is clear that the driving cycle for each API is different at some points on the route and quiet similar at other points along the routes. The generated driving cycles will be used in the next section to develop the power profile for the electric vehicle. Therefore, the energy estimation can be performed and the battery dynamics can be captured.
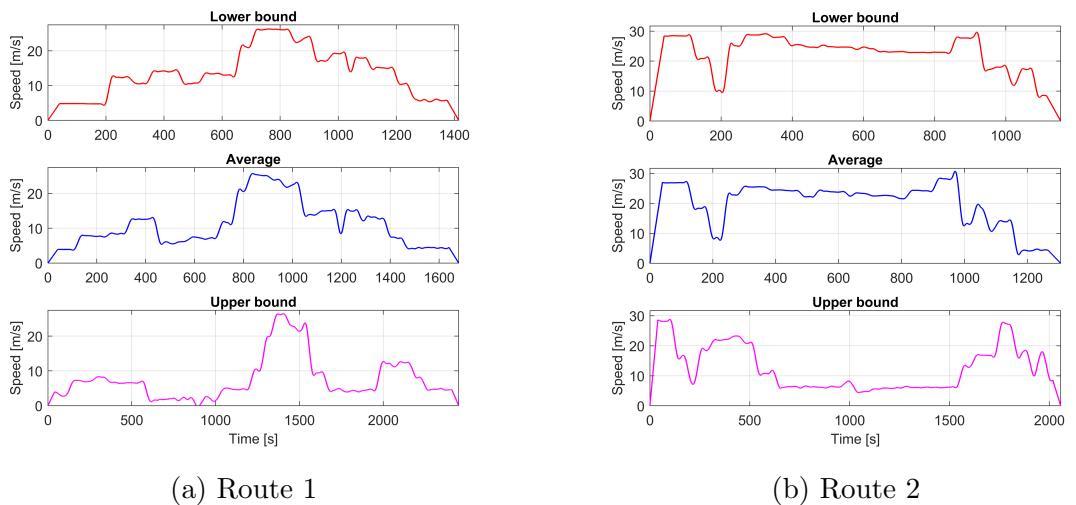
(a) Route 1

(b) Route 2

Figure 4.14: Google Maps driving cycles
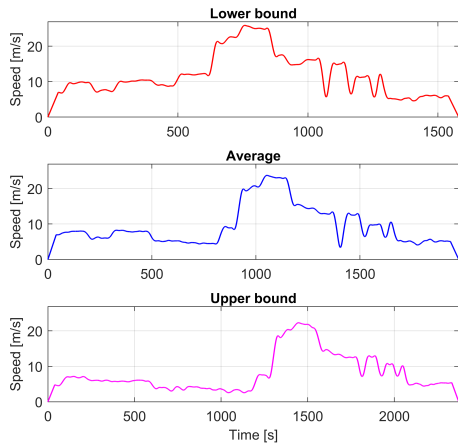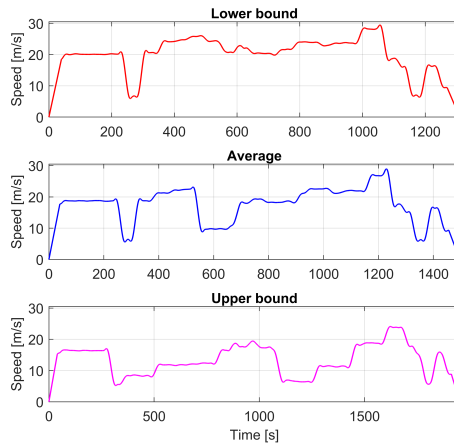
(a) Route 1   (b) Route 2

Figure 4.15: HERE Maps driving cycles
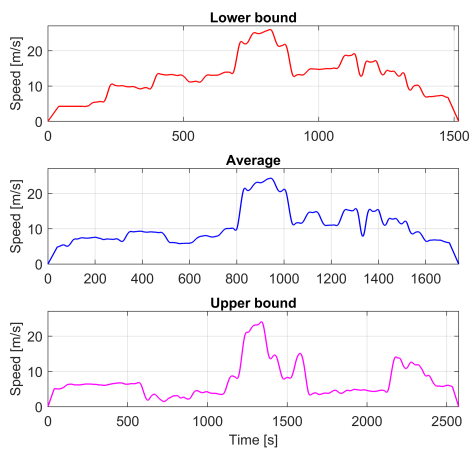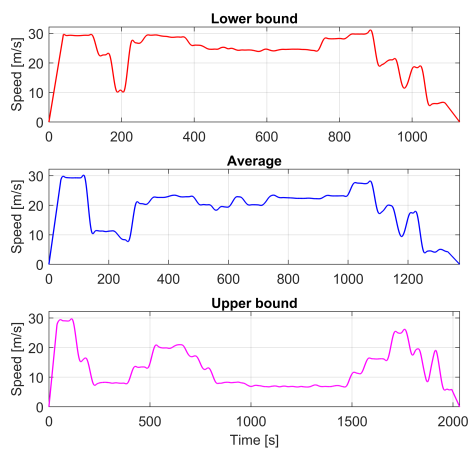
(a) Route 1   (b) Route 2

Figure 4.16: TomTom Maps driving cycles

4.6 Generating the power demand using electric vehicle's dynamics

This section considers an electric vehicle model based on existing Nissan Leaf to perform the power demand generation and the state of charge estimation based on the data used on this chapter. With the vehicle speed determined in the driving cycle, we calculate the power consumed to generate the vehicle, or, in case of braking, the power provided back to the battery pack [52].
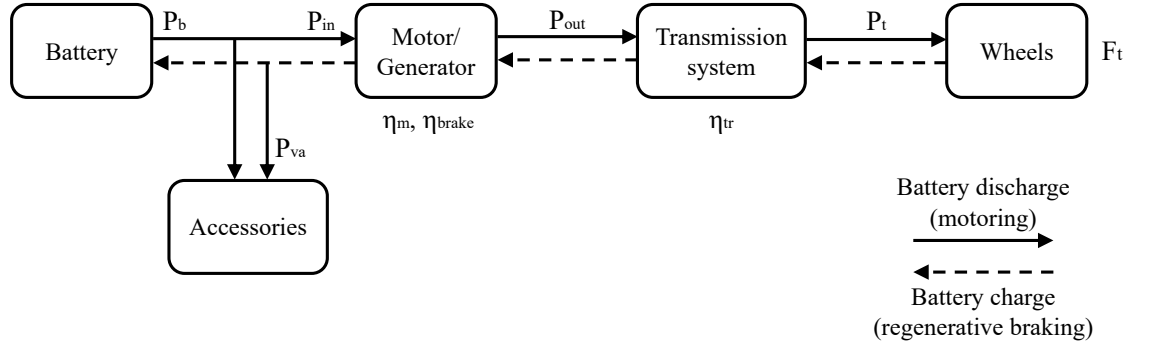
Figure 4.17: Electric vehicle power transition diagram

$$F_t(t) = F_r(t) + F_g(t) + F_d(t) + F_a(t) \tag{4.7}$$

Starting at the wheels, the traction force F_t required for the vehicle's motion is expressed by the sum of opposing forces, which is the rolling friction, grade resistance, aerodynamic drag, and acceleration force [52, 167]. We consider the road slope $\alpha = 0$ for the full extension of the routes. Even though the road slope data is available from some API map providers, it was impossible to obtain it accurately in this approach. Elevation was affected by the waypoint's manual selection. Therefore, obtaining the road slope has been a complex task in this approach due to the uneven route segment length. In addition, the road elevation data is obtained and considered in the following chapter.

- The rolling resistance, force resisting the movement of the tires on the road surface:

$$F_r(t) = \mu_r m_v g \cos a = \mu m_v g \tag{4.8}$$

- Grade resistance, gravitational force acting on the vehicle when it travels along a sloping road:

$$F_g(t) = m_v g \sin a = 0 \tag{4.9}$$

- Aerodynamic drag, force opposing the vehicle motion through the air, in which the wind speed is not considered:

$$F_d(t) = \frac{1}{2}\rho C_d A_{vf} v(t)^2 \tag{4.10}$$

- Acceleration force, in which the rotational acceleration is expressed with an additional mass m_r, representing the inertia of rotating components:

$$F_a(t) = (m_r + m_v)a(t) \tag{4.11}$$

Where:

$$m_r = (0.04 + 0.0025G^2) \times m_c \tag{4.12}$$

- The traction power at the wheels is function of the traction force and the vehicle speed.

Vehicle's and environment parameters	
Abbreviation	Parameter
α	road slope
a	acceleration $[m/s]^2$
A_{vf}	Vehicle frontal area $[m^2]$
C_d	Drag coefficient
F_a	acceleration force [N]
F_d	aerodynamic drag [N]
F_g	grade resistance [N]
F_r	rolling resistance [N]
F_t	traction force [N]
g	gravity acceleration $[m/s]^2$
G	gear ratio
m_c	curb weight, vehicle mass including battery pack [kg]
m_r	vehicle mass increase representing the inertia of rotating components
m_v	total vehicle mass, including passengers [kg]
η_{brake}	efficiency of regenerative braking
η_m	motor efficiency
η_{ns}	transmission system efficiency
ρ	acceleration force [N]
P_t	traction power [W]
P_{in}	motor input power [W]
P_{out}	motor output power [W]
μ_r	rolling resistance coefficient
V	speed of the vehicle

Table 4.8: vehicle and environmental parameters

$$P_t(t) = F_t(t) \times v(t) \tag{4.13}$$

- To calculate the output power of the motor, we consider the efficiency of the transmission system $\eta_t s$. Therefore, in case of motoring (battery discharge), P_t is positive, and P_{out} is expressed by:

$$P_{out}(t) = \frac{P_t(t)}{\eta_{ts}} \tag{4.14}$$

- In case of battery charge, when P_t is negative, the efficiency of the regenerative braking η_{brake} must be considered in P_{out} as well. η_{brake} is a function of the speed, as proposed in [44].

$$P_{out}(t) = P_t \times \eta_{ts} \times \eta_{brake} \tag{4.15}$$

$$n_{brake} = \begin{cases} 0 & if \ \ 0 \leq v(t) < l_1 \\ k_1 \times v(t) + k_2 & if \ \ l_1 \leq v(t) < l_2 \\ 1 & if \ \ \ \ \ \ v(t) \geq l_2 \end{cases}$$

where l_1 and l_2 are speed thresholds, based on the characteristics of the vehicle, and k_1 and k_2 are fitting constants. l_1 is the speed from which the vehicle starts recuperating energy. For higher speeds l_2, the regenerative factor reaches its maximum value, 1. Between l_1 and l_2, the behavior of η_{brake} is assumed to be linear, starting at 0 and finishing at 1.

- The input power of the motor is function of its output power and efficiency as motor or generator, determined with look-up tables proposed in [52]. In case of motoring, $P_{out} > 0$ and P_{in} is expressed by:

$$P_{in}(t) = \frac{P_{out}(t)}{\eta_m} \tag{4.16}$$

- In case of regenerative braking, $P_{out} < 0$ and P_{in} is:

$$P_{in}(t) = P_{out}(t) \times \eta_m \tag{4.17}$$

- Finally, the power provided or received by the battery P_b is the sum of the motor input power and the power consumed by vehicle accessories P_{va}, such as air conditioner and light system, which is considered constant.

$$P_b(t) = P_{in}(t) + P_{va}(t) \tag{4.18}$$

Abbreviation	Parameter
SOC	state of charge [%]
V_{oc}	open-circuit voltage [V]
I	battery current [A]
t, τ	time [s]
F_a	acceleration force [N]
C_r	battery rated capacity
R_s	internal resistance, in series with load

Table 4.9: Battery parameters

4.6.1 Battery model dynamics and energy consumption estimation

The implementation of the battery model, was considering the Rint model proposed in [37]. This model includes a voltage source V_{oc}, representing the open-circuit voltage, in series with the parallel branch of internal resistance. Any battery model can be implemented in this part of the research to estimate the state of charge based on our power profiles. The current model is less complex and validated in previous studies such as in [37].
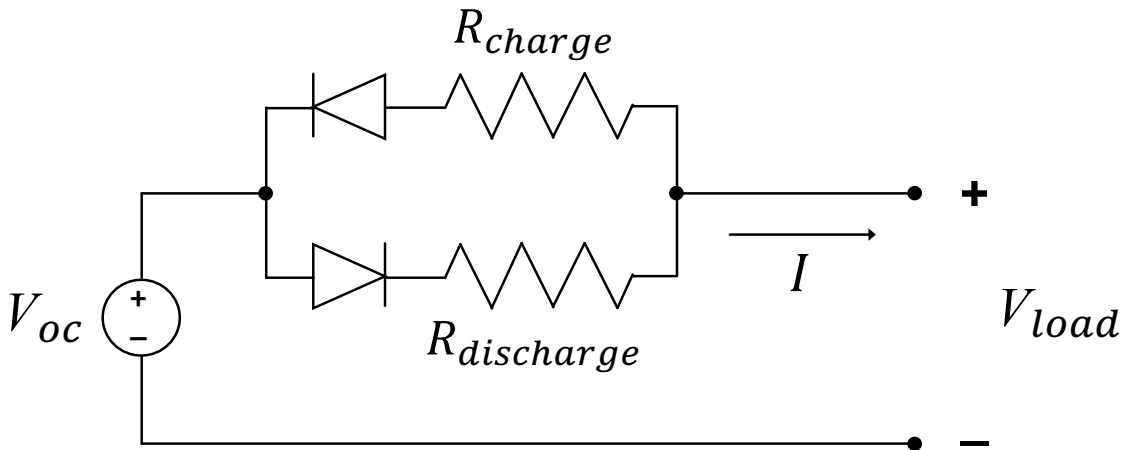
Figure 4.18: The equivalent circuit model based on Rint with two resistors in parallel

Ideal diodes represent the current flow in the resisting branch. For example, when the battery is discharging, the diode in series with the discharging resistance ($R_{discharge}$) conducts the current; contrarily, in the case of battery charge, the diode conducting the current is in series with charging resistance (R_{charge}). Given an initial state-of-charge, we start by calculating open-circuit voltage V_{oc} in terms of the state-of-charge (SOC), where ln is the natural logarithm, K, a, b, c and d are constants that were taken from [52] and adjusted for a better response. This adjustment was empirical and can be improved in the future.

$$
\begin{aligned}
V_{oc}(t) = K &- a \times SOC(t) - b\tfrac{1}{SOC(t)} \\
&+ \text{c} \times \ln(SOC(t)) = d \times ln(1 - SOC(t))
\end{aligned}
\tag{4.19}
$$

The charging or discharging resistance R_s in the following equation is a function of the SOC and is determined based on look-up tables obtained from [52]. Then, the battery current is calculated by:

$$
I(t) = \frac{V_{oc}(t) - \sqrt{V_{oc}(t)^2 - 4R_sP_b(t)}}{2R_s}
\tag{4.20}
$$

The current is positive if the battery is discharging, and negative if it is charging. Finally, the SOC is estimated with the coulomb counting method [150], in which the battery current is integrated over time to calculate the transferred charge.

$$
SOC(t) = SOC(t_0) - \frac{1}{C_r} \int_{t_0}^{t} I\Delta\tau
\tag{4.21}
$$

$$
SOC(t) = SOC(t-1) + \frac{I(t)\Delta\tau}{C_r}
\tag{4.22}
$$

Where $SOC(t)$ is the current state-of-charge, $SOC(t_0)$ is the initial state-of-charge, C_r is the rated capacity, I is the current flowing in or out of the battery, t_0 is the initial time and t, the current time. Alternatively, the SOC can be expressed in terms of its previously estimated value $SOC(t-1)$ and the current for the time interval of $\Delta\tau = [t-1, t]$.

The equations of V_{oc}, I and SOC are applied iteratively over time to obtain the profiles for a full driving cycle.

4.7   Results

This section presents the power needed for each journey based on each API and route. It also shows the battery voltage and the state of charge estimation.

4.7.1   Google Maps API

The results in Figure 4.19, show the power profiles needed for cycles obtained using data from the Google Maps API. The first graph (a) shows the power profile for the lower bound in the first route, and as a result of many segments containing traffic lights and roundabouts, we notice the power profile fluctuating due to change in speed and excessive acceleration. It also contains segments in higher speed limits where there is a higher power demand.

The state of charge estimation for the lower bound shows that the fully charged battery dropped to 92% in almost 23 minutes, this was the lower bound in using Google Maps data, and it involves higher speed due to less dense traffic.

Figure 4.19 (b), illustrate the power profiles for the same route but for the upper bound with a high traffic density. This journey consumes an almost similar amount of energy as the lower bound; however, this is mainly because of the driving at lower speeds and the regenerative braking functionality. This journey time was around 41 minutes.

(a) Lower bound
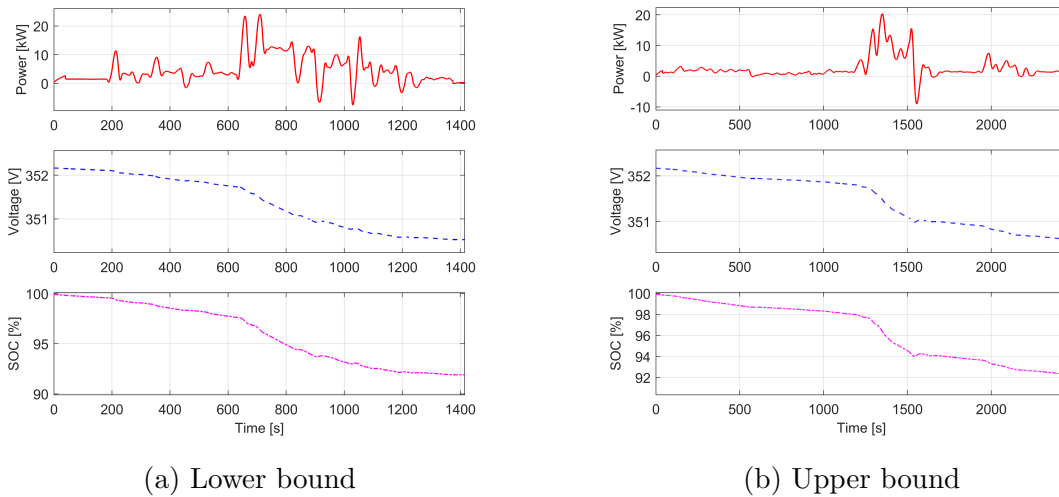
(b) Upper bound

Figure 4.19: Lower and Upper bounds for Google Maps data Route 1

Figure 4.20 show the same plots presented for route two illustrating that motor driving leads to higher power demand; hence, the efficiency is less due to the higher speed. Figure 4.20 (a), shows the state of charge in lower bound dropped from 100% to 86% even though the time taken for this journey is approximately 18 minutes. Unlike in Figure 4.20 (b), the journey duration was almost 34 minutes; however, in the upper bound the state of charge was captured at nearly 88% from fully charged cycle.

(a) Lower bound
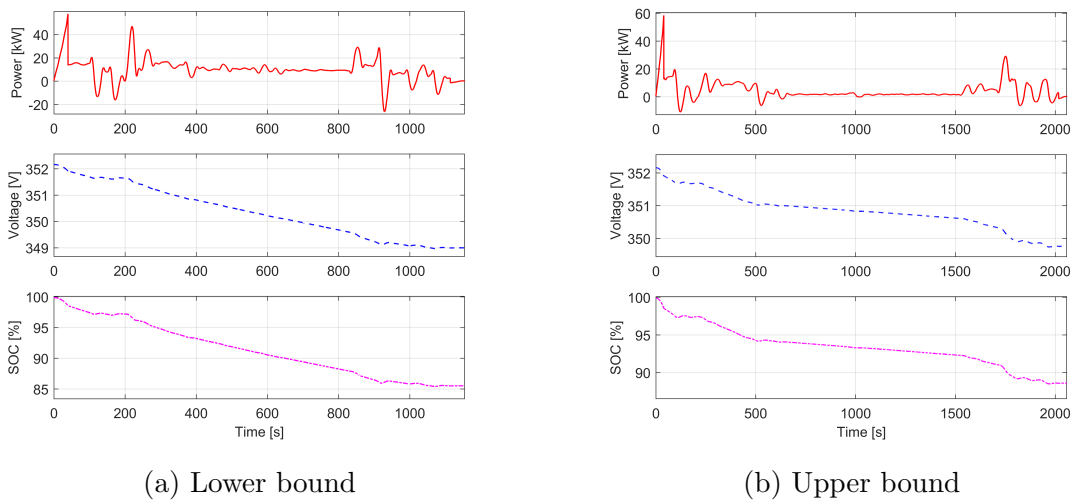
(b) Upper bound

Figure 4.20: Lower and Upper bounds for Google Maps data Route 2

4.7.2   HERE Maps API

Figure 4.21, show the power profiles and SOC estimation for the experiments based on the data obtained from HERE Maps API. As for the power profile in the first route, the data shows a slightly similar appearance to the previous API profiles. In addition, the state of charge for that profile dropped to 93% in the lower and lower bounds.

(a) Lower bound   (b) Upper bound
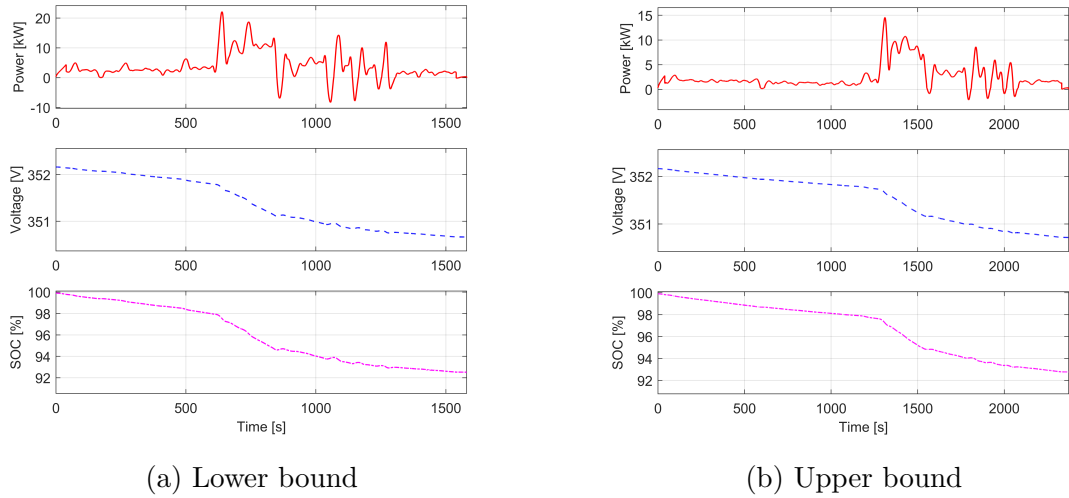
Figure 4.21: Lower and Upper bounds for HERE Maps data Route 1

(a) Lower bound   (b) Upper bound
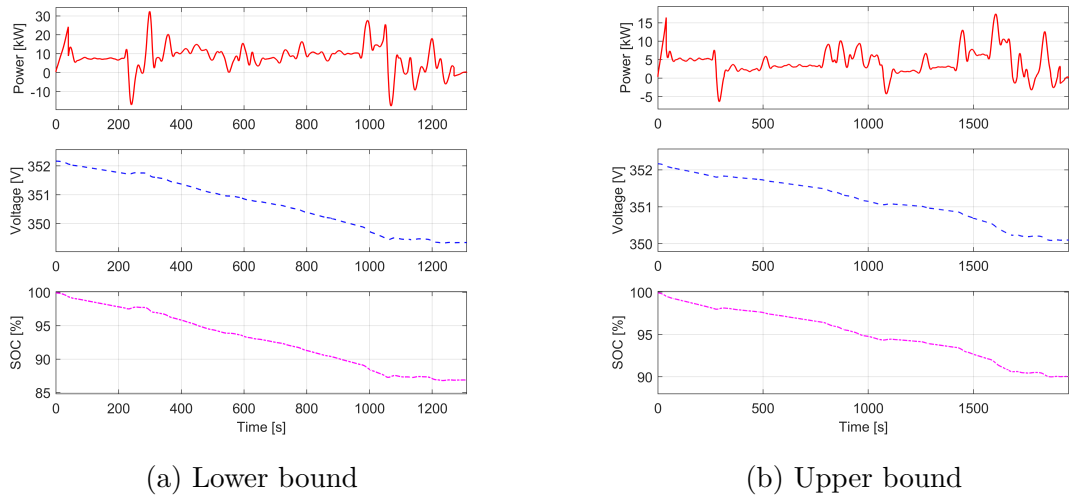
Figure 4.22: Lower and Upper bounds for HERE Maps data Route 2

Figure 4.22, shows the profiles for the second route, and it is slightly different compared to Google and TomTom, where it shows less power consumption, but it has more variation, mainly when the speed is restricted by traffic. This variations in the lower bound led the SOC to drop from fully charged to almost 87%.

4.7.3   TomTom Maps API

Figure 4.23, shows the results based on TomTom Maps API for the first route. The power profiles generated for the first route is quite similar to the same profiles using Google Maps API data for both bounds. However, the journey time was slightly longer with slightly less power consumption. The SOC estimation for the upper bound of the first route was 92% in 44 minutes. The next power profiles in Figure 4.24 showed more energy consumption on the motorway in the lower bound as a result of driving at the highest speed limit.

(a) Lower bound   (b) Upper bound
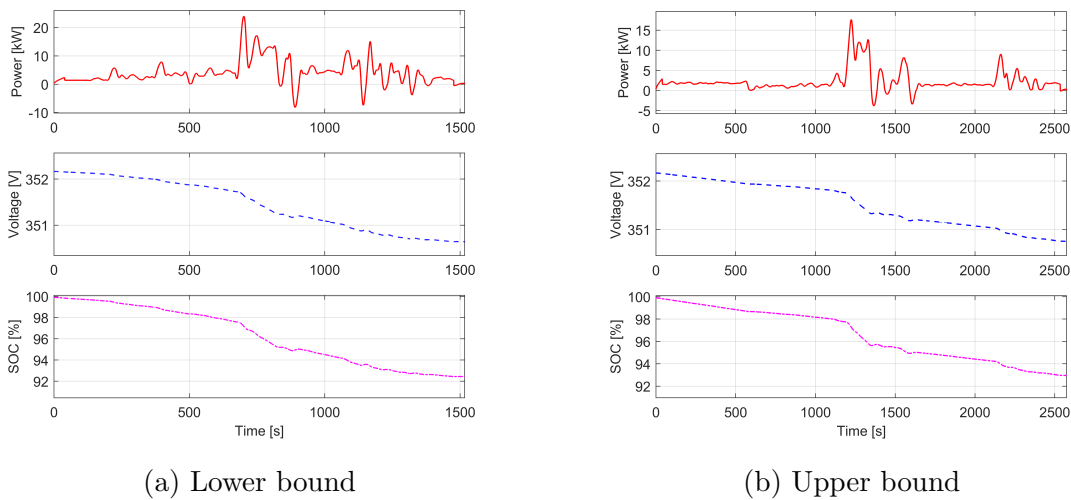
Figure 4.23: Lower and Upper bounds for TOMTOM Maps data Route 1

(a) Lower bound   (b) Upper bound
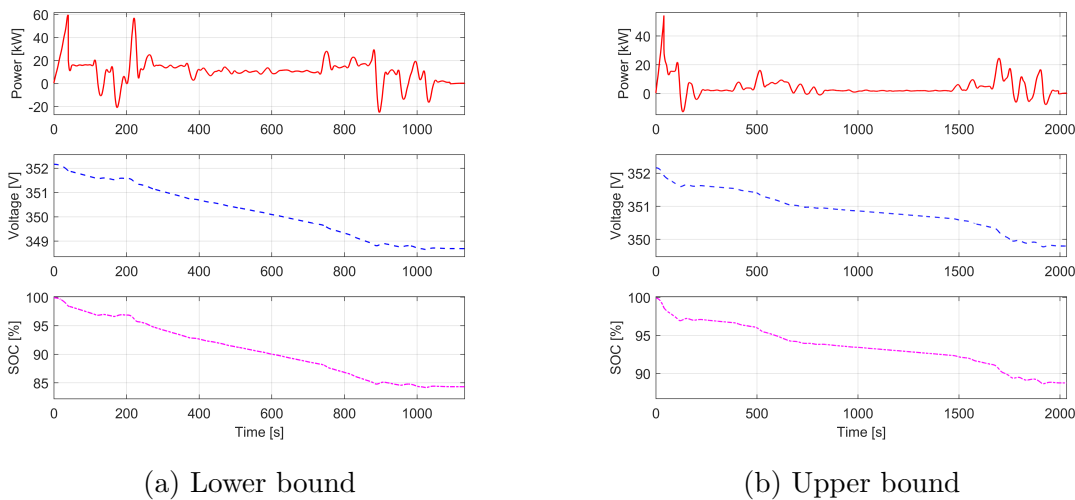
Figure 4.24: Lower and Upper bounds for TOMTOM Maps data Route 2

4.8   Conclusion

This chapter constructed different driving cycles based on three API data and two routes. A data collection framework was developed, which gathered the same data from different APIs and processed the data to generate representative driving cycles. We divided the routes into segments using the route segmentation technique. The data contained the distance, the time taken for the whole journey, the average speed for the entire journey, and the way-points. We developed a velocity model algorithm and introduced variations using a random function based on Gaussian normal distribution.

After introducing some randomness to the mean data extracted from the APIs, we used the locally-weighted scatter-plot smoothing function "LOWESS" in MATLAB to fit a smooth curve to the randomised data and eliminate any sharp edges. The data selection was based on data classification and statistical analysis. Finally, an electric vehicle model based on the Nissan Leaf was implemented to calculate the power demand and the remaining range for each cycle.

The results showed that the driving cycles are within the range of the existing industrial driving cycles, and the vehicle's constraints are satisfied. Moreover, it stimulated the driving patterns for each cycle. The results also show the variation between the different data sources and the times for the data collection. The state of charge estimation for each cycle and route varies for each route and data source. The route includes motorway driving, shows massive energy consumption when the vehicle manages to drive at the highest speed limit and shows less energy consumption when the traffic density restricts the speed. By contrast, the results also show less energy efficiency for city driving when the traffic is dense because the journey time is longer.

The proposed velocity model in this chapter work with any dataset that includes the average speed and road segments. It can produce a real-time velocity profile construction without collecting more data for extended periods. Unfortunately, it was almost impossible to integrate weather API and traffic lights detection techniques due to the restrictions in the map service provider. This drawback makes the accuracy of the constructed velocity less; however, adding these features will not require any significant modification to the proposed velocity model. The following chapter aims to overcome these limitations and consider more data over the route.

5

REMAINING RANGE ESTIMATION BASED ON DYNAMIC ROUTE DATA RETRIEVAL

Contents

5.1   Summary

This chapter implements another approach to obtain the data from map services API. This approach retrieves the API data and processes at the run-time. The route segmentation in this approach is more dynamic and applied by the API algorithm, which results in more segmentation for the route. In addition, we can use it for any road as long as the API source has the information we require for the road. The data we obtain includes speed, average time, time considering traffic, way-points and road slope.

5.2   Introduction

Many APIs in this chapter have demonstrated the concept of using external APIs in pairs with map APIs to obtain more information. The main one is the HERE Maps API, which retrieves detailed route information. In addition, another OpenStreetMap-based API is used in conjunction with the Overpass API to obtain traffic light coordinates. This API only allows us to obtain the vehicle's maximum speed on a specific route. However, it cannot be used because it does not take into account real-time traffic. In addition, as they both collect data from the same server, this API works seamlessly with the Overpass API. As a result, we examined the impact of traffic lights and how much they affect energy consumption. Finally, we used OpenWeather to gather wind speed and direction data. The weather data was combined with the HERE Maps information, and the data was then prepared and processed in order to construct the driving cycles using various techniques. As a result, we generated the power profiles and estimated the SOC for each driving cycle using the EV and battery models implemented in the previous chapter.

5.3   Dynamic data collection

The data collected in this chapter is different from the one in the previous chapter. It contains more information about the route, and it processes the data and constructs the driving cycle as soon as the data returns from the API. Furthermore, the API applies the route segmentation and is not restricted to our desire, which means that the waypoints can differ in each API call. This technique makes the driving cycle generation more generic, and we can apply it to any route on the map. In the forthcoming sections, we will explain the data collection process and the driving cycles generation. Figure 5.1 illustrates the overview of the data collection along with the data process.
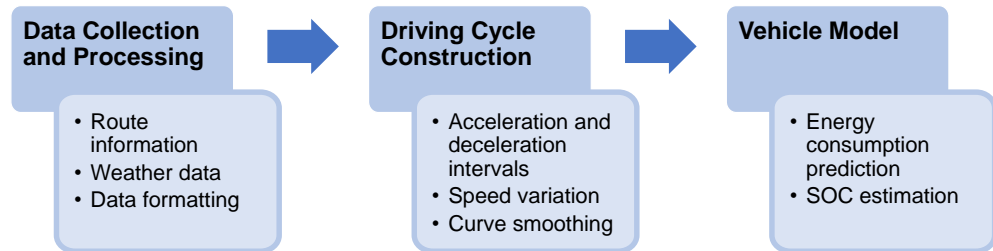
Figure 5.1: The general workflow for the data collection, driving cycle development and the energy consumption estimation

5.3.1   Impact of traffic lights on electrical energy balance

In order to assess the limitation of API usage for retrieving traffic lights' geographical locations, we aim to evaluate their impact on electrical energy balance numerically. For simplification, we simulate a driving cycle with a constant speed, considering acceleration and deceleration at the beginning and end of the route. The exact vehicle and battery parameters applied in the previous chapter are used. Regarding the route information, we consider the road slope and the wind speed equal to zero and the temperature at $20°$. We set the constant speed for the first simulation at $15\ m/s$ and the travel duration at $2000\ s$. Without the stops, the travelled distance is $27\ km$, and for each stop corresponding to the traffic lights, the vehicle decelerates, stops for $30\ s$ and accelerates, returning to the speed of $15\ m/s$. It is essential to mention that, with stops, the route duration increases to conserve the travel distance. Therefore, the time required for the vehicle to finish the route at constant speed is added before the deceleration at the end of the driving cycle. Figures 5.2 and 5.3 show the simulated driving cycles along with their respective power profiles and SOC estimations. Finally, we calculate the energy balance from the power profiles, which is the sum of the energy provided and received by the battery, for the two presented cases and simulations with one and three stops, Table 5.1. Each stop represents an increase in energy consumption, which, in this simulation, is equivalent to approximately 11 Wh. By simulating different values of constant speed, we notice that, between 5 and 20 m/s, the balance increases with the number of stops, while between 25 and 45 m/s, it decreases. Therefore, we conclude that the impact of stops on energy balance depends primarily on the travelling speed and the number of stops in the route; nonetheless, it represents a small portion of energy balance (less than 1 per cent) in all cases of our simulation.

Furthermore, the status of traffic lights is not provided by the APIs, which makes it necessary to consider the probability of them being green or red. Thus, considering traffic lights or not, we admit uncertainty in energy prediction and SOC estimation. Given the liability of APIs and the low impact on energy balance, traffic lights are not considered in our latest implementation. However, strategies for overcoming these limitations in routes can be investigated in future work.
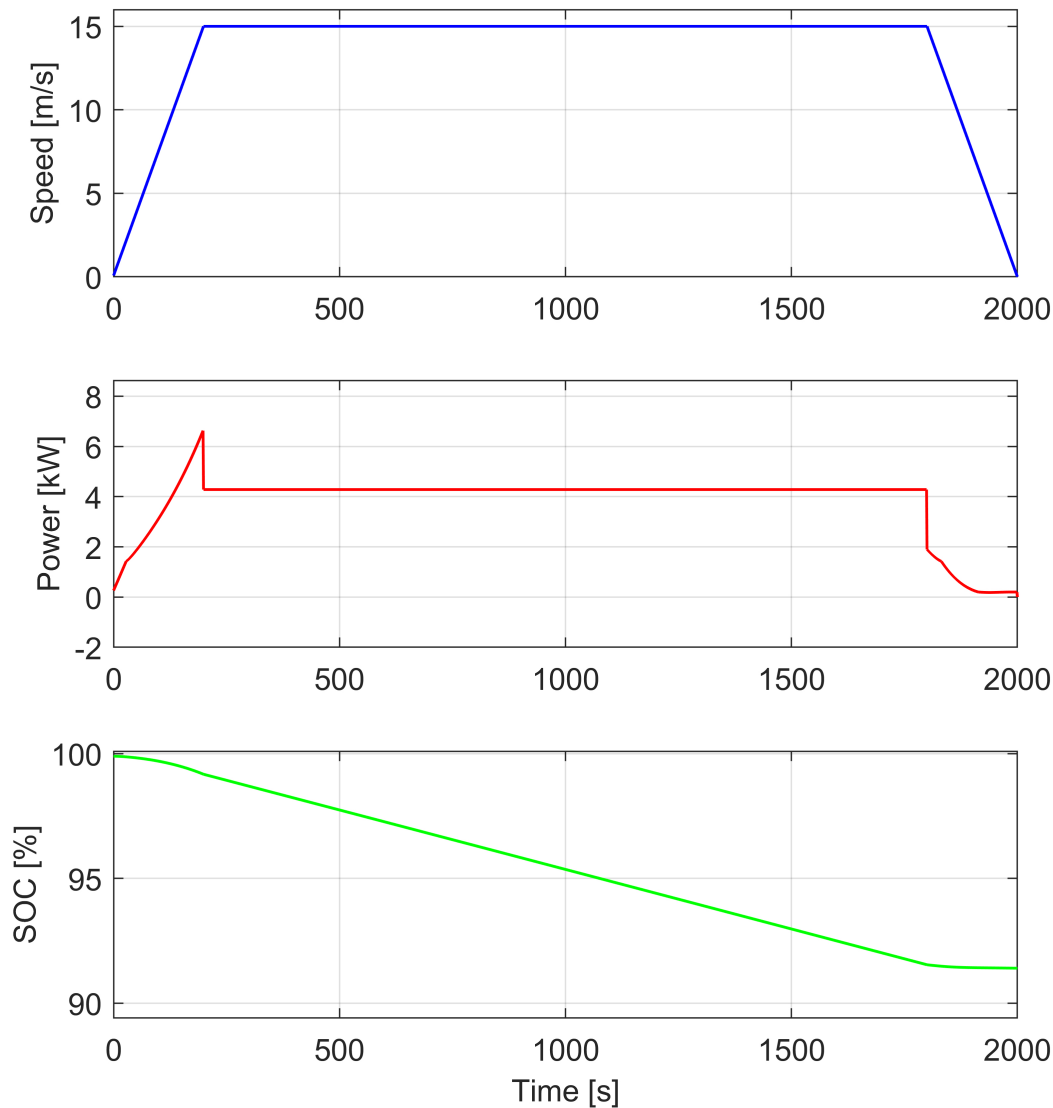
Figure 5.2: Simulated driving cycle (constant speed of 15 m/s) and the respective power profile with SOC estimation without traffic lights
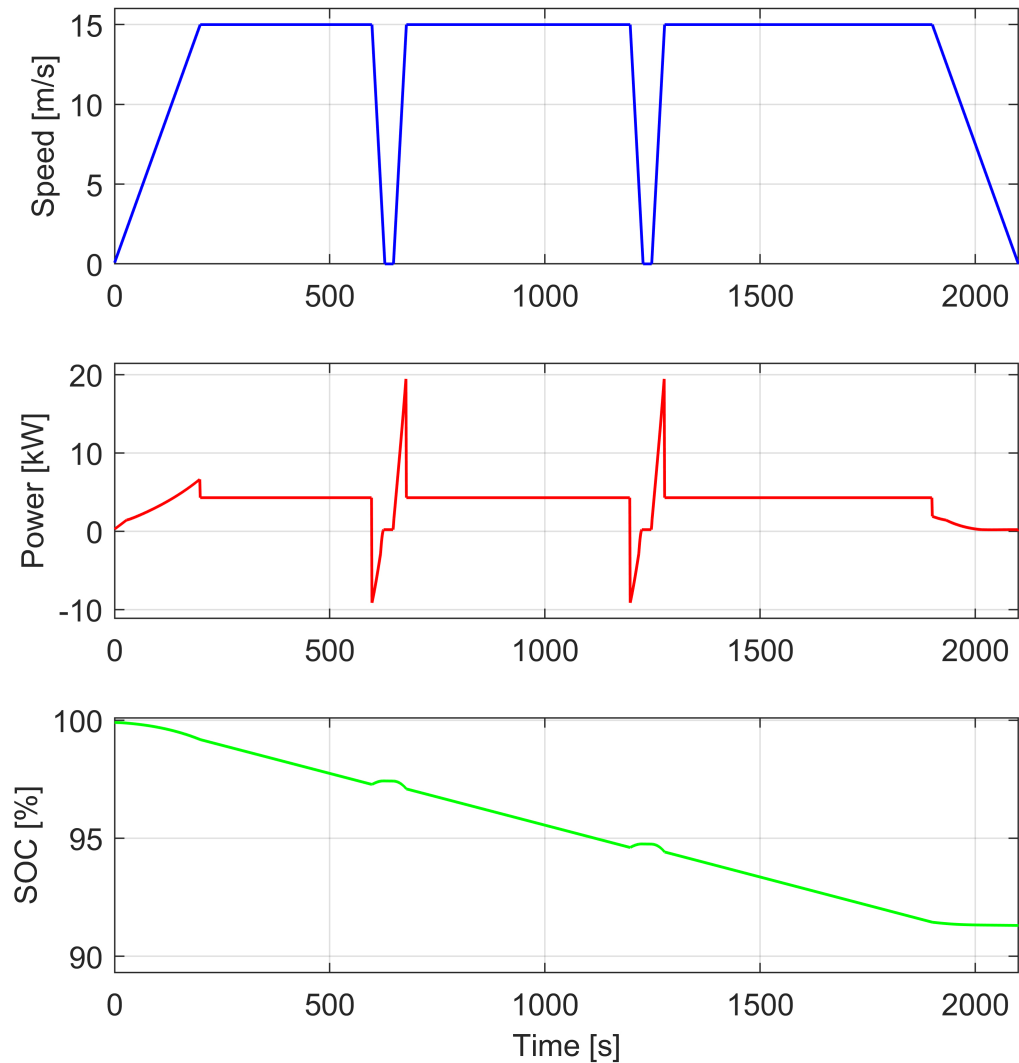
Figure 5.3: Simulated driving cycle (constant speed of 15 m/s) and the respective power profile with SOC estimation with two traffic lights

Number of traffic lights	Energy balance [kWh]
0	2.1185
1	2.1295
2	2.1405
3	2.1515

Table 5.1: Energy balance for simulated routes with and without stops at a constant speed of 15 m/s

5.3.2   Data collection

In this part HERE Map and OpenWeather APIs were used to collect the relevant data to construct the driving cycles and consider the weather conditions that possibly influence the energy consumption for electric vehicles.

5.3.2.1   Graphhopper API data (OSM)

Graphhopper is a Java-based open-source routing library and server that offers a web-based Maps interface and a routing API via HTTP. It uses OpenStreetMap data for routing information and elevation data. This API is fast and efficient and works with Overpass API to obtain the coordinates for any traffic light in a given route. However, the drawback of this API is that it doesn't consider real-time traffic and only returns the maximum possible speed. The real-time traffic can be only considered when routing applications purchased from graphhopper for business purposes such as good's delivery. The speed profile using this API in conjustion with Overpass API for the traffic light is shown in figure 5.4
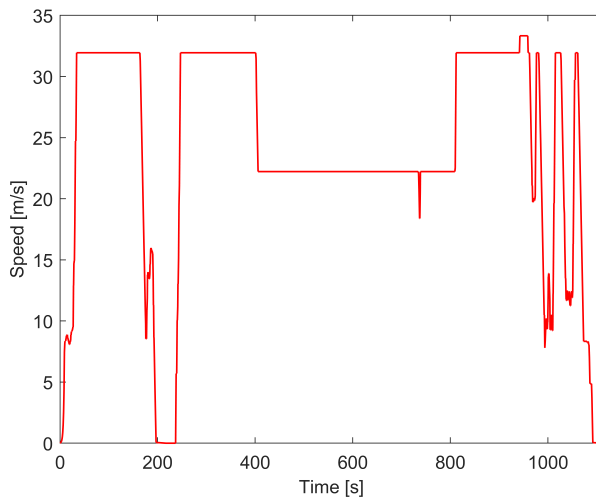
Figure 5.4: Driving cycle obtained from graphhopper API showing the maximum speed and the traffic lights on the route

5.3.2.2   HERE Map API

The HERE Routing API is a JSON RESTful HTTP API that calculates routes between two or more places in various areas across the globe. The HERE Routing API enables users to provide parameters that affect route computation and request extra information about a route to meet particular requirements [164]. The HERE Maps API documentation is provided in the Appendix section.

5.3.2.3 OpenWeatherMap API

OpenWeatherMap API is one of the most popular options for accessing free weather data. Users may make up to 60 requests per minute using the API's extensive free plan. It includes access to current weather data, predictions, and weather maps for many cities around the globe [168]. The inputs for this API and the other related documentation are illustrated in the Appendix section.

5.3.2.4 Comparison with previous implementation

■ Definition on way points:

The manual segmentation performed on the first implementation was based on prior knowledge of the route. Due to the extension of the segments the resolution, and therefore, the accuracy of road data, such as the slope, are compromised. Therefore, the average speed is not returned by the API, but calculated based on time and distance, and the road slope is not applied in the power calculations. With the automatic segmentation, performed by the API at the request, the small length of segments allow the road slope to be considered and the average speed to be returned along with other solicited variables. In this case, we admit the possibility of minor changes in the route according to the traffic at the requested time. These variations are considered acceptable, although a point of attention when validating results. Overall, the number of segments in automatic way-point selection is substantially higher than the one in manual selection. For instance, in Route 1 the number of segments in automatic selection is approximately 5 times the one in manual selection.

■ Integration of data collection and processing:

In the current application, API data are processed immediately after collection on MATLAB. In the previous implementation, data collection is executed on Python, and the API response is saved in a csv file. The driving cycle generation and power calculations are processed in MATLAB. The need to manipulate data and execute scripts between the two platforms is a disadvantage compared to the current application. Table 5.2 and Table 5.3 illustrate the main differences between the data collection in Chapter 4 and Chapter 5.

	Data Collection	Previous Implementation	Current Implementation
API Calling	Version	7	8
	Defining waypoints	Manual	Automatic\Dynamic
Platform	Python		MATLAB
Output Format	.csv Files		MATLAB array/matrix
Integration of data collection and processing	No		Yes

Table 5.2: API data collection main differences between two different implementation

API response	Previous Implementation	Current Implementation
Departure time	Yes	Yes
Departure coordinates	Yes	Yes
Arrival time	Yes	Yes
Arrival coordinates	Yes	Yes
Average speed without traffic	No	Yes
Average speed with traffic	No	Yes
Length	Yes	Yes
Duration without traffic	Yes	Yes
Duration with traffic	Yes	Yes
Road elevation	No	Yes
Speed limit	No	Yes

Table 5.3: API data responses comparison between two different implementation

5.3.3 HERE API response

5.3.3.1 Polyline

- Data decoding (flexible polyline) in Python to obtain list of coordinates.

- Data type conversion (Python tuple to MATLAB matrix containing coordinates "latitude and longitude" and route elevation).

5.3.3.2 Data formatting

- Relevant information is extracted from the Data structure and stored in arrays to facilitate indexing.

- Road slope is calculated based on route elevation for each segment.

5.3.4 OpenWeatherMap response

- Wind speed in driving direction

- Ambient temperature

Segment	1	2	3	...	N -1	N
Distance [m]	5	25	449	...	63	38
Speed In Traffic [m/s]	7.8	7.8	23.3	...	8.1	6.4
Road Elevation [m]	100	100	110	...	95	90
Wind Speed [m/s]	2	2.2	2	...	1.9	1.8
Wind Direction [°]	30	30	31	...	27	27
Ambient Temperature [°C]	20	20	20	...	21	21

Rows "Distance", "Speed In Traffic" and "Road Elevation" belong to **HERE API**. Rows "Wind Speed", "Wind Direction" and "Ambient Temperature" belong to **OpenWeather Map API**.

Table 5.4: Data samples obtained from each API for each segment along the route

5.4 Driving cycle construction and energy estimation

5.4.0.1 Speed profile

The acceleration method used in Chapter 4 is applied in this chapter. To smooth the transition of speed between intervals, we apply acceleration and deceleration rate to the beginning and end of intervals. Based on Nissan Leaf's 2019 performance for acceleration from 0 to 100 km/h, we determine the maximum acceleration on the car (Electric vehicle database). In the equation below, the variables v_1 and v_2 are the speeds of two consecutive intervals. The speed variation Δ_v denotes if the vehicle is accelerating - $\Delta_v > 0, a > 0$ - or decelerating - $\Delta_v < 0, a < 0$. If the speed remains constant between intervals ($\Delta_v = 0$), the acceleration is zero.

It is determined that, for a speed variation equals or greater than 10 km/h, the acceleration function saturates at its maximum value, 3.5 m/s^2. In case of deceleration, the saturation occurs at -3.5 m/s^2. For a variation between 0 and 10 km/h, the acceleration function is linear, in which the coefficient multiplying Δ_v ensures the curve continuity at $\Delta_v = \pm 100 km/h$.

$$a = \begin{cases} \frac{\Delta v}{28.49} \text{ m/s} & \text{if } |\Delta v| < 100 \text{ km/h} \\ \pm 3.51 \text{ m/s} & \text{if } |\Delta v| \geq 100 \text{ km/h} \end{cases} \quad \text{for } \Delta v = v_2 - v_1 \quad (5.1)$$

For each segment, the acceleration and deceleration intervals are based on the speeds from the previous $i - 1$, the actual i and the next $i + 1$ segments. The acceleration occurs at the beginning of the segment, while the deceleration occurs at the end. If none of the conditions below are satisfied, the speed along the segment is constant.

$$\begin{cases} \text{if } v_i > v_{i-1} \text{ then accelerate } (a > 0) \\ \text{if } v_i > v_{i+1} \text{ then decelerate } (a < 0) \end{cases} \quad (5.2)$$
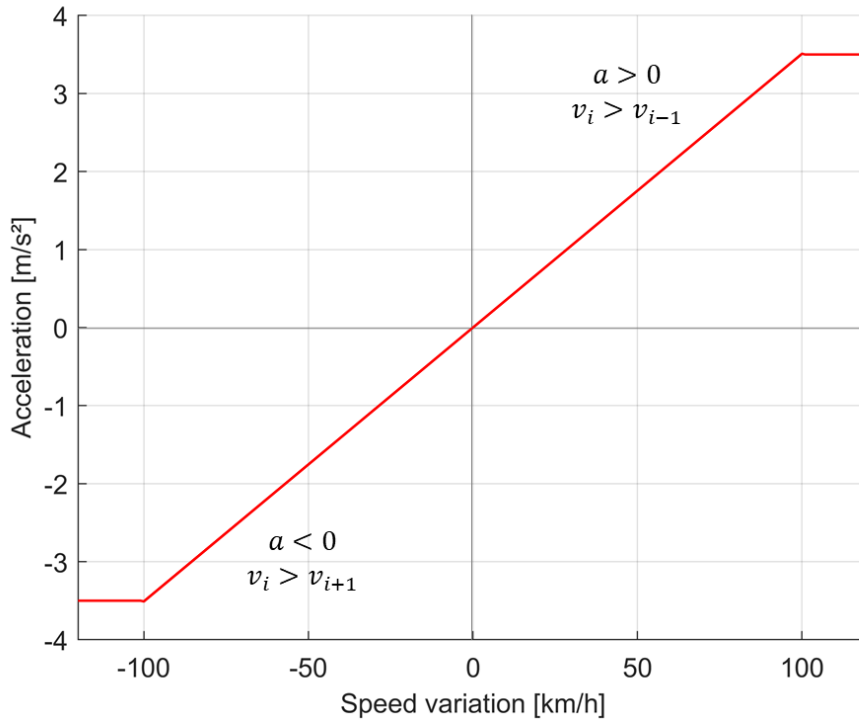
Figure 5.5: Acceleration (a) in function of speed variation (Δv)

In case there is an acceleration, deceleration, or both, we calculate the distance (s_a) and time (t_a) required in acceleration/deceleration. If s_a or t_a are lower than the length of (s_s) or duration (t_s) of the segment, the remaining time of the segment ($t_s - t_a$) has a constant speed (v_i).

If s_a or t_a are higher than the length or duration of the segment, t_a becomes the duration of the segment. In case of acceleration, the speed of actual segment is reduced to the value reached by the end of the segment. In case of deceleration, the speed of the next segment is increased to the value reached by the end of the previous segment. For both cases, we consider the acceleration/deceleration calculated with the original speed values.

$$t_a = \begin{cases} \frac{v_i - v_{i-1}}{a} & \text{if } a > 0 \text{ (acceleration)} \\ \frac{v_{i+1} - v_i}{a} & \text{if } a < 0 (\text{ deceleration }) \end{cases}$$
$$s_a = v_{i-1}t_a + a\frac{t_a{}^2}{2}$$

(5.3)

5.4.1 Adding noise to the speed profile

To simulate the real driving cycle, we add noise to the intervals in which the speed has low variation. The noise is generated as a random numbers based on Gaussian normal distribution in a range $[a, b]$. Given that we admit low variations in speed, a and b are defines as functions of the maximum and minimum speeds in an interval i. The noise addition method was used in Chapter 4 and it can be expressed as:

$$a = -5 \times \frac{1}{\text{minimum}\,(v_i)}$$
$$b = 5 \times \frac{1}{\text{maximum}\,(v_i)} \quad (5.4)$$

To ensure that the noise addition does not interfere in the travelled distance and the average speed we used the same equation in Chapter 4 to correct it as follows:

$$n_{i\ corrected} = n_i - \overline{n}, \quad i = 1, 2, \cdots, N \quad (5.5)$$

5.4.2 Smoothing function

Moreover, the smoothing function used in the previous chapter was used to deal with sharp edges on the speed profile due to speed change or noise addition to representing the actual driving patterns. Figure 5.6 shows the initial driving cycle of untreated data from the API and the one after processing using the above methodology. It can be noticed that this driving cycle was performed in the early morning when the route is busier than usual, and that appears when the speeds drop down in the Motorway. Moreover, we receive more segments from the API when we apply the dynamic segmentation selected by the API instead of manually configuring the waypoints to identify the route segments, such as the one in chapter 4. This method enhances the accuracy of the average speed of each segment and enables us to obtain the road slope for them. LOESS (locally estimated scatterplot smoothing) is a method of non-parametric regression that produces a smooth curve by locally fitting polynomial functions. Thus the fitted values of the velocity over time, in this case, are determined with neighbouring subsets of data [169]. This method and its percentage of samples are chosen based on a qualitative evaluation of the final driving cycle. The main criteria are the decrease of sharp edges, preservation of noise-induced variations and preservation of the cycle when compared to its pre-processing shape. The cycle must start and end at or near the speed of $0\ m/s$, which is only sometimes possible in the smoothing function. Furthermore, to overcome this situation, the speed curve is linearly interpolated from zero to the speed value of the nearest speed provided in the first and last segments at the start and the end of the route.
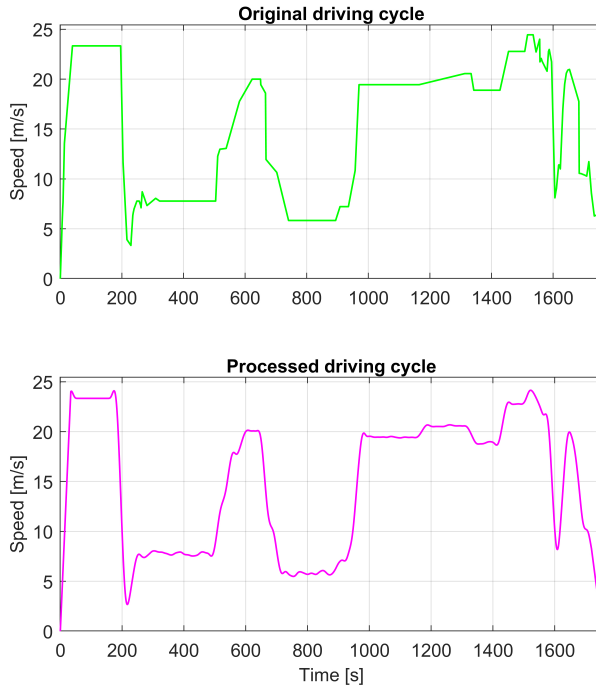
Figure 5.6: Driving cycles for Route 2 using HERE Map Data

5.5   Power profile generation

In Figure 4.17 in chapter 4; the diagram of components, power, and force on the applied EV model is depicted. With the vehicle's speed determined in the driving cycle, we calculate the power consumed to propel the vehicle or, in the case of braking, the power provided to the battery. In the previous implementation, we considered the road slope $a = 0$. However, we obtain the road slope at every segment in this chapter. The traction force F_t is composed of rolling friction, grade resistance, aerodynamic drag, and acceleration force. We can obtain the total force by using the following equation:

$$F_t(t) = F_r(t) + F_g(t) + F_d(t) + F_a(t) \tag{5.6}$$

Starting

- The rolling resistance, force resisting the movement of the tires on the road surface:

$$F_r(t) = \mu_r m_v g \, \cos a \tag{5.7}$$

- Grade resistance, gravitational force acting on the vehicle when it travels along a sloping road:

$$F_g(t) = m_v g \sin a \tag{5.8}$$

- Aerodynamic drag, force opposing the vehicle motion through the air, where the wind speed is considered this time:

$$F_d(t) = \frac{1}{2}\rho C_d A_{vf}(v(t) - W(t))^2 \tag{5.9}$$

- Acceleration force, in which the rotational acceleration is expressed with an additional mass m_r, representing the inertia of rotating components:

$$F_a(t) = (m_r + m_v)a(t) \tag{5.10}$$

Where:

$$m_r = (0.04 + 0.0025G^2) \times m_c \tag{5.11}$$

In Addition to the list of variables used in Chapter 4, Table 4.9 we added the following variables:

Environment parameters	
Abbreviation	Parameter
ρ	air density
T_{amb}	average ambient temperature along the route
W	wind speed in driving direction $[m/s]$

Table 5.5: environmental parameters obtained from OpenWeatherMaps API

- The traction power at the wheels is function of the traction force and the vehicle speed.

$$P_t = F_t(t) \times v(t) \tag{5.12}$$

- To calculate the output power of the motor, we consider the efficiency of the transmission system $\eta_t s$. Therefore, in case of motoring (battery discharge), P_t is positive, and P_{out} is expressed by:

$$P_{out}(t) = \frac{P_t(t)}{\eta_{ts}} \tag{5.13}$$

5.5.1   Regenerative braking

In case of battery charge, when P_t is negative, and a regeneration factor η_{brake} must be considered in P_{out} as well. Expressed in terms of the speed, η_{brake} denotes the power available for recuperation in regenerative braking, considering torque and speed condition [44].

$$P_{out}(t) = P_t \times \eta_{ts} \times \eta_{brake} \tag{5.14}$$

$$n_{brake} = \begin{cases} 0 & \text{if } 0 \leq v(t) < l_1 \\ k_1 \times v(t) + k_2 & \text{if } l_1 \leq v(t) < l_2 \\ 1 & \text{if } v(t) \geq l_2 \end{cases}$$

where l_1 and l_2 are speed thresholds, based on the characteristics of the vehicle, and k_1 and k_2 are fitting constants. l_1 is the speed from which the vehicle starts recuperating energy. For higher speeds l_2, the regenerative factor reaches its maximum value, 1. Between l_1 and l_2, the behavior of η_{brake} is assumed to be linear, starting at 0 and finishing at 1.

- The input power of the motor is function of its output power and efficiency as motor or generator, determined with look-up tables proposed in [52]. In case of motoring, $P_{out} > 0$ and P_{in} is expressed by:

$$P_{in}(t) = \frac{P_{out}(t)}{\eta_m} \tag{5.15}$$

- In case of regenerative braking, $P_{out} < 0$ and P_{in} is:

$$P_{in}(t) = P_{out}(t) \times \eta_m \tag{5.16}$$

- Finally, the power provided or received by the battery P_b is the sum of the motor input power and the power consumed by vehicle accessories P_{va}, such as air conditioner and light system.

$$P_b(t) = P_{in}(t) + P_{va} \tag{5.17}$$

5.5.2 Auxiliary system and ambient temperature

The power consumed by the auxiliary system is considered as a function of the average ambient temperature along the route (T_{amb}) as it is associated with heating and air conditioning. Between $-15°$ and $20°$, the power varies linearly from 6000 W to 200 W [52]. In order to cover a wider range of ambient temperature, we consider the samve variation of temperature and power and determine a symmetric linear function for the interval from $20°$ to $55°$. For temperature values outside the range from $-15°$ to $55°$, the power is considered constant at its maximum.

$$\begin{cases} \text{if } -15 \leq T_{amb} < 20 \text{ then } P_{va} = -165.71 \times T_{amb} + 3514.3 \\ \text{if } 20 \leq T_{amb} \leq 55 \text{ then } P_{va} = 165.71 \times T_{amb} - 3114.3 \\ \text{if } T_{amb} < -15 \text{ or } T_{amb} > 55 \text{ then } P_{va} = 600 \end{cases}$$
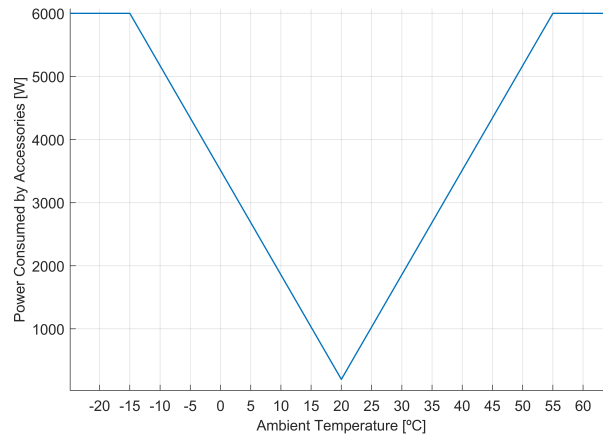
Figure 5.7: Power consumed by accessories (P_{va}) in function of ambient temperature along the route (T_{amb})

5.5.3 Temperature and auxiliary power

In order to demonstrate the impact of auxiliary consumption during a trip, we run the application for Route 2 with different levels of average ambient temperature as shown in Tables 5.6 and 5.7. The tests are executed sequentially to achieve a low variation of average speed, which allows us to compare the energy balance and final SOC values obtained. Comparing the results for maximum and minimum values auxiliary power, we observe a variation of 2.07 kWh in the energy balance. This variation represents approximately 66% of the basic energy balance (not considering auxiliary power) for this route. The percentage impact of auxiliary consumption is less substantial in situations where the basic energy balance higher in longer routes, or in higher levels of average speed, for example. Nonetheless, with a higher basic consumption, the power consumed by accessories can became an important contribution and a concern in terms of driving range. Therefore, it is important to consider the auxiliary power, especially as a function of driving conditions, when predicting the EV energy consumption.

Test (~6 pm GMT)	Duration [s]	Length [m]	Average Speed [m/s]	Temperature [°C]	Auxiliary Power [kW]	Energy Balance [kWh]	SOC [%]	Balance variation [kWh]	SOC Variation [%]
1	1313	26033.24	19.83	-15	6.000	5.36	78.11	0.31	-1.26
2	1321	26040.76	19.71	-10	5.171	5.05	79.37	0.30	-1.23
3	1317	26054.06	19.78	-5	4.343	4.75	80.60	0.30	-1.26
4	1299	26028.12	20.04	0	3.514	4.45	81.86	0.29	-1.15
5	1300	26035.53	20.03	5	2.686	4.16	83.01	0.27	-1.12
6	1291	26028.78	20.16	10	1.857	3.89	84.13	0.29	-1.17
7	1278	26069.51	20.40	15	1.029	3.6	85.30	0.31	-1.26
8	1285	26077.53	20.29	20	0.200	3.29	86.56	-	-
AVERAGE	1300.5	26045.94	20.03	-	-	-	82.37	0.30	-1.21
STD DEVIATION	15.53	19.00	0.25	-	-	-	2.93	0.01	0.06

Auxiliary Consumption [kWh]	Max Power	Min Power
	2.1883	0.0714

Table 5.6: Tests on evaluating the auxiliary consumption in kWh by tuning the temperature from the lowest to the optimal temperature.

Test (~6 pm GMT)	Duration [s]	Length [m]	Average Speed [m/s]	Temperature [ºC]	Auxiliary Power [kW]	Energy Balance [kWh]	SOC [%]	Balance variation [kWh]	SOC Variation [%]
8	1285	26077.53	20.29	20	0.2	3.29	86.56	-0.31	1.26
9	1286	26134.15	20.32	25	1.028	3.60	85.30	-0.35	1.42
10	1261	26085.97	20.69	30	1.857	3.95	83.88	-0.29	1.22
11	1272	26005.87	20.44	35	2.685	4.24	82.66	-0.27	1.09
12	1272	26013.09	20.45	40	3.514	4.51	81.57	-0.29	1.17
13	1276	26008.26	20.38	45	4.343	4.80	80.40	-0.28	1.15
14	1274	26016.31	20.42	50	5.171	5.08	79.25	-0.31	1.29
15	1273	26023.49	20.44	55	6	5.39	77.96	-	-
AVERAGE	**1274.875**	**26045.58**	**20.43**	-	-	-	**82.20**	**-0.30**	**1.23**
STD DEVIATION	**7.94**	**47.61**	**0.12**	-	-	-	**2.98**	**0.03**	**0.11**

Table 5.7: Tests on evaluating the auxiliary consumption in kWh by tuning the temperature from the optimal to the highest temperature.

5.5.3.1 SOC estimation

For the state-of-charge estimation we used the model proposed in [37]. This model was used also in Chapter 4, and it has been validated against a real battery experiments. The battery model characteristics shown in Figure 4.18. Figure 5.8 shows the power profile and the SOC estimation for Route 1, this journey was captured during the afternoon when the traffic is smooth and quiet.
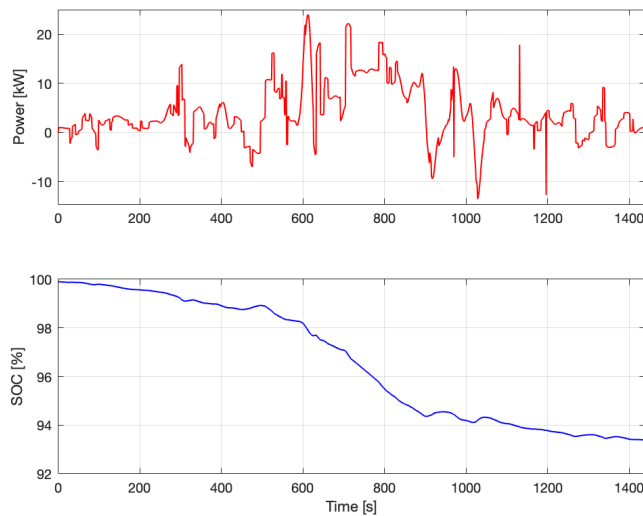
Figure 5.8: Power profile and SOC estimation for Route 1 during the middle of the day

5.6 Results and discussion

In this section, three driving cycles were constructed using HERE Maps API. We considered an extended route to the previous routes as this implementation does not need previous way-points configuration.

5.6.1 Route 1

Figure 5.9 illustrates the driving cycle for Route 1. Compared to the driving cycles of the same route presented in the previous chapter Figure 4.15, we can notice a slight similarity in the speed patterns; however, there is a higher variation due to the intensive route segmentation. Contrarily to manual segmentation, which requires prior knowledge from the user, the routing technique in this section is route-independent and follows the fastest route in every execution. Therefore, this method leads to variations in the speed profile, as we notice in Figure 5.9.

Figure 5.9: Route 1 driving cycle performed in early morning using HERE Maps API

The power consumption and the SOC estimation for the above journey are depicted in Figure 5.10. The power profile presents higher variation due to many factors, such as regenerative braking, road slope resistance and wind direction/speed consideration. Moreover, the higher number of segments on this implementation also contributes to the power variation. The higher and lower power are similar to the ones for the same journey performed using previous implementation in Figure 4.21.
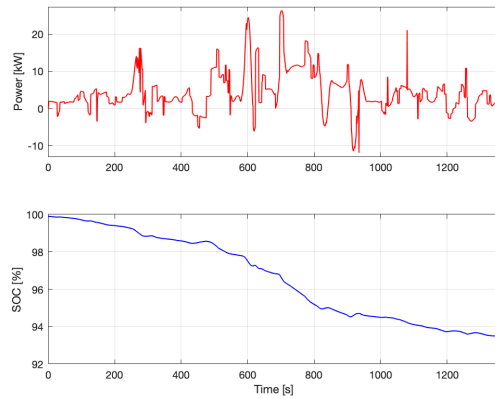
Figure 5.10: Power profile and energy consumption estimation for Route 1 driving cycle

5.6.2 Route 2

For Route 2, the driving cycle is shown in Figure 5.11. It presents close resemblance to the lower bound profile, shown in Figure 4.15, in terms of shape, although it has different speed limits. We observe higher levels of acceleration and deceleration due to the increased number of segments provided by the API and the presence of a motorway in the route. Therefore, the power profile in Figure 5.12 shows higher variation and higher power consumption compared to the power profile in Figure 4.22.

Figure 5.11: Route 2 driving cycle performed in early morning using HERE Maps API
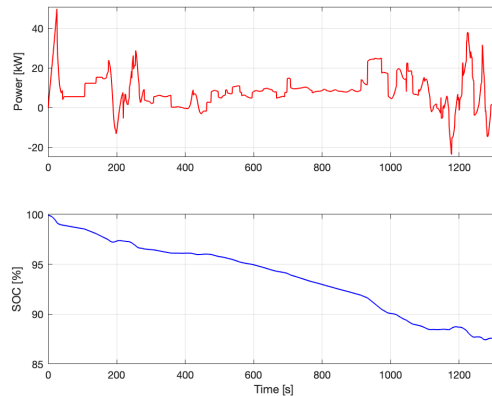
Figure 5.12: Power profile and energy consumption estimation for Route 2 driving cycle

5.6.3 Extended Route

The following route demonstrates the flexibility of adapting the application to any route covered by HERE Maps. It shows a long route with various road structures involving a motorway, city driving, dual and single carriageways. It also has different road characteristics, such as different road gradients and many direction changes. For instance, the driving cycle in Figure 5.13 shows a lower speed at the beginning and the end of the route with significant variations due to the city, village driving, different speed limits and traffic. However, the middle of the route shows higher speed and lower variation where the journey passes through the motorway. The power profile and the SOC estimation show this journey's intensive power demand and energy consumption Figure 5.14. The length of the journey is 64.17 miles, and it consumes more than 60% of a fully charged battery considering the Nissan Leaf EV's battery model, as considered in the previous chapter.

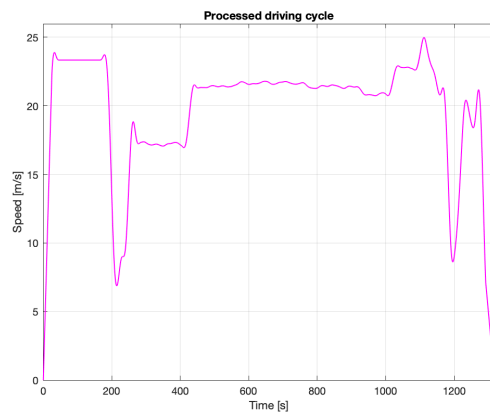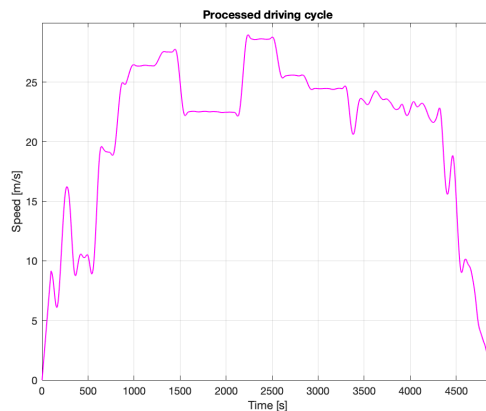Figure 5.13: The extended Route driving cycle performed in early morning using HERE Maps API
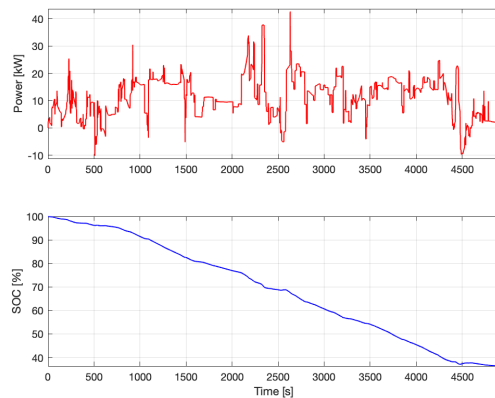
Figure 5.14: Power profile and energy consumption estimation for the extended Route driving cycle

5.7 Conclusion

This chapter uses HERE Map API as the primary data source to request and retrieve the routing and traffic-related required data for developing driving cycles and calculating electric vehicles' energy consumption.

With the methods discussed in chapter 4 for the driving cycle construction, acceleration/deceleration, noise and smoothing, we can approximate the retrieved API data to a real driving cycle. The generated speed profile is feasible in speed transition and considers slight variations through the noise and curve smoothing, keeping a low error in travelled distance and route duration. We managed to improve the results by collecting data at execution time and processing more variables, such as wind speed and ambient temperature. These improvements allow us to have more precise accuracy in energy consumption prediction and SOC estimation. This accuracy can be validated by performing real journeys using the actual EV. In addition, we have faster responses and more reliable applications to retrieve and process the required data.

The results validated the driving cycles' range in chapter 4 and introduced more variations within the journey. This chapter also presented and examined the impact of traffic lights on the route and evaluated their influence. It also evaluated the impact of using the auxiliary systems on the EV when using the AC and the heating system on several journeys. Even though the traffic lights consideration does not contribute significantly to energy consumption, it was impossible to integrate the Overpass API with HERE Map API to allocate the traffic lights within the route and predict whether they are green or red. This process might limit the driving cycles from being more accurate and realistic. Therefore, finding a reliable, more compatible data source that works with maps API to identify the traffic lights on any route on the map on the run-time will be interesting.

6

EXPERIMENTAL RESULTS FOR ALL GENERATED DRIVING CYCLES

Contents

6.1   Summary

This chapter illustrates part of the laboratory experiments for battery dynamics and SOC estimation. In addition, it presents an overview of the equipment used for validation, including batteries, software and hardware. Finally, these results are compared to SOC and power profiles generated with the implemented battery model.

In the experiments, the battery experts extract the current profiles of the driving cycles considering their battery characteristics. Then, they import the current as an urban driving cycle load to discharge the battery. The output, which consists of battery voltage and current, is recorded with the EC-Lab software and exported to a spreadsheet.

The experimental data are compared to our model's power, SOC and energy balance results. We estimate the SOC from both sources with the Coulomb counting methods. The analysis of the validation will be discussed in the forthcoming sections.

6.2   Introduction

Even though the constructed driving cycles in this research are realistic and within the range of the current standard driving cycles, we can validate them using several techniques. One validation approach is to analyse and evaluate the generated driving cycles against the driving cycles in the literature. Another approach is to generate a real journey physically using the same route and the exact vehicle's specification and trip time. However, this approach is time-consuming and can add congestion to the traffic, which is not efficient and environmentally friendly. Therefore, the driving cycle's validity is possible when used to discharge a real battery available in some laboratories; then, we can analyse the battery's outputs and compare them to the model's output, including power demand and SOC estimation.

6.3   Testing tools and equipment

6.3.1   Battery specifications

The battery module used for these experiments is from first generation Nissan Leaf EV with 56 Ah capacity and up to $\pm$ 100 A. The driving cycles were converted to current profiles for each cycle, then imported to EC-lab software as urban profile to cycle the module. The data was recorded in the EC-lab, exported to Excel files, and plotted in terms of voltage, energy and capacity. Figure 6.1 shows the battery module used for performing the validation tests.

Figure 6.1: Battery module from first generation Nissan Leaf EV (li-ion)

6.3.2 Software

The software used to control the validation process is called: BioLogic EC-Lab Software [170]. EC-Lab helps to control multiple devices using a single interface, providing centralised experiments control. It is mainly used to analyse the performance of energy, fuel cells and batteries. The software is user-friendly; it simplifies the workflow and helps the user to work more efficiently.

6.4 Battery dynamics, power profile and SOC validation for driving cycles based on three APIs data

This section will provide insight into the validated results carried out at the lab using the above techniques and tools. It will illustrate the battery dynamics for one cycle for each API, including the voltage, current, power and SOC profiles. Furthermore, it will focus on the energy statistical data and show the differences in energy consumption on each cycle. This section includes the driving cycles produced in Chapter 4 based on three different APIs. The SOC and the power profiles were considered in the following comparisons for four driving cycles. The other driving cycles and the battery dynamics, such as voltage and current profiles, will be added to the appendices. The driving cycles generated using dynamic route data retrievals, as described in chapter 5, can be validated using the same techniques and equipment. The longer route driving cycles need further analysis before performing any validation process.
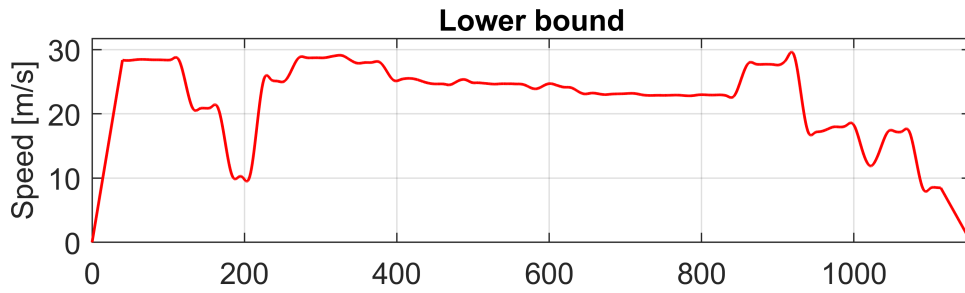
Figure 6.2: Speed profile for Route 2 recorded on February 11$^{\text{th}}$, 2020 at 00:23 (Data source: Google API)
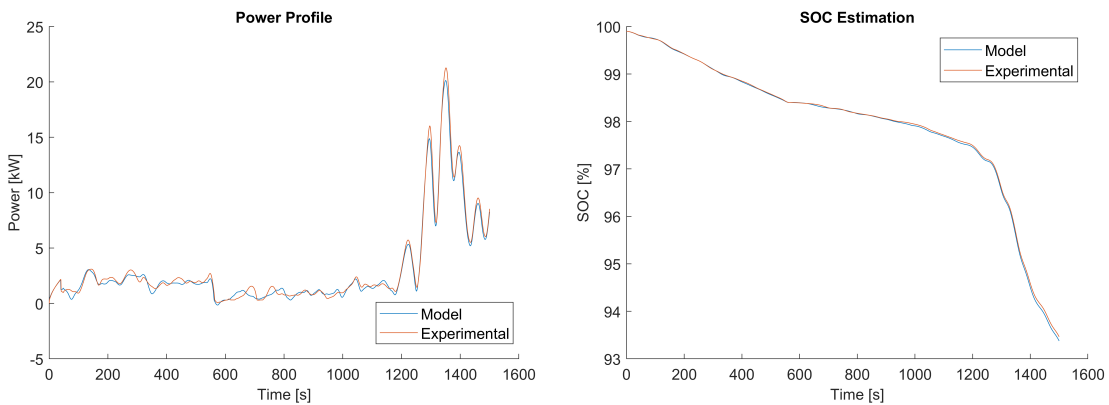
(a) Power profile

(b) SOC estimation

Figure 6.3: Model and experiment output for Route 1 on February 11$^{\text{th}}$, 2020, at 00:00 (Data source: Google Map API)
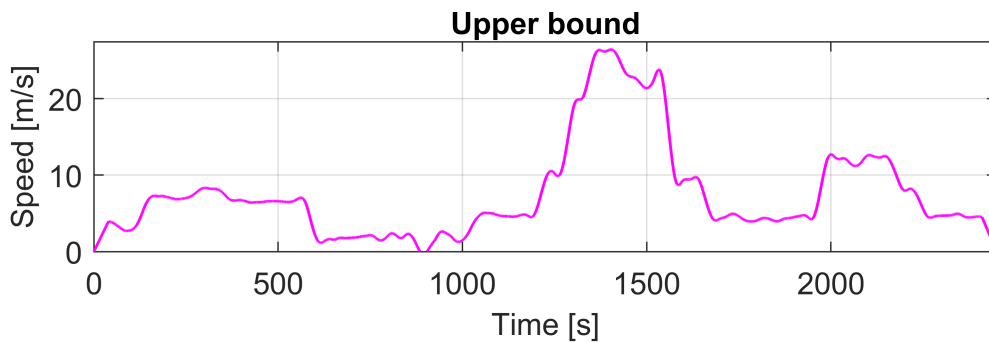
Figure 6.4: Speed profile for Route 1 recorded on October 23$^{\text{rd}}$, at 16:45 (Data source: Google API)

(a) Power profile

(b) SOC estimation
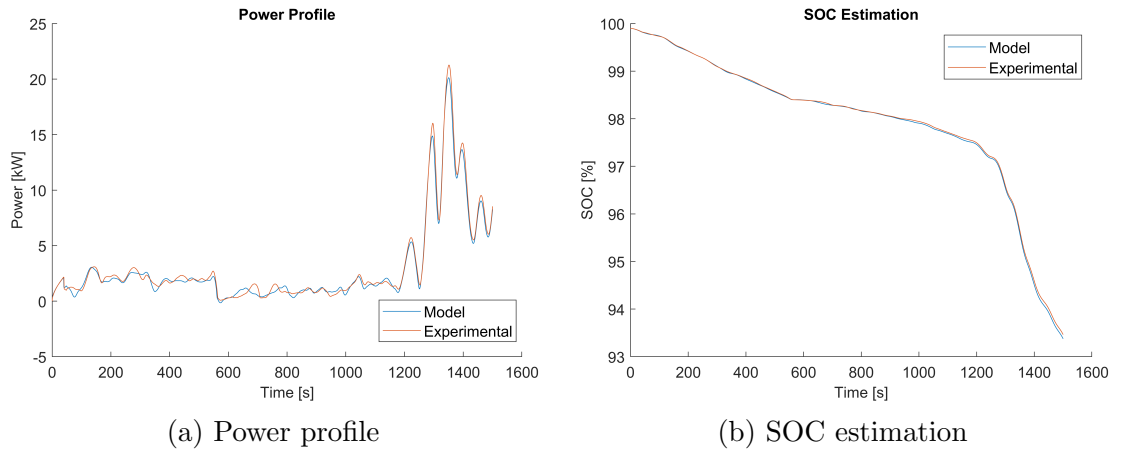
Figure 6.5: Model and real experiment output for Route 1 on October 23$^{\text{rd}}$, 2019, at 16:45 (Data source: Google API)
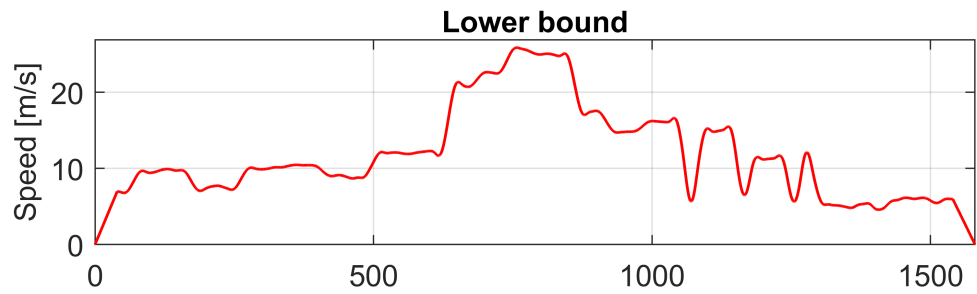
Figure 6.6: Speed profile for Route 1 on September 19$^{\text{th}}$, 2019, at 00:30 (Data source: HERE Maps API)

(a) Power profile

(b) SOC estimation
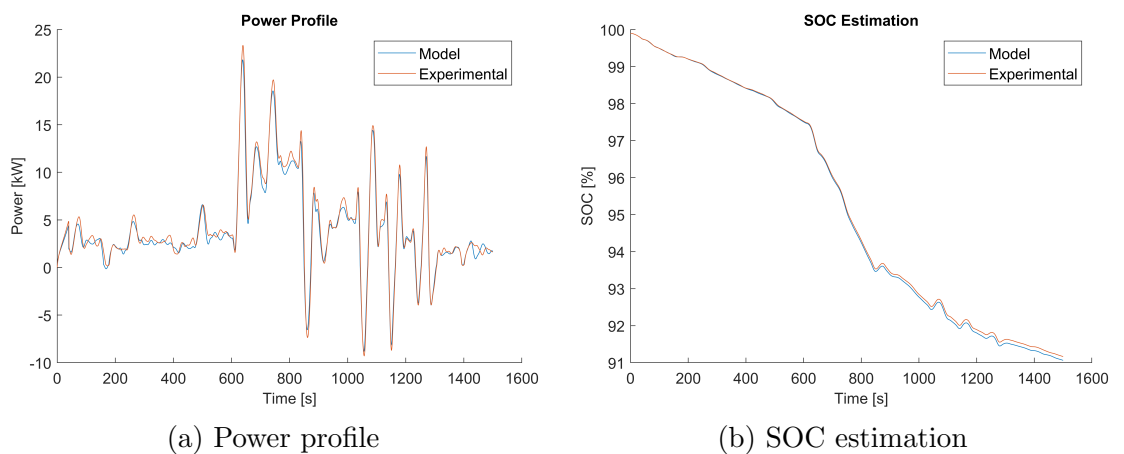
Figure 6.7: Model and real experiment output for Route 1 on September 19$^{\text{th}}$, 2019, at 00:30 (Data source: HERE Maps API)
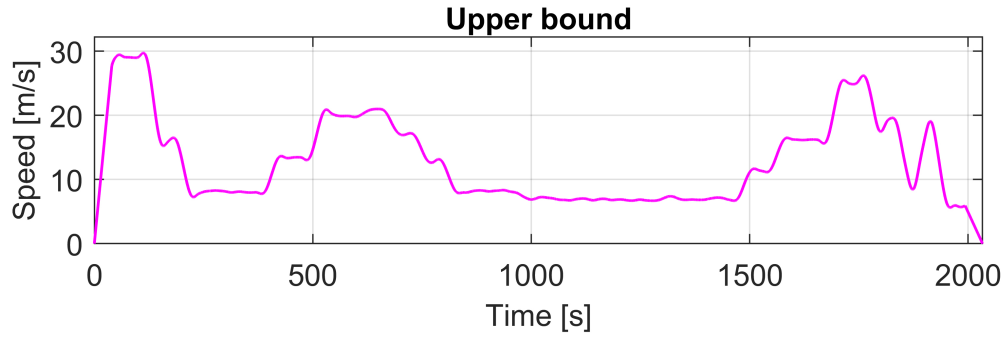
Figure 6.8: Speed profile for Route 2 on October 3rd, 2019, at 16:45 (Data source: TomTom API)

(a) Power profile

(b) SOC estimation
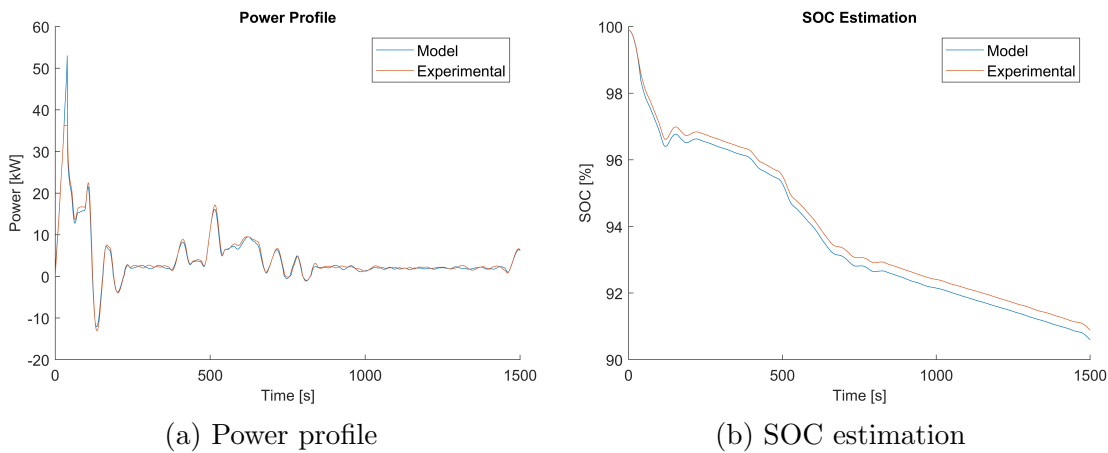
Figure 6.9: Model and real experiment output for Route 2 on October 3rd, 16:45 (Data source: TomTom API)

6.4.1   Comparison analysis

This section compared theoretical and experimental results for some of the driving cycles with high and low traffic (Upper and lower bounds for speed). The theoretical results refer to the data obtained with the presented model. Experimental data was generated in the university laboratory using the EC-Lab software. Figures 6.2, 6.4, 6.6 and 6.8 above present the speed profiles for the corresponding driving cycles we validated. In addition, power profiles and SOC estimation of the above driving cycles are illustrated in Figures 6.3, 6.5, 6.7 and 6.9.

Theoretical and experimental battery power and SOC curves present very similar behaviour in all the studied cycles. Overall, by comparing the speed cycle with the power profile and the SOC estimation, we observe that power peaks coincide with the most significant variations in speed. In high deceleration, we notice negative peaks in power and ceases in SOC provided by the regenerative braking. Contrarily, in the case of high acceleration, the power profile shows positive peaks, while the SOC estimation varies.

Route	API	Traffic	Median Absolute Percentage Error [%]		
			Current	Power	Energy Balance
1	Google	High	11.24	11.00	5.14
		Low	7.16	10.01	9.44
	HERE	High	8.87	10.08	6.46
		Low	9.13	12.04	8.54
	TomTom	Low	6.87	8.71	7.59
2	Google	Low	5.94	9.70	4.90
	HERE	Low	5.91	5.91	2.66
	TomTom	High	6.22	7.68	2.77

Table 6.1: Median Absolute Percentage Error in Power Profiles by Drive Cycle.

In the SOC estimation, the curves grow apart throughout the route as our SOC estimation decreases faster than the experimental curve. This variation is explained by the difference in battery capacity values considered in the model and the experiment.

Due to memory limitations of the testing device used in the experiments, two of the upper-bound speed cycles - Google's data for Route 1 Figures 6.4 and 6.5 and Tom-Tom's data for Route 2 Figures 6.8 and 6.9 are partially analysed. The respective power and SOC profiles present 61% and 73% of the total route duration.

6.4.2   Statistical analysis

To assess the model performance, we start by calculating the absolute percentage error between validation and model values for each point in a cycle. Then, given the resulting right-skewed error distributions, we choose the median as a central tendency measure, allowing us to summarise these calculations for each cycle. This choice also reduces the impact of extreme error values, derived mainly from power peaks, beginnings, and ending of cycles. Table 6.1 presents the median absolute percentage errors for current, power and energy balance. Across all cycles, the average error is 7.7% for current, 9.4% for power, and 5.9% for energy balance. Furthermore, this shows that power curves represent the most significant area for development. However, considering that several functions and parameters in the model are approximations, we consider these acceptable ranges of error. Finally, comparing our results with the experimental data allows us to validate the model response. It also provides a reference for future improvements, such as adjusting parameters and refining or adding auxiliary functions, for instance, estimating the rolling resistance coefficient and power consumed by accessories.

6.5   Conclusion

This chapter used four driving cycles from 3 different map APIs, twelve in total, to compare the battery model output to the actual experiments performed. In addition, eight driving cycle outputs were used for the statistical analysis to illustrate an insight into the percentage error and behaviour similarity between the model and the actual

battery. Finally, we generated battery current and power demand for each journey, and the battery experts used these profiles to discharge the Nissan Leaf battery in the laboratory. In addition, comparing our results with the experimental data allows us to confirm the model's consistency. This validation will also support us as a reference for further improvements, such as adjusting parameters and refining or adding auxiliary functions, i.e. the estimation of the rolling resistance coefficient and power consumed by accessories. Furthermore, the software used to capture the battery dynamics in the lab has limited memory leading to some inconsistency in some of the validation results; therefore, some validation will be repeated. In addition, more driving cycles can be validated using the method we implemented in chapter 5 after we studied the possible approach to avoid any memory issues or data inconsistency caused by longer routes.

Conclusions, Limitations and Future work

7.1 Summary

This chapter summarises the whole thesis, emphasises the contributions and outlines the work achieved in each chapter. In addition, it will present the limitations and challenges of this domain. Finally, it outlines and discusses the potential future work.

7.2 Thesis summary

Chapter 2: This chapter provided an overview of the technology behind electric vehicles, discussing its history and the obstacles it faces. In addition, it has analysed the previously conducted research on this area. Finally, it focused on research that considers outside factors in predicting the energy consumption of EVs.

Chapter 3 This chapter presented power profiles for four standard driving cycles. First, it processed the driving cycle data, which consists of velocity versus time, to find the parameters to calculate the power profile for each cycle. Then, it generated power profiles to show the differences in the SOC when the traffic conditions influence the driving patterns. Each profile was used as power inputs for two generic battery models, namely the Equivalent Circuit and Shepherd's mathematical models. These models were configured using MATLAB scripts and SIMULINK blocks to estimate the SOC and capture the voltage and current dynamics of the battery. The models were explained in detail, along with their limitations. Finally, the simulation, SOC estimation and voltage measurement results were discussed and analysed.

Chapter 4 This chapter constructed different driving cycles based on three API data and two routes. It presented a data collection framework to gather the same data from different APIs and process the data to generate realistic driving cycles. We divided the routes into slices using the route segmentation technique. The data contain the distance, the time taken for the whole journey, the average speed for the whole journey, and the waypoints. We developed a velocity model algorithm and introduced variations using a random function based on Gaussian normal distribution. After introducing randomness to the mean data extracted from the APIs, we used the locally weighted scatterplot smoothing function "LOWESS" in MATLAB to fit a smooth curve to the

randomised data and eliminate any sharp edges. The data selection is based on data classification and statistical analysis. An electric vehicle model based on the Nissan Leaf was implemented to calculate each cycle's power demand and the remaining range.

Furthermore, this chapter shows that the generated driving cycles are within the range of the existing ones, and the vehicle's constraints are satisfied. Moreover, it stimulates an acceptable driving pattern for each cycle. The results also show the variation between the different data sources and the times for the data collection. The state of charge estimation for each cycle and route varies for each route and data source. The route includes motorway driving, shows massive energy consumption when the vehicle manages to drive at the highest speed limit and shows less energy consumption when the traffic density restricts the speed. In contrast, the results also show less energy efficiency for city driving when the traffic is dense because the journey time is longer.

Chapter 5 and retrieve the routing and traffic-related required data for developing driving cycles and calculating electric vehicles' energy consumption.

With methods discussed in chapter 4 for the driving cycle construction, acceleration/deceleration, noise and smoothing, we can approximate the retrieved API data to a real driving cycle. The generated speed profile is feasible in speed transition and considers slight variations through the noise and curve smoothing, keeping the minimal error in travelled distance and route duration. We improved the results by collecting data at execution time and processing more variables, such as wind speed and ambient temperature, which have a less significant impact in normal conditions. These improvements allow us to achieve higher energy consumption prediction and SOC estimation accuracy. In addition, we have faster responses and more reliable applications to retrieve and process the required data. The results validated the driving cycles' range in chapter 4 and introduced more variations within the journey. This chapter also presented and examined the impact of traffic lights on the route and evaluated their influence. It also evaluated the impact of using the auxiliary systems on the EV when using the AC and the heating system on several journeys.

Chapter 6 This chapter used four driving cycles from 3 different map APIs, twelve in total, to compare the battery model output to the actual experiments performed. In addition, eight driving cycle outputs were used for the statistical analysis to illustrate an insight into the percentage error and behaviour similarity between the model and the actual battery. Finally, we generated battery current and power demand for each journey, and the battery experts used these profiles to discharge the Nissan Leaf battery in the laboratory. In addition, comparing our results with the experimental data allows us to confirm the model's consistency. This validation will also support us as a reference for further improvements, such as adjusting parameters and refining or adding auxiliary functions, i.e. the estimation of the rolling resistance coefficient and power consumed by accessories. Furthermore, the software used to capture the battery dynamics in the lab has limited memory leading to some inconsistency in some of the validation results; therefore, some validation will be repeated. In addition, more driving cycles can be validated using the method we implemented in chapter 5 after we studied the possible approach to avoid any memory issues or data inconsistency caused by longer routes.

The proposed approach could also be improved by applying different techniques to

enhance the estimation accuracy. For instance, machine learning techniques can be considered to use the real world for driving and traffic and energy consumption measurements. In addition, combining the presented model with other techniques could also improve the accuracy of the proposed approach. These techniques include but are not limited to, using deep learning to detect vehicle speed based on video streams and neural network methods to predict vehicle velocity based on real-traffic information. It is also possible to investigate and study the driving behaviours of multiple regions and cities. The driving patterns of each driver are different; therefore, it significantly impacts energy consumption. Understanding how the driver reacts to the traffic situation is an exciting area; this could be combined with existing models to estimate the power demand for EVs better. However, this involves many challenges, such as accessing the drivers' data and sensing the driving behaviours. In addition, the map service providers are expanding and improving the data quality and reliability. Therefore, it can help improve EV estimation by providing more detailed data for the routes and traffic.

7.3 Limitations

The limitations in this thesis can be classified in five categories:

7.3.1 Capturing the real-time traffic precisely

The map's real-time traffic situation can only be obtained using the existing maps service providers. The existing maps information providers are competing with one another, and they are careful of collecting their data; therefore, they have introduced some obstacles to avoid any competitors from gathering the data regularly. They offered to sell some of their historical data; however, it is less valuable since they are minimal. This limitation made it quite difficult for us to collect more data that can allow us to study the traffic patterns to improve the velocity estimation within the route.

7.3.2 Predicting the driving behaviours

This is one of the most challenging parts of this domain, even with conventional vehicles. Although the roads are restricted with speed limits and traffic congestion, it has been vital to estimate the driver's behaviours over the route. Every driver is unique, and the driving patterns can be influenced by multiple factors, including emotional, psychological and cultural behaviours. These factors might significantly impact the rate of acceleration and deceleration. Hence, this will significantly affect the battery discharging rate and energy consumption.

7.3.3 Smooth integration of different data sources

The data needed to have a better estimation on electric vehicles, including but not limited to; traffic status, speed limits, route information, weather information. These parameters cannot be obtained using a single data source to achieve real-time estimation or estimate the energy consumption for the route ahead before starting the journey. For instance, the route and traffic information can be collected using Tom-Tom Maps. However, it is challenging to integrate another API to collect the weather data for the same route. Another example can be integrating another API besides HERE Maps to collect the coordinates for every traffic light on the route, as discussed in chapter 5.

7.3.4 Accessing historical data

Many organisations can cooperate in providing historical data recorded for a single or multiple routes. These data might include the number of cars passing in a particular street, vehicle's speed, and much more. This kind of data can only be analysed within the road or city where the data was collected; therefore, it is less helpful to apply to other routes.

7.3.5 Making more generic estimation

Estimating the energy consumption for an electric vehicle can be challenging even if we have the necessary data for the estimation parameters. This challenge includes the variations on the current models of electric vehicles, and this variation includes the maximum range of each model that it can travel. Thus, if we managed to estimate the energy consumption for an average vehicle that can travel for 200 miles within a single charge, then the estimation can be less accurate for vehicles with less range.

7.4 Future direction

There are several future directions beyond the scope of this thesis; however, they are related directly or indirectly to the energy consumption estimation and the energy efficiency of EVs. These directions may address many existing challenges in addition to the energy estimation accuracy. These challenges include but are not limited to the following.

7.4.1 Behavioural-based energy consumption estimation analysis

One of the main unanswered questions for energy consumption estimation of EVs is how to predict driving patterns. The driver behaviour may have a degree of relevance to energy consumption. Attaching sensory devices to a sufficient number of actual

vehicles may reveal behavioural patterns of interest. For instance, real-time sensors are attached to the battery management systems on the vehicles for a sufficient amount of time helps understand drivers' driving patterns. Thus, future work will consider the impact of driving behaviours on the energy consumption estimation. Predicting the driver's behaviours will improve the accuracy of the energy consumption estimation. However, this will need a considerable amount of data collected from many drivers and vehicles.

7.4.2 The influence of energy consumption estimation on planning the power generation

The concept of electric vehicles is one of the main components of a typical smart grid architecture [171]. Therefore, it would be interesting to see how energy consumption is relevant to other components. For instance, energy consumption may increase planning and estimating power generation accuracy and reliability. In addition, Integrating a significant number of EVs into the power grid can help the power generators to understand the energy consumption levels in EVs. However, some complex issues associated with this process need to be further investigated and assessed to analyse the economic consequences. For instance, the distribution of charging stations and faster chargers is expanding inside cities and workplaces. As a result, the effects of EV charging are likely to impact the power grid systems' distribution directly. These consequences vary from overheated power transformers to the need for additional facilities of power distribution infrastructure.

BIBLIOGRAPHY

[1] S. Alateef and N. Thomas, "Battery models investigation and evaluation using a power demand generated from driving cycles," in *Proceedings of the 12th EAI International Conference on Performance Evaluation Methodologies and Tools*, 2019, pp. 189–190.

[2] S. Alatef and N. Thomas, "Energy consumption estimation for electric vehicles using routing api data," in *18th European Performance Engineering Workshop*. EPEW, 2022.

[3] S. Alateef and N. Thomas, "Trip driving cycle development and energy consumption estimation based on route api information for battery powered vehicles." in *36th Annual UK Performance Engineering Workshop*. Newcastle University, 2020.

[4] Department of Transport. Vehicle licensing statistics data tables. [Online]. Available: https://www.gov.uk/government/statistical-data-sets/vehicle-licensing-statistics-data-tables (Accessed: February 29, 2022)

[5] J. Meng, G. Luo, M. Ricco, M. Swierczynski, D.-I. Stroe, and R. Teodorescu, "Overview of lithium-ion battery modeling methods for state-of-charge estimation in electrical vehicles," *Applied Sciences*, vol. 8, no. 5, p. 659, 2018.

[6] United Nations. The Paris agreement. [Online]. Available: https://www.unfccc.int/process-and-meetings/the-paris-agreement/the-paris-agreemen (Accessed: November 12, 2020)

[7] S. Brown, D. Pyke, and P. Steenhof, "Electric vehicles: The role and importance of standards in an emerging market," *Energy Policy*, vol. 38, no. 7, pp. 3797–3806, 2010.

[8] J. Larminie and J. Lowry, *Electric Vehicle Technology Explained*. John Wiley & Sons, 2012.

[9] T. F. Fuller, M. Doyle, and J. Newman, "Simulation and optimization of the dual lithium ion insertion cell," *Journal of the Electrochemical Society*, vol. 141, no. 1, pp. 1–10, 1994.

[10] H. Hermanns, J. Krčál, and G. Nies, "Recharging probably keeps batteries alive," in *International Workshop on Design, Modeling, and Evaluation of Cyber Physical Systems*. Springer, 2015, pp. 83–98.

[11] M. R. Jongerden and B. R. Haverkort, "Battery aging, battery charging and the kinetic battery model: a first exploration," in *International Conference on Quantitative Evaluation of Systems*. Springer, 2017, pp. 88–103.

[12] Y. Chen and Y. Fan, "Transportation fuel portfolio design under evolving technology and regulation: a california case study," *Transportation Research Part D: Transport and Environment*, vol. 24, pp. 76–82, 2013.

[13] "International Energy Agency (Paris, France)," https://www.iea.org/reports/global-ev-outlook-2019/, accessed: 2020-09-03.

[14] P. Hertzke, N. Müller, S. Schenk, and T. Wu, "The global electric-vehicle market is amped up and on the rise," *McKinsey Centre For Future Mobility*, pp. 1–8, 2018.

[15] M. Smuts, B. Scholtz, and J. Wesson, "A critical review of factors influencing the remaining driving range of electric vehicles," in *2017 1st International Conference on Next Generation Computing Applications (NextComp)*. IEEE, 2017, pp. 196–201.

[16] W. Li, R. Long, H. Chen, and J. Geng, "A review of factors influencing consumer intentions to adopt battery electric vehicles," *Renewable and Sustainable Energy Reviews*, vol. 78, pp. 318–328, 2017.

[17] H. Jiang, Y. Zhang, Y. Chen, C. Zhao, and J. Tan, "Power-traffic coordinated operation for bi-peak shaving and bi-ramp smoothing–a hierarchical data-driven approach," *Applied Energy*, vol. 229, pp. 756–766, 2018.

[18] C. Chan, "The state of the art of electric and hybrid vehicles," *Proceedings of the IEEE*, vol. 90, no. 2, pp. 247–275, 2002.

[19] C. C. Chan and Y. Wong, "Electric vehicles charge forward," *IEEE Power and Energy Magazine*, vol. 2, no. 6, pp. 24–33, 2004.

[20] O. D. Momoh and M. O. Omoigui, "An overview of hybrid electric vehicle technology," in *2009 IEEE Vehicle Power and Propulsion Conference*, 2009, pp. 1286–1292.

[21] J. Walters, H. Husted, and K. Rajashekara, "Comparative study of hybrid powertrain strategies," *SAE Transactions*, pp. 1944–1953, 2001.

[22] G. Zorpette, "The smart hybrid," *IEEE Spectrum*, vol. 41, no. 1, pp. 44–51, 2004.

[23] T. Katrasnik, F. Trenc, and S. R. Opresnik, "Analysis of energy conversion efficiency in parallel and series hybrid powertrains," *IEEE Transactions on Vehicular Technology*, vol. 56, no. 6, pp. 3649–3659, 2007.

[24] M. Morimoto, "Which is the first electric vehicle?" *Electrical Engineering in Japan*, vol. 192, no. 2, pp. 31–38, 2015.

[25] H.-K. Tseng, J. S. Wu, and X. Liu, "Affordability of electric vehicles for a sustainable transport system: An economic and environmental analysis," *Energy policy*, vol. 61, pp. 441–447, 2013.

[26] R. Sharma, C. Manzie, M. Bessede, M. Brear, and R. Crawford, "Conventional, hybrid and electric vehicles for australian driving conditions–part 1: Technical and financial analysis," *Transportation Research Part C: Emerging Technologies*, vol. 25, pp. 238–249, 2012.

[27] Statista, "Electric vehicles worldwide," http://www.statista.com/study/11578/electric-vehicles-statista-dossier/, accessed: 2020-09-30.

[28] N. Adnan, S. M. Nordin, I. Rahman, P. M. Vasant, and A. Noor, "A comprehensive review on theoretical framework-based electric vehicle consumer adoption research," *International Journal of Energy Research*, vol. 41, no. 3, pp. 317–335, 2017.

[29] J. Neubauer and E. Wood, "The impact of range anxiety and home, workplace, and public charging infrastructure on simulated battery electric vehicle lifetime utility," *Journal of power sources*, vol. 257, pp. 12–20, 2014.

[30] P. Piatkowski and W. Puszkiewicz, "Electric vehicles: problems or solutions," *Journal of Mechanical and Energy Engineering*, vol. 2, 2018.

[31] E. Macioszek, "Electric vehicles-problems and issues," in *Scientific And Technical Conference Transport Systems Theory And Practice*. Springer, 2019, pp. 169–183.

[32] T. Anegawa, "Development of quick charging system for electric vehicle," 2010.

[33] R. C. Majhi, P. Ranjitkar, M. Sheng, G. A. Covic, and D. J. Wilson, "A systematic review of charging infrastructure location problem for electric vehicles," *Transport Reviews*, vol. 41, no. 4, pp. 432–455, 2021.

[34] F. Badin, F. Le Berr, H. Briki, J. Dabadie, M. Petit, S. Magand, and E. Condemine, "Evaluation of evs energy consumption influencing factors, driving conditions, auxiliaries use, driver's aggressiveness," *World Electric Vehicle Journal*, vol. 6, no. 1, pp. 112–123, 2013.

[35] H. A. Bonges III and A. C. Lusk, "Addressing electric vehicle (EV) sales and range anxiety through parking layout, policy and regulation," *Transportation Research Part A: Policy and Practice*, vol. 83, pp. 63–73, 2016.

[36] T. A. Becker, I. Sidhu, and B. Tenderich, "Electric vehicles in the united states: a new model with forecasts to 2030," *Center for Entrepreneurship and Technology, University of California, Berkeley*, vol. 24, 2009.

[37] R. Maia, M. Silva, R. Araújo, and U. Nunes, "Electrical vehicle modeling: A fuzzy logic model for regenerative braking," *Expert Systems with Applications*, vol. 42, no. 22, pp. 8504–8519, 2015.

[38] N. Chang, D. Baek, and J. Hong, "Power consumption characterization, modeling and estimation of electric vehicles," in *2014 IEEE/ACM International Conference on Computer-Aided Design (ICCAD)*. IEEE, 2014, pp. 175–182.

[39] C. Bingham, C. Walsh, and S. Carroll, "Impact of driving characteristics on electric vehicle energy consumption and range," *IET Intelligent Transport Systems*, vol. 6, no. 1, pp. 29–35, 2012.

[40] J. Thomas, S. Huff, and B. West, "Fuel economy and emissions effects of low tire pressure, open windows, roof top and hitch-mounted cargo, and trailer," *SAE International Journal of Passenger Cars-Mechanical Systems*, vol. 7, no. 2014-01-1614, pp. 862–872, 2014.

[41] M. A. Hannan, M. H. Lipu, A. Hussain, and A. Mohamed, "A review of lithium-ion battery state of charge estimation and management system in electric vehicle applications: challenges and recommendations," *Renewable and Sustainable Energy Reviews*, vol. 78, pp. 834–854, 2017.

[42] J. Bi, Y. Wang, S. Shao, and Y. Cheng, "Residual range estimation for battery electric vehicle based on radial basis function neural network," *Measurement*, vol. 128, pp. 197–203, 2018.

[43] K. Kambly and T. H. Bradley, "Geographical and temporal differences in electric vehicle range due to cabin conditioning energy consumption," *Journal of Power Sources*, vol. 275, pp. 468–475, 2015.

[44] K. N. Genikomsakis and G. Mitrentsis, "A computationally efficient simulation model for estimating energy consumption of electric vehicles in the context of route planning applications," *Transportation Research Part D: Transport and Environment*, vol. 50, pp. 98–118, 2017.

[45] K. M. Sentoff, L. Aultman-Hall, and B. A. Holmén, "Implications of driving style and road grade for accurate vehicle activity data and emissions estimates," *Transportation Research Part D: Transport and Environment*, vol. 35, pp. 175–188, 2015.

[46] X. Wu, X. He, G. Yu, A. Harmandayan, and Y. Wang, "Energy-optimal speed control for electric vehicles on signalized arterials," *IEEE Transactions on Intelligent Transportation System*, vol. 16, no. 5, pp. 2786–2796, 2015.

[47] S. M. Rezvanizaniani, Z. Liu, Y. Chen, and J. Lee, "Review and recent advances in battery health monitoring and prognostics technologies for electric vehicle (EV) safety and mobility," *Journal of Power Sources*, vol. 256, pp. 110–124, 2014.

[48] M. Mruzek, I. Gajdáč, L. Kučera, and D. Barta, "Analysis of parameters influencing electric vehicle range," *Procedia Engineering*, vol. 134, pp. 165–174, 2016.

[49] N. Rauh, T. Franke, and J. F. Krems, "Understanding the impact of electric vehicle driving experience on range anxiety," *Human Factors*, vol. 57, no. 1, pp. 177–187, 2015.

[50] M. Eisel, I. Nastjuk, and L. M. Kolbe, "Understanding the influence of in-vehicle information systems on range stress–insights from an electric vehicle field experiment," *Transportation Research Part F: Traffic Psychology and Behaviour*, vol. 43, pp. 199–211, 2016.

[51] Z. Zhang, W. Li, C. Zhang, and J. Chen, "Climate control loads prediction of electric vehicles," *Applied Thermal Engineering*, vol. 110, pp. 1183–1188, 2017.

[52] P. Iora and L. Tribioli, "Effect of ambient temperature on electric vehicles' energy consumption and range: Model definition and sensitivity analysis based on nissan leaf data," *World Electric Vehicle Journal*, vol. 10, no. 1, p. 2, 2019.

[53] S. M. Lukic, J. Cao, R. C. Bansal, F. Rodriguez, and A. Emadi, "Energy storage systems for automotive applications," *IEEE Transactions on Industrial Electronics*, vol. 55, no. 6, pp. 2258–2267, 2008.

[54] A. Khaligh and Z. Li, "Battery, ultracapacitor, fuel cell, and hybrid energy storage systems for electric, hybrid electric, fuel cell, and plug-in hybrid electric vehicles: State of the art," *IEEE Transactions on Vehicular Technology*, vol. 59, no. 6, pp. 2806–2814, 2010.

[55] S. F. Tie and C. W. Tan, "A review of energy sources and energy management system in electric vehicles," *Renewable and Sustainable Energy Reviews*, vol. 20, pp. 82–102, 2013.

[56] E. A. Grunditz and T. Thiringer, "Performance analysis of current bevs based on a comprehensive review of specifications," *IEEE Transactions on Transportation Electrification*, vol. 2, no. 3, pp. 270–289, 2016.

[57] Y. Li, L. Zhang, H. Zheng, X. He, S. Peeta, T. Zheng, and Y. Li, "Evaluating the energy consumption of electric vehicles based on car-following model under non-lane discipline," *Nonlinear Dynamics*, vol. 82, no. 1, pp. 629–641, 2015.

[58] C. Fiori, K. Ahn, and H. A. Rakha, "Power-based electric vehicle energy consumption model: Model development and validation," *Applied Energy*, vol. 168, pp. 257–268, 2016.

[59] X. Wu, D. Freese, A. Cabrera, and W. A. Kitch, "Electric vehicles' energy consumption measurement and estimation," *Transportation Research Part D: Transport and Environment*, vol. 34, pp. 52–67, 2015.

[60] O. Travesset-Baro, M. Rosas-Casals, and E. Jover, "Transport energy consumption in mountainous roads. a comparative case study for internal combustion engines and electric vehicles in andorra," *Transportation Research Part D: Transport and Environment*, vol. 34, pp. 16–26, 2015.

[61] R. Maia, M. Silva, R. Araújo, and U. Nunes, "Electric vehicle simulator for energy consumption studies in electric mobility systems," in *2011 IEEE Forum on Integrated and Sustainable Transportation Systems*. IEEE, 2011, pp. 227–232.

[62] G. M. Fetene, S. Kaplan, S. L. Mabit, A. F. Jensen, and C. G. Prato, "Harnessing big data for estimating the energy consumption and driving range of electric vehicles," *Transportation Research Part D: Transport and Environment*, vol. 54, pp. 1–11, 2017.

[63] M. Masikos, K. Demestichas, E. Adamopoulou, and M. Theologou, "Mesoscopic forecasting of vehicular consumption using neural networks," *Soft Computing*, vol. 19, no. 1, pp. 145–156, 2015.

[64] S. Sun, J. Zhang, J. Bi, and Y. Wang, "A machine learning method for predicting driving range of battery electric vehicles," *Journal of Advanced Transportation*, vol. 2019, 2019.

[65] R. Zhang and E. Yao, "Electric vehicles' energy consumption estimation with real driving condition data," *Transportation Research Part D: Transport and Environment*, vol. 41, pp. 177–187, 2015.

[66] H. Wang, D. Zhao, Y. Cai, Q. Meng, and G. P. Ong, "A trajectory-based energy consumption estimation method considering battery degradation for an urban electric vehicle network," *Transportation Research Part D: Transport and Environment*, vol. 74, pp. 142–153, 2019.

[67] D. Jiménez, S. Hernández, J. Fraile-Ardanuy, J. Serrano, R. Fernández, and F. Alvarez, "Modelling the effect of driving events on electrical vehicle energy consumption using inertial sensors in smartphones," *Energies*, vol. 11, no. 2, p. 412, 2018.

[68] J. Vepsäläinen, K. Otto, A. Lajunen, and K. Tammi, "Computationally efficient model for energy demand prediction of electric city bus in varying operating conditions," *Energy*, vol. 169, pp. 433–443, 2019.

[69] P. Egede, *Environmental assessment of lightweight electric vehicles.* Springer, 2017.

[70] J. Yao and A. Moawad, "Vehicle energy consumption estimation using large scale simulations and machine learning methods," *Transportation Research Part C: Emerging Technologies*, vol. 101, pp. 276–296, 2019.

[71] J. G. Hayes and K. Davis, "Simplified electric vehicle powertrain model for range and energy consumption based on epa coast-down parameters and test validation by argonne national lab data on the nissan leaf," in *2014 IEEE Transportation Electrification Conference and Expo (ITEC)*. IEEE, 2014, pp. 1–6.

[72] C. De Cauwer, J. Van Mierlo, and T. Coosemans, "Energy consumption prediction for electric vehicles based on real-world data," *Energies*, vol. 8, no. 8, pp. 8573–8593, 2015.

[73] W. J. Sweeting, A. R. Hutchinson, and S. D. Savage, "Factors affecting electric vehicle energy consumption," *International Journal of Sustainable Engineering*, vol. 4, no. 3, pp. 192–201, 2011.

[74] C. Fiori and V. Marzano, "Modelling energy consumption of electric freight vehicles in urban pickup/delivery operations: analysis and estimation on a real-world dataset," *Transportation Research Part D: Transport and Environment*, vol. 65, pp. 658–673, 2018.

[75] J. Romero Schmidt, J. Eguren, and F. Auat Cheein, "Profiling the instantaneous power consumption of electric machinery in agricultural environments: Algebraic approach," *Sustainability*, vol. 11, no. 7, p. 2146, 2019.

[76] F. Ye, G. Wu, K. Boriboonsomsin, and M. J. Barth, "A hybrid approach to estimating electric vehicle energy consumption for ecodriving applications," in *2016 IEEE 19th International Conference on Intelligent Transportation Systems (ITSC)*. IEEE, 2016, pp. 719–724.

[77] J.-b. Wang, K. Liu, T. Yamamoto, and T. Morikawa, "Improving estimation accuracy for electric vehicle energy consumption considering the effects of ambient temperature," *Energy Procedia*, vol. 105, pp. 2904–2909, 2017.

[78] H. Wang, D. Zhao, Q. Meng, G. P. Ong, and D.-H. Lee, "Network-level energy consumption estimation for electric vehicles considering vehicle and user heterogeneity," *Transportation Research Part A: Policy and Practice*, vol. 132, pp. 30–46, 2020.

[79] W. Li, P. Stanula, P. Egede, S. Kara, and C. Herrmann, "Determining the main factors influencing the energy consumption of electric vehicles in the usage phase," *Procedia Cirp*, vol. 48, pp. 352–357, 2016.

[80] Z. Qi, J. Yang, R. Jia, and F. Wang, "Investigating real-world energy consumption of electric vehicles: A case study of shanghai," *Procedia Computer Science*, vol. 131, pp. 367–376, 2018.

[81] Y. Zhang, W. Wang, Y. Kobayashi, and K. Shirai, "Remaining driving range estimation of electric vehicle," in *2012 IEEE International Electric Vehicle Conference*. IEEE, 2012, pp. 1–7.

[82] R. Galvin, "Energy consumption effects of speed and acceleration in electric vehicles: Laboratory case studies and implications for drivers and policymakers," *Transportation Research Part D: Transport and Environment*, vol. 53, pp. 234–248, 2017.

[83] K. Liu, J. Wang, T. Yamamoto, and T. Morikawa, "Exploring the interactive effects of ambient temperature and vehicle auxiliary loads on electric vehicle energy consumption," *Applied Energy*, vol. 227, pp. 324–331, 2018.

[84] B. Luin, S. Petelin, and F. Al-Mansour, "Microsimulation of electric vehicle energy consumption," *Energy*, vol. 174, pp. 24–32, 2019.

[85] R. Zhang and E. Yao, "Mesoscopic model framework for estimating electric vehicles' energy consumption," *Sustainable Cities and Society*, vol. 47, p. 101478, 2019.

[86] X. Yuan, C. Zhang, G. Hong, X. Huang, and L. Li, "Method for evaluating the real-world driving energy consumptions of electric vehicles," *Energy*, vol. 141, pp. 1955–1968, 2017.

[87] Y. Xu and K. Wang, "Research on estimation method of mileage power consumption for electric vehicles," in *2018 International Conference on Computer Science, Electronics and Communication Engineering (CSECE 2018)*. Atlantis Press, 2018.

[88] M. Bartłomiejczyk, "Driving performance indicators of electric bus driving technique: Naturalistic driving data multicriterial analysis," *IEEE Transactions on Intelligent Transportation Systems*, vol. 20, no. 4, pp. 1442–1451, 2018.

[89] D. Wu, D. C. Aliprantis, and K. Gkritza, "Electric energy and power consumption by light-duty plug-in electric vehicles," *IEEE Transactions on Power Systems*, vol. 26, no. 2, pp. 738–746, 2010.

[90] D. F. Specht *et al.*, "A general regression neural network," *IEEE Transactions on Neural Networks*, vol. 2, no. 6, pp. 568–576, 1991.

[91] J. Felipe, J. C. Amarillo, J. E. Naranjo, F. Serradilla, and A. Díaz, "Energy consumption estimation in electric vehicles considering driving style," in *2015 IEEE 18th International Conference on Intelligent Transportation Systems*. IEEE, 2015, pp. 101–106.

[92] R. Abousleiman and O. Rawashdeh, "Energy consumption model of an electric vehicle," in *2015 IEEE Transportation Electrification Conference and Expo (ITEC)*. IEEE, 2015, pp. 1–5.

[93] L. Kessler and K. Bogenberger, "Forecast of the energy consumption of bev based on dynamic traffic information," *Mobil. TUM*, 2015.

[94] Y. Wang, J. Jiang, and T. Mu, "Context-aware and energy-driven route optimization for fully electric vehicles via crowdsourcing," *IEEE Transactions on Intelligent Transportation Systems*, vol. 14, no. 3, pp. 1331–1345, 2013.

[95] J. Wang, I. Besselink, and H. Nijmeijer, "Battery electric vehicle energy consumption prediction for a trip based on route information," *Proceedings of the Institution of Mechanical Engineers, Part D: Journal of Automobile Engineering*, vol. 232, no. 11, pp. 1528–1542, 2018.

[96] A. D. Alvarez, F. S. Garcia, J. E. Naranjo, J. J. Anaya, and F. Jimenez, "Modeling the driving behavior of electric vehicles using smartphones and neural networks," *IEEE Intelligent Transportation Systems Magazine*, vol. 6, no. 3, pp. 44–53, 2014.

[97] K. Liu, T. Yamamoto, and T. Morikawa, "Impact of road gradient on energy consumption of electric vehicles," *Transportation Research Part D: Transport and Environment*, vol. 54, pp. 74–81, 2017.

[98] E. Yao, Z. Yang, Y. Song, and T. Zuo, "Comparison of electric vehicle's energy consumption factors for different road types," *Discrete Dynamics in Nature and Society*, vol. 2013, 2013.

[99] J. Wang, I. Besselink, and H. Nijmeijer, "Electric vehicle energy consumption modelling and prediction based on road information," *World Electric Vehicle Journal*, vol. 7, no. 3, pp. 447–458, 2015.

[100] K. Hu, J. Wu, and T. Schwanen, "Differences in energy consumption in electric vehicles: An exploratory real-world study in beijing," *Journal of Advanced Transportation*, 2017.

[101] K. Liu, J. Wang, T. Yamamoto, and T. Morikawa, "Modelling the multilevel structure and mixed effects of the factors influencing the energy consumption of electric vehicles," *Applied Energy*, vol. 183, pp. 1351–1360, 2016.

[102] D. Kowalsky, "Quantifying behavioral impacts on electric vehicle efficiency," Ph.D. dissertation, University of Rhode Island, 2017.

[103] X. Qi, M. J. Barth, G. Wu, K. Boriboonsomsin, and P. Wang, "Energy impact of connected eco-driving on electric vehicles," in *Road Vehicle Automation 4*. Springer, 2018, pp. 97–111.

[104] D. Baek and N. Chang, "Runtime power management of battery electric vehicles for extended range with consideration of driving time," *IEEE Transactions on Very Large Scale Integration (VLSI) Systems*, vol. 27, no. 3, pp. 549–559, 2018.

[105] X. Qi, G. Wu, K. Boriboonsomsin, and M. J. Barth, "Data-driven decomposition analysis and estimation of link-level electric vehicle energy consumption under real-world traffic conditions," *Transportation Research Part D: Transport and Environment*, vol. 64, pp. 36–52, 2018.

[106] N. Schwertner, "Driving behavior energy consumption estimation for electric vehicles," Master's thesis, 2018.

[107] Y. Chen, D. Baek, J. Kim, S. Di Cataldo, N. Chang, E. Macii, S. Vinco, and M. Poncino, "A systemc-ams framework for the design and simulation of energy management in electric vehicles," *IEEE Access*, vol. 7, pp. 25 779–25 791, 2019.

[108] C. Zhang, F. Yang, X. Ke, Z. Liu, and C. Yuan, "Predictive modeling of energy consumption and greenhouse gas emissions from autonomous electric vehicle operations," *Applied Energy*, vol. 254, p. 113597, 2019.

[109] S. Chen, W. Sun, Y. Li, and L. Shi, "On the relationship between energy consumption and driving behavior of electric vehicles based on statistical features," IEEE. Chinese Control Conference (CCC), 2019, pp. 3782–3787.

[110] G. Wu, F. Ye, P. Hao, D. Esaid, K. Boriboonsomsin, and M. J. Barth, "Deep learning–based eco-driving system for battery electric vehicles," *A Research Report from the National Center for Sustainable transportation UC Davies*.

[111] R. Basso, B. Kulcsár, B. Egardt, P. Lindroth, and I. Sanchez-Diaz, "Energy consumption estimation integrated into the electric vehicle routing problem," *Transportation Research Part D: Transport and Environment*, vol. 69, pp. 141–167, 2019.

[112] A. Fotouhi, N. Shateri, D. Shona Laila, and D. J. Auger, "Electric vehicle energy consumption estimation for a fleet management system," *International Journal of Sustainable Transportation*, vol. 15, no. 1, pp. 40–54, 2020.

[113] S. Modi, J. Bhattacharya, and P. Basak, "Estimation of energy consumption of electric vehicles using deep convolutional neural network to reduce driver's range anxiety," *ISA Transactions*, vol. 98, pp. 454–470, 2020.

[114] S. Yang, M. Li, Y. Lin, and T. Tang, "Electric vehicle's electricity consumption on a road with different slope," *Physica A: Statistical Mechanics and its Applications*, vol. 402, pp. 41–48, 2014.

[115] J. C. Ferreira, V. D. F. Monteiro, and J. L. Afonso, "Data mining approach for range prediction of electric vehicle," *Conference on Future Automotive Technology - Focus Electromobility*, pp. 1–15, 2012.

[116] J. C. Ferreira, V. Monteiro, and J. L. Afonso, "Dynamic range prediction for an electric vehicle," in *2013 World Electric Vehicle Symposium and Exhibition (EVS27)*. IEEE, 2013, pp. 1–11.

[117] T. Bär, D. Nienhüser, R. Kohlhaas, and J. M. Zöllner, "Probabilistic driving style determination by means of a situation based analysis of the vehicle data," in *2011 14th International IEEE Conference on Intelligent Transportation Systems (ITSC)*. IEEE, 2011, pp. 1698–1703.

[118] B. D. Ziebart, A. L. Maas, J. A. Bagnell, A. K. Dey *et al.*, "Maximum entropy inverse reinforcement learning." in *AAAI Conference on Artificial Intelligence*, vol. 8. Chicago, IL, USA, 2008, pp. 1433–1438.

[119] C. De Cauwer, W. Verbeke, T. Coosemans, S. Faid, and J. Van Mierlo, "A data-driven method for energy consumption prediction and energy-efficient routing of electric vehicles in real-world conditions," *Energies*, vol. 10, no. 5, p. 608, 2017.

[120] S. Javanmardi, E. Bideaux, J.-F. Trégouët, R. Trigui, H. Tattegrain, and E. N. Bourles, "Driving style modelling for eco-driving applications," *IFAC-PapersOnLine*, vol. 50, no. 1, pp. 13 866–13 871, 2017.

[121] D. Delling, A. V. Goldberg, T. Pajor, and R. F. Werneck, "Customizable route planning in road networks," *Transportation Science*, vol. 51, no. 2, pp. 566–591, 2017.

[122] M. Baum, J. Dibbelt, T. Pajor, and D. Wagner, "Energy-optimal routes for electric vehicles," in *Proceedings of the 21st ACM SIGSPATIAL International Conference on Advances in Geographic Information Systems*, 2013, pp. 54–63.

[123] J. A. Oliva, C. Weihrauch, and T. Bertram, "Model-based remaining driving range prediction in electric vehicles by using particle filtering and markov chains," IEEE. 2013 World Electric Vehicle Symposium and Exhibition (EVS27), 2013, pp. 1–10.

[124] D. Wang, F. Yang, L. Gan, and Y. Li, "Fuzzy prediction of power lithium ion battery state of function based on the fuzzy c-means clustering algorithm," *World Electric Vehicle Journal*, vol. 10, no. 1, p. 1, 2019.

[125] T. Zahid, K. Xu, W. Li, C. Li, and H. Li, "State of charge estimation for electric vehicle power battery using advanced machine learning algorithm under diversified drive cycles," *Energy*, vol. 162, pp. 871–882, 2018.

[126] H. Yavasoglu, Y. Tetik, and K. Gokce, "Implementation of machine learning based real time range estimation method without destination knowledge for BEVs," *Energy*, vol. 172, pp. 1179–1186, 2019.

[127] J. Brady and M. O'Mahony, "Development of a driving cycle to evaluate the energy economy of electric vehicles in urban areas," *Applied Energy*, vol. 177, pp. 165–178, 2016.

[128] S. Qiu, J. Meyer, F. Tseng, and S. Sangameswaran, "Predicting energy consumption for an electric vehicle using variations in past energy consumption," May 24 2016, US Patent 9,346,452.

[129] Z. Gao, T. LaClair, S. Ou, S. Huff, G. Wu, P. Hao, K. Boriboonsomsin, and M. Barth, "Evaluation of electric vehicle component performance over eco-driving cycles," *Energy*, vol. 172, pp. 823–839, 2019.

[130] L. Zhu and J. D. Gonder, "A driving cycle detection approach using map service api," *Transportation Research Part C: Emerging Technologies*, vol. 92, pp. 349–363, 2018.

[131] K. Young, C. Wang, L. Y. Wang, and K. Strunz, "Electric vehicle battery technologies," in *Electric Vehicle Integration into Modern Power Networks*. Springer, 2013, pp. 15–56.

[132] A. Fotouhi, D. J. Auger, T. Cleaver, N. Shateri, K. Propp, and S. Longo, "Influence of battery capacity on performance of an electric vehicle fleet," IEEE. 2016 IEEE International Conference on Renewable Energy Research and Applications (ICRERA), 2016, pp. 928–933.

[133] M. R. Jongerden and B. R. Haverkort, "Which battery model to use?" *IET software*, vol. 3, no. 6, pp. 445–457, 2009.

[134] S. C. Hageman, "Simple PSpice models let you simulate common battery types," *EDN*, vol. 38, no. 22, p. 117, 1993.

[135] S. Gold, "A pspice macromodel for lithium-ion batteries," IEEE. The Twelfth Annual Battery Conference on Applications and Advances, 1997, pp. 215–222.

[136] A. A.-h. Hussein and I. Batarseh, "An overview of generic battery models." Power and Energy Society General Meeting, 2011 IEEE, 2011, pp. 1–6.

[137] T. Huria, M. Ceraolo, J. Gazzarri, and R. Jackey, "High fidelity electrical model with thermal dependence for characterization and simulation of high power lithium battery cells," in *International Electric Vehicle Conference*. IEEE, 2012, pp. 1–8.

[138] H. He, R. Xiong, and J. Fan, "Evaluation of lithium-ion battery equivalent circuit models for state of charge estimation by an experimental approach," *Energies*, vol. 4, no. 4, pp. 582–598, 2011.

[139] B. Wu and B. Chen, "Study the performance of battery models for hybrid electric vehicles," IEEE/ASME. Tenth International Conference on Mechatronic and Embedded Systems and Applications (MESA), 2014, pp. 1–6.

[140] S. Raël, M. Urbain, and H. Renaudineau, "A mathematical lithium-ion battery model implemented in an electrical engineering simulation software." IEEE 23rd International Symposium on Industrial Electronics (ISIE), 2014, pp. 1760–1765.

[141] J. Feng, Y. He, and G. Wang, "Comparison study of equivalent circuit model of li-ion battery for electrical vehicles," *Research Journal of Applied Sciences*, vol. 6, no. 20, pp. 3756–3759, 2013.

[142] J. Fang, L. Qiu, and X. Li, "Comparative study of thevenin model and gnl simplified model based on kalman filter in soc estimation," *International Journal of Advanced Research in Computer Engineering and Technology*, vol. 6, pp. 1660–1663, 2017.

[143] D. N. Rakhmatov and S. B. Vrudhula, "An analytical high-level battery model for use in energy management of portable electronic systems," in *Proceedings of the 2001 IEEE/ACM International Conference on Computer-Aided Design*. IEEE Press, 2001, pp. 488–493.

[144] J. F. Manwell and J. G. McGowan, "Lead acid battery storage model for hybrid energy systems," *Solar Energy*, vol. 50, no. 5, pp. 399–405, 1993.

[145] L. M. Rodrigues, C. Montez, R. Moraes, P. Portugal, and F. Vasques, "A temperature-dependent battery model for wireless sensor networks," *Sensors*, vol. 17, no. 2, p. 422, 2017.

[146] S. Moore and M. Eshani, "An empirically based electrosource horizon lead-acid battery model," *SAE Transactions*, pp. 421–424, 1996.

[147] J. F. Manwell, J. G. McGowan, U. Abdulwahid, and K. Wu, "Improvements to the hybrid2 battery model," in *Windpower 2005 Conference*, 2005.

[148] H. Fang, X. Zhao, Y. Wang, Z. Sahinoglu, T. Wada, S. Hara, and R. A. De Callafon, "State-of-charge estimation for batteries: A multi-model approach," in *2014 American Control Conference*. IEEE, 2014, pp. 2779–2785.

[149] A. Falconi, "Electrochemical li-ion battery modeling for electric vehicles," Ph.D. dissertation, Communaute Universite Grenoble Alpes, 2017.

[150] M. Murnane and A. Ghazel, "A closer look at state of charge (soc) and state of health (soh) estimation techniques for batteries," *Analog Devices*, vol. 2, pp. 426–436, 2017.

[151] T. Kim and W. Qiao, "A hybrid battery model capable of capturing dynamic circuit characteristics and nonlinear capacity effects," *IEEE Transactions on Energy Conversion*, vol. 26, no. 4, pp. 1172–1180, 2011.

[152] B. Y. Liaw, G. Nagasubramanian, R. G. Jungst, and D. H. Doughty, "Modeling of lithium ion cells—a simple equivalent-circuit model approach," *Solid state ionics*, vol. 175, no. 1-4, pp. 835–839, 2004.

[153] O. Tremblay, L.-A. Dessaint, and A.-I. Dekkiche, "A generic battery model for the dynamic simulation of hybrid electric vehicles." Vehicle Power and Propulsion Conference, VPPC IEEE, 2007, pp. 284–289.

[154] R. Ahmed, J. Gazzarri, S. Onori, S. Habibi, R. Jackey, K. Rzemien, J. Tjong, and J. LeSage, "Model-based parameter identification of healthy and aged li-ion batteries for electric vehicle applications," *SAE International Journal of Alternative Powertrains*, vol. 4, no. 2, pp. 233–247, 2015.

[155] T. J. Barlow, S. Latham, I. McCrae, and P. Boulter, *A reference book of driving cycles for use in the measurement of road vehicle emissions*, 2009.

[156] A. Esteves-Booth, T. Muneer, H. Kirby, J. Kubie, and J. Hunter, "The measurement of vehicular driving cycle within the city of edinburgh," *Transportation Research Part D: Transport and Environment*, vol. 6, no. 3, pp. 209–220, 2001.

[157] M. Uzunoglu and M. Alam, "Dynamic modeling, design and simulation of a pem fuel cell/ultra-capacitor hybrid system for vehicular applications," *Energy Conversion and Management*, vol. 48, no. 5, pp. 1544–1553, 2007.

[158] A. K. Singh, A. Dalal, and P. Kumar, "Analysis of induction motor for electric vehicle application based on drive cycle analysis," in *2014 IEEE International Conference on Power Electronics, Drives and Energy Systems (PEDES)*. IEEE, 2014, pp. 1–6.

[159] M. Montazeri-Gh and M. Naghizadeh, "Development of car drive cycle for simulation of emissions and fuel economy," in *Proceedings of 15th European Simulation Symposium*, 2003.

[160] S. A. Miers, R. W. Carlson, S. S. McConnell, H. K. Ng, T. Wallner, and J. L. Esper, "Drive cycle analysis of butanol/diesel blends in a light-duty vehicle," SAE Technical Paper, Tech. Rep., 2008.

[161] N. Juul and P. Meibom, "Road transport and power system scenarios for northern europe in 2030," *Applied Energy*, vol. 92, pp. 573–582, 2012.

[162] M. Knowles, H. Scott, and D. Baglee, "The effect of driving style on electric vehicle performance, economy and perception," *International Journal of Electric and Hybrid Vehicles*, vol. 4, no. 3, pp. 228–247, 2012.

[163] "Google maps api (developers portal)," https://cloud.google.com/maps-platform/, accessed: 2019-09-03.

[164] "Here maps api (developers portal)," https://developer.here.com/products/maps/, accessed: 2019-08-22.

[165] "Tomtom maps api," https://developer.tomtom.com/products/maps-api/, accessed: 2019-09-05.

[166] J. Bi, Y. Wang, Q. Sai, and C. Ding, "Estimating remaining driving range of battery electric vehicles based on real-world data: A case study of Beijing, China," *Energy*, vol. 169, pp. 833–843, 2019.

[167] H. Rahimi-Eichi and M.-Y. Chow, "Big-data framework for electric vehicle range estimation," in *IECON 2014-40th Annual Conference of the IEEE Industrial Electronics Society*. IEEE, 2014, pp. 5628–5634.

[168] "Openweather maps api (developers portal)," https://openweathermap.org/api, accessed: 2021-08-22.

[169] R. Isnanto, "Comparation on several smoothing methods in nonparametric regression," *Jurnal Sistem Komputer*, vol. 1, no. 1, pp. 41–48, 2011.

[170] "Biologic ec-lab® software," Aug 2007. [Online]. Available: https://www.biologic.net/support-software/ec-lab-software/

[171] F. Mwasilu, J. J. Justo, E.-K. Kim, T. D. Do, and J.-W. Jung, "Electric vehicles and smart grid interaction: A review on vehicle to grid and renewable energy sources integration," *Renewable and sustainable energy reviews*, vol. 34, pp. 501–516, 2014.